




12-2015

Novel Thermoplastic Elastomers based on Benzofulvene: Synthesis and Mechanical Properties

Weiyu Wang

University of Tennessee - Knoxville, wwang41@vols.utk.edu

Follow this and additional works at: https://trace.tennessee.edu/utk_graddiss

 Part of the [Materials Chemistry Commons](#), [Polymer and Organic Materials Commons](#), and the [Polymer Chemistry Commons](#)

Recommended Citation

Wang, Weiyu, "Novel Thermoplastic Elastomers based on Benzofulvene: Synthesis and Mechanical Properties." PhD diss., University of Tennessee, 2015.
https://trace.tennessee.edu/utk_graddiss/3558

This Dissertation is brought to you for free and open access by the Graduate School at TRACE: Tennessee Research and Creative Exchange. It has been accepted for inclusion in Doctoral Dissertations by an authorized administrator of TRACE: Tennessee Research and Creative Exchange. For more information, please contact trace@utk.edu.

To the Graduate Council:

I am submitting herewith a dissertation written by Weiyu Wang entitled "Novel Thermoplastic Elastomers based on Benzofulvene: Synthesis and Mechanical Properties." I have examined the final electronic copy of this dissertation for form and content and recommend that it be accepted in partial fulfillment of the requirements for the degree of Doctor of Philosophy, with a major in Chemistry.

Jimmy W. Mays, Major Professor

We have read this dissertation and recommend its acceptance:

Michael Kilbey, Alexei Sokolov, Michael Best

Accepted for the Council:

Carolyn R. Hodges

Vice Provost and Dean of the Graduate School

(Original signatures are on file with official student records.)

**Novel Thermoplastic Elastomers based on Benzofulvene:
Synthesis and Mechanical Properties**

A Dissertation Presented for the
Doctor of Philosophy
Degree
The University of Tennessee, Knoxville

Weiyu Wang
December 2015

Copyright © 2015 by Weiyu Wang
All rights reserved.

Acknowledgements

First of all, I gratefully thank my advisor Dr. Jimmy W. Mays for his mentorship which is beyond support, encouragement and guidance throughout my doctoral study throughout pass four and half years. His spirit of collaboration, wisdom of interpersonal skills and passion of career pursuits, constructively influenced my mind-set within and outside graduate school.

I would like to thank my doctoral committee members: Dr. Michael Best for his valuable time and advising, Dr. Michael Kilbey and Dr. Alexei Sokolov for bringing me on board on fascinating fundamental research projects and expanding my knowledge about polymeric materials. I enjoyed and would like to continue our collaboration in my future career.

I sincerely thank Dr. Nam-Goo Kang, Dr. Kunlun Hong (ORNL), Dr. Sang-Woog Ryu (Chungbuk National University, Korea), Dr. Suxiang Deng (GM, China) and Dr. David Uhrig (ORNL) for coaching me with essential experiment techniques when I started in UTK.

Working in Mays' group provided me with various opportunities to interact with world leading polymer scientists and engineers including: Dr. Mario Beiner and Dr. Ralf Schlegel from Fraunhofer institute in German (mechanical properties). Dr. Samuel Gido and Katherine Williams from the University of Massachusetts (TEM and SAXS). Dr. Frank Bates and Yiming Zeng from the University of Minnesota (Parr reactor hydrogenation). Dr. Shi-Qing Wang and Jianning Liu from the University of Akron (rheology).

Additionally, I would also like to thank Dr. Herbert Chao (Total Valley), Dr. Zhiyi Bao (Zeon Chemical), Dr. Naixiong Jin (Eastman) and Ilir Koliqi (Tosoh Bioscience LLC.) for their career advices.

I am also very fortunate to work with professors, post-docs and fellow graduate students in the University of Tennessee and Oak Ridge National Lab including: Dr. Mark Dadmun, Dr. Adam Imel, Dr. Jihua Chen (ORNL) and Halie Martin for TEM. Dr. Yangyang Wang (ORNL), Dr. Shiwang Chen, Dr. Fei Fan, Adam Holt for rheology and dielectric spectroscopy. Dr. Jesse Davis and Kamlesh R. Bornani for light scattering. Dr. Dimitry Voyloy for AFM. Dr. Carlos Steren for NMR. Dr. Chunhui Bao for ATRP and RAFT. Also current and ex- group members in Mays' group including: Dr. Shahinur Rahman, Dr. Kostas Mischronis, Dr. Beomgoo Kang, Tom Malmgren, Dr. Xiaojun Wang, Dr. Justin Roop, Dr. Vikram Srivastava, Dr. Sachin Bobade, Andrew Goodwin, Christopher Hurley, Wei Lu, Xinyi Lu, Hongbo Feng, Benjamin Ripy, Huiqun Wang and Tyler White. It has been a great pleasure to work with all of them. The presence of all these people during my doctoral study are vital for my growth and success. I sincerely appreciate every one of them.

Finally, I would like to thank my father Jimin Wang and my mother Yun Wang for their patience, sacrifice and selfless love which makes today possible. To my grandfather who passed away shortly after I came to Knoxville in 2011, may he rest in peace.

Weiyu Wang

Abstract

Thermoplastic elastomers (TPEs) are of great importance both academically and technologically. Currently TPEs are the predominant form of styrene-diene copolymers. However, these styrenic TPEs have serious limitations in applications, especially at higher temperature, because of their low upper service temperature (UST). The work described in this dissertation is aimed toward developing thermoplastic elastomers with a higher UST and lower cost.

In order to develop TPEs with a higher UST, we employed benzofulvene, an anionically polymerizable monomer in hydrocarbon solvent at room temperature, as the glassy block and copolymerized it with isoprene to prepare polybenzofulvene-polyisoprene-polybenzofulvene (FIF) triblock copolymers. Among all triblock copolymers studied, FIF with 14 vol% [volume percentage] of PBF [polybenzofulvene] exhibited a maximum stress of 14.3 MPa [megapascal] and strain at break of 1394 % from tensile tests. Dynamic mechanical analysis showed that the upper service temperature of FIF is 145 °C. Microphase separation of FIF triblock copolymers was observed by small angle X-ray scattering, however, without long range order.

Additionally, we report the effects of partial and complete hydrogenation on the thermal stability, mechanical and morphological properties of high temperature thermoplastic elastomers comprised of polybenzofulvene-polyisoprene-polybenzofulvene (FIF) triblock copolymers. After hydrogenation of polyisoprene and unsaturated carbon bonds in the five member ring of PBF, ultimate tensile stress was reduced to 11.2 MPa with strain at break of 750 %. The upper service temperature also decreased to 125 °C. The

fully hydrogenated triblock copolymer demonstrated an ultimate stress of 17.4 MPa at 744 % strain. The glass transition temperature (T_g) of fully hydrogenated PBF was 130 °C. Thermal stability was greatly improved by both partial and complete hydrogenation.

Lastly, we developed a cost efficient method to prepare high molecular weight “comb-shaped” graft copolymers, poly(isoprene-*g*-styrene), with polyisoprene as the backbone and polystyrene as side chains. The grafted polymers were synthesized via free radical emulsion polymerization by copolymerization of isoprene with a polystyrene macromonomer synthesized using anionic polymerization. A material incorporating 29 wt% [weigh percentage] polystyrene exhibits a disordered microphase separated morphology and elastomeric properties. These materials show promise as new, highly tunable, and potentially low cost thermoplastic elastomers.

Table of Contents

Chapter 1: Recent Advances in Thermoplastic Elastomers based on Synthetic	
Polymers.....	1
1.1 Introduction:.....	2
1.2 ABA triblock copolymer type TPEs:	6
1.2.1 Polymers prepared by anionic polymerization:	6
1.2.2 Polymers prepared by cationic polymerization:	16
1.2.3 Polymers prepared by metal catalyzed ring opening polymerization:.....	22
1.2.4 Polymers prepared by controlled radical polymerization techniques:	29
1.2.5 Polymers prepared by metathesis polymerization techniques:	33
1.3 Star branched polymers for TPEs:	38
1.4 Grafted polymers for TPEs:	42
1.5 Perspective:	52
References:.....	57
Chapter 2: Scope of the Dissertation.....	73
2.1 Research Motivation:	74
2.2 Outline:	76
References:.....	78
Chapter 3: Experimental Techniques	79
3.1 High Vacuum Manifold:	80
3.2 Anionic Polymerization by High Vacuum Techniques:	80
3.3 Synthesizing anionic initiator:	84

References:.....	86
Chapter 4: High Temperature Thermoplastic Elastomers Synthesized by Living Anionic Polymerization in Hydrocarbon Solvent at Room Temperature.....	87
Abstract:.....	88
4.1 Introduction:.....	89
4.2 Experimental Section:.....	92
4.2.1 Materials:	92
4.2.2 Anionic polymerization of BF monomer:.....	93
4.2.3 Anionic polymerization of BF monomer in the presence of additives:	94
4.2.4 Diblock copolymerization of BF and isoprene:	94
4.2.5 Triblock copolymerization of isoprene and BF:	95
4.2.6 Preparation of samples:.....	95
4.2.7 Measurements:	96
4.3 Results and Discussion:	98
4.3.1 Anionic polymerization of BF and glass transition temperature of PBF:.....	98
4.3.2 Effects of additives on glass transition temperature:	101
4.3.3 NMR analysis of PBF synthesized without additive and with DME as the additive:.....	106
4.3.4 Diblock Copolymerization of BF with Isoprene:.....	106
4.3.5 Triblock Copolymerization of BF with Isoprene:.....	109
4.3.6 Dynamic Mechanical Analysis (DMA):	113
4.3.7 Stress-strain behavior of FIF triblock copolymers:	117

4.3.8 Microphase separation behavior:	124
4.4 Conclusions:.....	127
References:.....	130
Chapter 5: Polybenzofulvene Based Thermoplastic Elastomers: Effects of Partial and Fully Hydrogenation	133
Abstract:.....	134
5.1 Introduction:.....	135
5.2 Experimental Section:.....	138
5.2.1 Materials:	138
5.2.2 Anionic polymerization:	139
5.2.3 Hydrogenation:	141
5.2.4 Preparation of samples:.....	144
5.2.5 Measurements:	144
5.3 Results and Discussion:	146
5.3.1 Anionic polymerization and complete hydrogenation of homopolybenzofulvene:.....	146
5.3.2 Anionic polymerization and hydrogenation of polybenzofulvene-b- polyisoprene-b-polybenzofulvene (FIF):.....	152
5.3.3 Thermal properties:	155
5.3.4 Dynamic mechanical analysis:.....	158
5.3.6 Atomic force microscopy:.....	160
5.4 Conclusions:.....	164

References:.....	165
Chapter 6: Synthesis and Characterization of Graft Copolymers Poly(isoprene-g-styrene) of High Molecular Weight by a Combination of Anionic Polymerization and Emulsion Polymerization.....	168
Abstract:	169
6.1 Introduction:.....	170
6.2 Experimental Section:.....	175
6.2.1 Materials:	175
6.2.2 Synthesis of PS macromonomer:	176
6.2.3 Synthesis of graft copolymers:.....	176
6.2.4 Characterization:	180
6.3 Results and Discussion	182
6.3.1 Synthesis of PS macromonomer:	182
6.3.2 Characterization of latex particles composed of graft copolymers:.....	186
6.3.3 Characterization of “comb” graft copolymers:	188
6.3.4 Microphase separation of graft copolymer:	191
6.3.5 Thermal properties of the graft copolymers:	196
6.3.6 Rheological properties of graft copolymers:.....	199
6.4 Conclusions:.....	201
References:.....	204
Chapter 7: Conclusions and Future Perspectives	208
7.1 Conclusions:.....	209

7.2. Future Perspectives:	210
7.2.1. Composition Dependence of the Morphology in PBF/PI block copolymers:	212
7.2.2 Effects of additives on the characteristic ratio of PBF:	214
7.2.3: Benzofulvene-Butadiene Rubber:	214
Vita	217

List of Tables

Table 1.1: Mechanical properties of ABA triblock copolymer type TPEs prepared by anionic polymerization in hydrogenation solvent.....	10
Table 1.2: Mechanical properties of ABA triblock copolymer type TPEs prepared by anionic polymerization in polar solvent.....	12
Table 1.3: Mechanical properties of ABA triblock copolymer type TPEs – all acrylic polymers.....	14
Table 1.4: Mechanical properties of ABA triblock copolymer type TPEs based on hydrogenated polymers.....	17
Table 1.5: Mechanical properties of ABA triblock copolymer type TPEs synthesized by cationic polymerization.....	19
Table 1.6: Mechanical properties of ABA triblock copolymer type TPEs – all vinyl ether polymers.....	21
Table 1.7: Mechanical properties of ABA triblock copolymer type TPEs synthesized by ring opening polymerization with PLA as the glassy segment.....	24
Table 1.8: Mechanical properties of ABA triblock copolymer type TPEs synthesized by ring opening polymerization with sustainable recourse.....	26

Table 1.9: Mechanical properties of ABA triblock copolymer type TPEs synthesized by ATRP	32
Table 1.10: Mechanical properties of ABA triblock copolymer type TPEs synthesized by RAFT polymerization	34
Table 1.11: Mechanical properties of ABA triblock copolymer type TPEs synthesized by coordination polymerization	37
Table 1.12: Mechanical properties of star-branched polymer type TPEs synthesized by anionic polymerization.....	40
Table 1.13: Mechanical properties of star-branched polymer type TPEs synthesized by cationic polymerization.....	43
Table 1.14: Mechanical properties of star-branched polymer type TPEs synthesized by ATRP	44
Table 1.15: Mechanical properties of grafted polymer type TPEs synthesized by anionic polymerization	48
Table 1.16: Mechanical properties of grafted polymer type TPEs synthesized by ring opening metathesis polymerization.....	50
Table 1.17: Mechanical properties of grafted polymer type TPEs based on architecture III.....	54
Table 4.1 Anionic polymerization of BF in benzene in the absence of additives:.....	99

Table 4.2 Anionic Polymerization of BF in benzene in the presence of additives.	104
Table 4.3 Diblock Copolymerization of isoprene and benzofulvene.	110
Table 4.4 Composition of FIF triblock copolymers.	114
Table 4.5 Mechanical property parameters of FIF.	119
Table 5.1: Anionic polymerization and complete hydrogenation of polybenzofulvene	140
Table 5.2 Anionic polymerization, partial and complete hydrogenation of FIF-14	142
Table 5.3 Mechanical properties of triblock copolymers.	160
Table 6.2 Average molecular weights and compositions of macromonomer and multigraft copolymers as measured by SEC and $^1\text{H-NMR}$	190
Table 7.1 Mechanical properties of PBF based TPEs	211

List of Figures

Figure 1.1: a) Applications of SBCs. b) Global Market of SBCs.....	4
Figure 1.2: Schematic of SIS TPEs.	8
Figure 1.3: CO ₂ separation plots for poly(6-acetoxyhexyl vinyl ether) and poly (2-(2-methoxyethoxy)ethyl vinyl ether) based triblock copolymers together with commodity polymers [polystyrene, natural rubber, and poly(vinyl chloride)] for comparison.....	23
Figure 1.4: (a) Total biosynthetic pathway for the production of MVL. (b) A semisynthetic route to produce MVL from mevalonate. (c) Conversion of MVL to an elastomeric triblock polymer that can be repeatedly stretched to 18 times its original length without breaking.	27
Figure 1.5: Illustration of a Zn ²⁺ /VHV hybrid via metal-ligand complexation.	31
Figure 1.6: Triblock TPEs based on PMCH and a-PP.....	36
Figure 1.7: S(IS') ₃ miktoarm star copolymer type TPEs.	41
Figure 1.8: a). Illustration of multigrafted copolymers based on PI backbone and PS branches. b). Chain conformation of multigrafted copolymers in microphase-separated state	46
Figure 1.9: Illustration of TPEs' architecture	51

Figure 1.10: Design concept and synthesis of nanostructured elastomers mimicking the mechanical properties of human skin. (a) ATRP macroinitiator, (b) Cross-linked brush polymers were synthesized and self-assembled into two-phase morphology. (c) Two phase morphology of CBPs can be reconfigured into that close to the skin microstructure model.....	53
Figure 3.1: High vacuum manifold.....	81
Figure 3.2: Glass apparatus for anionic polymerization of styrene	82
Figure 3.3: Distill benzene in anionic polymerization apparatus	83
Figure 3.4: Final reactor for anionic polymerization.....	84
Figure 3.5: Glass apparatus to prepare <i>sec</i> -BuLi.....	85
Figure 4.1 SEC curve of PBF synthesized in benzene at room temperature with <i>sec</i> -BuLi. (Denote: PBF is polybenzofulvene and R1 to R7 is run 1 to run 7 in Table 4.1). 100	
Figure 4.2 Additives for anionic polymerization of BF in benzene: (a) DME, (b) DABCO, (c) TMEDA, and (d) <i>sec</i> -BuOLi for anionic polymerization of BF.	103
Figure 4.3 T_g versus M_n of PBF synthesized with different additives: DME (red cycle), <i>sec</i> -BuOLi (blue triangle), TMEDA (pink triangle), DABCO (green square) and no additives (black square).	105
Figure 4.4 Possible dimers of PBF.....	107

Figure 4.5 ^{13}C -NMR of PBF: a) ^{13}C -NMR of PBF-10, b) DEPT of PBF-10, c) ^{13}C -NMR of PBF-DME-16, d) DEPT of PBF-DME-16	108
Figure 4.6 SEC curve of PI and PI- <i>b</i> -PBF diblock copolymer.....	111
Figure 4.7 SEC curve of FIF triblock copolymers.....	115
Figure 4.8 ^1H -NMR of FIF-22 measured in THF- <i>d</i> ₈	116
Figure 4.9 DMA of FIF triblock copolymers: (a) Storage Modulus vs. Temp. and (b) Loss Modulus vs. Temp.....	118
Figure 4.10 Stress-strain curve of FIF triblock copolymers	121
Figure 4.11 Non-affine tube model analysis of FIF triblock copolymers.....	122
Figure 4.12 SAXS data for FIF triblock copolymers.....	125
Figure 4.13 DSC measurement of FIF triblock copolymers, PBF-20 and polyisoprene homopolymers.....	126
Figure 4.14 AFM of FIF-10: a-1) topology, a-2) phase contrast, a-3) force modulation and FIF-14: b-1) topology, b-2) phase contrast, b-3) force modulation.	128
Figure 5.1: GPC of complete hydrogenation of a) PBF-12 and b) PBF-DME.....	148
Figure 5.2 NMR of complete hydrogenation of PBF-12	149
Figure 5.3: TGA of complete hydrogenation of PBF-12.....	150

Figure 5.4 DSC of complete hydrogenation of a) PBF-12 and b) PBF-DME	151
Figure 5.5 ¹ H-NMR of partial and complete hydrogenation of FIF-14.....	153
Figure 5.6: GPC of partial and complete hydrogenation of FIF-14.....	154
Figure 5.7 TGA of partial and complete hydrogenation of FIF-14	156
Figure 5.8 DSC of partial and complete hydrogenation of FIF-14	157
Figure 5.9 DMA of a) FIF-14 and b) FH-FIF-14.....	159
Figure 5.11: Tensile test of FH-FIF-20.....	162
Figure 5.12: AFM of a) Height Image of FIF-14, b) Phase Image of FIF-14, c) Height Image of FH-FIF-14, d) Phase Image of FH-FIF-14.	163
Figure 6.1 SEC chromatogram for polystyrene macromonomer.	183
Figure 6.2 ¹ H-NMR spectrum of polystyrene macromonomer.....	184
Figure 6.3 MALDI-TOF mass spectrum of PS macromonomer.	185
Figure 6.5. SEC chromatograms for PS macromonomer and multigraft copolymers before and after fractionation.....	189
Figure 6.6 a) The chain structure and ¹ H-NMR spectrum of MG-3-3 dissolved in CDCl ₃ ; b) ¹³ C-NMR spectrum of MG-3-3 dissolved in CDCl ₃	192
Figure 6.7: AFM phase image of MG-3-5 over an area of 2 μm x 2 μm.	193

Figure 6.8: TEM image of MG-3-5	194
Figure 6.9: TGA thermograms for poly(isoprene- <i>g</i> -styrene) multigraft copolymers....	197
Figure 6.10: DSC thermograms for PI homopolymer, MG-3-3, MG-3-5, and PS macromonomer.	198
Figure 6.11: Storage modulus G' (solid symbols) and loss modulus G'' (hollow symbols) for MG-3-3 (■, □) and MG-3-5 (▲, △) as a function of frequency.	200
Figure 6.12: Tan δ versus frequency for MG-3-3 and MG-3-5.....	202
Figure 7.1: Proposed research on composition dependence of the morphology in PBF/PI block copolymers	213
Figure 7.2: Proposed Study of Effects of Additives on PBF	215
Figure 7.3: Benzofulvene-Butadiene Rubber	216

List of Schemes

Scheme 4.1 DLI approach to synthesize FIF triblock copolymer	112
Scheme 5.1 Partial hydrogenation of FIF-14	143
Scheme 5.2 Complete hydrogenation of FIF-14	145
Scheme 6.1: Emulsion copolymerization strategy for obtaining graft copolymer by macromonomer method.	174
Scheme 6.2: The synthetic route to PS macromonomer. (a) the synthesis procedure for hydroxyl-terminated PS; (b) Steglich esterification reaction for synthesis of PS macromonomer.	176
Scheme 6.3 The synthetic route to poly(isoprene- <i>g</i> -styrene) multigraft copolymer via free radical emulsion copolymerization.	179

Chapter 1: Recent Advances in Thermoplastic Elastomers based on Synthetic Polymers

1.1 Introduction:

Thermoplastic elastomers (TPEs) are biphasic synthetic polymer materials consisting of a continuous soft rubbery matrix physically cross linked by glassy plastic domains.^{1,2} Such materials have the elasticity of conventional rubber but are suitable for high throughput plastic processing techniques such as injection molding and melt extrusion without requiring a curing process.^{3,4} This feature allows TPEs to be manufactured on a large scale using short production times, which makes TPEs one of the most commonly used polymeric materials in many fields.⁵

Based on chemical composition and morphology, commercially available TPEs can be categorized into six different groups:³ (1) thermoplastic polyurethanes (TPUs), (2) styrenic thermoplastic elastomers (S-TPEs), (3) rubbery-polyolefin blends (TPOs), (4) thermoplastic vulcanizates (TPVs), (5) copolyesters thermoplastic elastomers (TPC-ET) and (6) thermoplastic polyamides (TPA). These have been extensively reviewed in many handbooks.⁴⁻⁷

As a brief historical introduction of thermoplastic elastomers, polyurethanes fibers started to emerge in the plastic/rubber market in the early 1950s with the discovery and development of basic diisocyanate addition.⁸ In 1952, Snyder first patented multiblock linear copolyester fibers with stress and strain characteristics competitive with nature rubber. From the current point of view, these materials would be considered as multiblock

TPUs.⁹ Many other polyurethane based thermoplastic gum elastomers were introduced by Bayer, Dupont and Goodyear in late 1950s.¹⁰ Polyurethane based TPEs showing high abrasion resistance with excellent elasticity and tensile strength were commercialized by B.F Goodrich in 1960s.¹¹

A significant event in the development of TPEs was in 1965, when Milkovich and Holden from Shell Development Company synthesized and characterized ABA triblock copolymers based on polystyrene as the hard segment (A block) and polyisoprene as the rubbery matrix (B block) by living anionic polymerization.¹² The termination free (living) anionic polymerization technique allowed styrenic TPEs to be prepared with predicted molecular weight, narrow molecular weight distribution and quantitative yield with negligible impurities in a short production cycle.¹³ The stress-strain and elongation recovery of styrenic TPEs displayed similar behavior to conventional vulcanized rubber without filler reinforcement or crosslinking.¹⁴ This new type of TPE with lower cost and well-defined structure, along with living anionic polymerization,^{15,16} stimulated numerous research activities in polymer thermodynamics,¹⁷ self-consistent field theory¹⁸ and polymer solution properties¹⁹ for the interest of both academic research and industrial applications.

Shell Chemical quickly realized the potential of processing styrenic TPEs (later given the trade name Kraton[®]) with injection molding and melt extrusion. After almost 50 years, styrenic block copolymers (SBCs) have developed into one of the major products in

the field of plastic/elastomer industry, and they are used in many fields such as paving, roofing, footwear, coatings, adhesives, sealants, medical tubing and some other advanced systems.²⁰ The global consumption of styrenic block copolymers, meanwhile, was predicted to increase from 1.8 million tons (5.5 billion US dollars) in 2013 to 2.5 million tons (8.4 billion US dollars) in 2020 with an annual growth rate of 4.5% (**Figure 1.1**).²¹

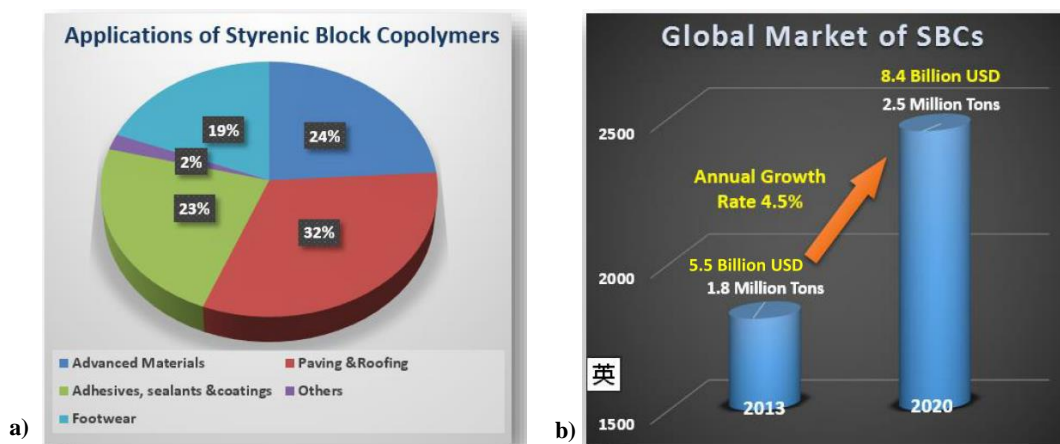


Figure 1.1: a) Applications of SBCs. b) Global Market of SBCs.²¹

Many other types of TPEs were introduced from the 1960s to 1980s. Hercules Inc. in 1966 patented the first thermoplastic polyolefin blends (TPO) based on mixtures of elastic poly(ethylene-co-propylene) (PEP) with over 50% of crystalline polypropylene (PP).²² In late 1970s, Monsanto Company started to focus on a dynamic vulcanization process to chemically crosslink blends of PEP-diene and PP, which was commercialized with trade name of Santoprene® (TPV).²³ Copolyester thermoplastic elastomers (TPC-ET)

named Hytrel[®], commercialized by DuPont in 1972, combined good mechanical properties with chemical and heat resistance.⁵ Dow Chemical Company developed Estamid[®] in 1982, a segmented polyamide based thermoplastic elastomer (TPA) with low density, superior mechanical properties at low temperature (-40°C) and service temperature above 200°C.⁸

Starting from the 1990s, many companies strategized their TPE research focus on specific market applications by adding new monomers, functionalities and using sustainable resources to improve properties of existing TPEs systems. In scientific research communities, fascinating polymers with various functionalities, well-defined structures and advanced macromolecular architectures were prepared thanks to developments in living/controlled polymerization techniques such as living anionic^{16,24}/cationic polymerization,²⁵ atomic transfer radical polymerization (ATRP),²⁶ ring opening metathesis polymerization (ROMP),²⁷ reversible addition-fragmentation chain transfer polymerization (RAFT),²⁸ nitroxide mediated radical polymerization (NMRP)²⁹ and so on. However, a large gap still exists between reactions on a laboratory scale and synthesis at the scale of pilot plants. Along with innovations in synthetic polymer chemistry, this chapter summarizes recent advances in thermoplastic elastomers based on synthetic polymers from the aspect of polymer architectures including: (1) ABA type triblock polymers, (2) grafted polymers and (3) star branched polymers. Service temperature, tensile properties of stress and strain at break will be summarized for different composition

and architectures. The difference between TPE research in academia and industry will be addressed as the perspective.

1.2 ABA triblock copolymer type TPEs:

1.2.1 Polymers prepared by anionic polymerization:

The most common ABA triblock copolymers type TPEs are polystyrene-*b*-polyisoprene-*b*-polystyrene (SIS) and polystyrene-*b*-polybutadiene-*b*-polystyrene (SBS) triblock copolymers. Three things need to be taken into consideration when designing the composition of SIS type triblock copolymers for TPEs applications: (1) Under the designed composition, PI needs to form a continuous rubbery matrix to provide enough elasticity. (2) Overall molecular weight needs to be high enough to drive micro-phase separation for efficient stress reinforcement. (3) Molecular weight should also not be too high considering that high viscosity may cause difficulty in processing and achieving ordered phase separation in the melt.³⁰

In a typical SIS TPE, the molecular weight (M_n) of PS is generally targeted at 10 to 15 kg/mol whereas the M_n of PI is targeted at 50 to 70 kg/mol.³¹ Due to the thermodynamic incompatibility between PS and PI, the minor component PS will micro-phase separate from PI, forming either spherical (less than 20 vol% PS) or cylindrical (20 vol% to 35 vol% of PS) glassy domains, which act as physical crosslinks and reinforce the entangled PI

rubbery matrix (**Figure 1.2**). In a dynamic mechanical analysis of SIS with temperature ramp/frequency sweep, SIS behaves like a glassy plastic with a high storage modulus (G') when the temperature is below the glass transition temperature of PI ($T_g \sim -56^\circ\text{C}$). As the temperature increases but remains lower than the T_g of PS (95°C), the polyisoprene chains start to move and G' reaches the rubbery plateau value. This temperature range is considered as the service temperature range where such polymers act as elastomer with typical stress-strain behavior. When the temperature is above 95°C , the polymer enters the melt flow zone and behaves as a viscous liquid. Most TPEs are processed by melt extrusion or injection molding with processing temperature higher than T_g or melting temperature (T_m) where elastic and glassy domains are miscible and the system is in one phase.

As many applications benefit from low cost S-TPEs, high temperature applications and other advanced consumptions of S-TPEs, such as in tire rubber, are largely limited by the relative low glass transition temperature of PS. When the service conditions approach 95°C , softening of PS domains dramatically reduces the tensile stress of S-TPEs. One major research interest in the field of anionic polymerization is to increase the upper service temperature of S-TPEs without changing the polymerization procedure, which has already existed in pilot plants for almost 50 years.¹⁴

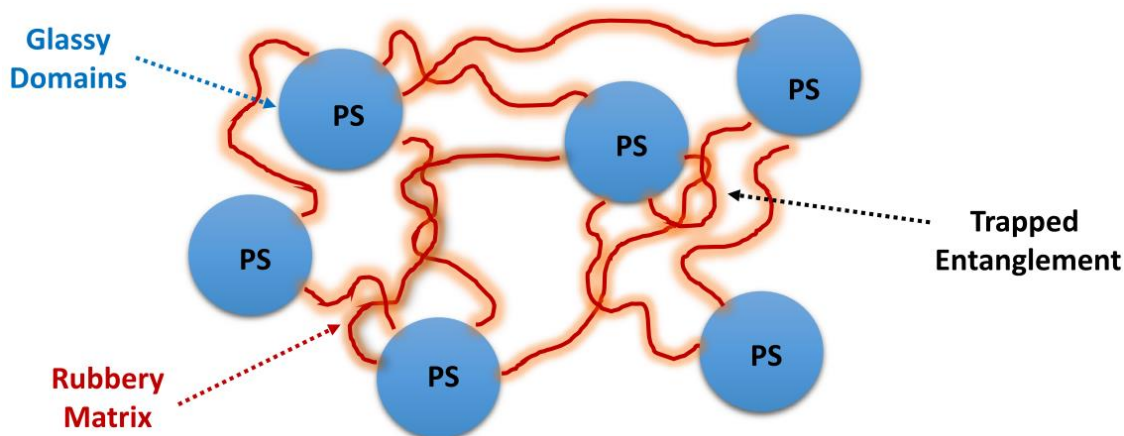


Figure 1.2: Schematic of SIS TPEs.

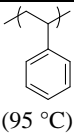
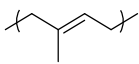
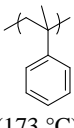
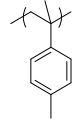
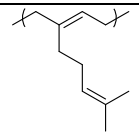
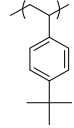
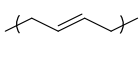
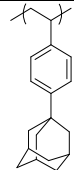
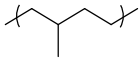
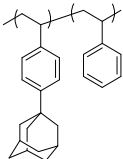
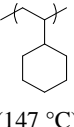
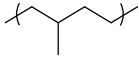
Many strategies and alternative monomers have been explored by using anionic polymerization in order to improve the upper service temperature (UST) of TPEs. The first strategy was to use *styrene derivatives* with functionalities at α - or *para*- position such as poly(α -methyl styrene) ($T_g \sim 173$ °C),³² poly(α -methyl *p*-methyl styrene) ($T_g \sim 183$ °C),³³ poly(*tert*-butyl styrene) (PtBS, $T_g \sim 130$ °C)³⁴ and poly(*p*-adamantyl styrene) (P-AdmS, $T_g \sim 203$ °C).^{35,36} In order to achieve quantitative yield, anionic polymerization of α -methyl styrene generally requires low polymerization temperature (-78 °C) in polar solvent (THF) due to the low monomer ceiling temperature caused by the bulky methyl group at the α position.³² High T_g polystyrene derivatives with bulky pendent groups such as *tert*-butyl or adamantyl, at the *para* position will cause phase blending with polydienes due to the lipophilic nature of the *tert*-butyl or adamantyl group. In order to increase the strength of phase separation and generate effective physical crosslinking, high overall molecular

weight is required for polybutadiene/poly(tert-butyl styrene) (PtBS, $T_g \sim 130$ °C) systems³⁴. Another approach to increase stress was through catalytic hydrogenation of polydienes into polyolefin, which was used in designing TPEs based on polyisoprene and poly(padamantyl styrene).³⁶ Catalytic hydrogenation to fully saturate PS, forming poly(vinylcyclohexane) (PVCH, $T_g \sim 147$ °C), produced TPEs with higher UST and better thermal stabilities.^{37,38} Mechanical properties and service temperatures of all the above mentioned TPEs are summarized in **Table 1.1**, no 1-5.

A second anionic polymerization strategy to improve UST was to use methyl methacrylate and its derivatives as the hard segment with polybutadienes (PB) or poly(n-butyl acrylate) (PnBA) as the soft segment.

Since the glass transition temperature of poly(alkyl methacrylate) depends both on tacticity and size of alkyl substituents,^{39,40} incorporating methacrylate derivatives with different tacticities as the hard segment in ABA type triblock copolymers could tune the service condition over a large temperature range.⁴¹ When using polydienes as the elastic matrix, methacrylate derivatives were initiated in THF at -78 °C through a difunctional polydiene anion, which was synthesized in a hydrocarbon solvent since anionic polymerization of butadiene or isoprene in polar solvents forms less cis-1,4 microstructure, and thus dramatically increased the T_g .^{42,43} Methyl methacrylate

Table 1.1: Mechanical properties of ABA triblock copolymer type TPEs prepared by anionic polymerization in hydrogenation solvent

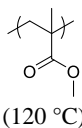
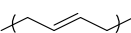
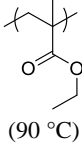
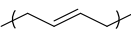
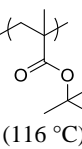
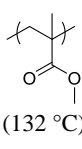
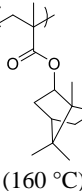
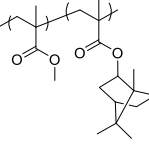
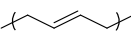
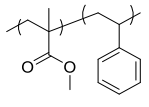
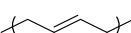
No	Hard Segment (T_g , °C)	Soft Segment (T_g , °C)	Mechanical Properties			Synthetic Methods	Ref
			Stress / MPa	Strain / %	wt %		
1	 (95 °C)	 (-64 °C)	25.5MPa	1200%	33%	Anionic PLZ (THF, -78 °C)	32
	 (173 °C)		44.6MPa	1100%	33%		
2	 (182 °C)	 (-39 °C)	0.5 to 10.8 MPa	525% to 1340%		Anionic PLZ (THF, -78 °C) Coupling Reaction	33
3	 (130 °C)	 (-90 °C)	24.6 MPa	1080%	50%	Anionic PLZ (benzene, r.t.)	34
4	 (180 °C)	 (-60 °C)	22.3 MPa	590%	45%	Anionic PLZ (CHx, 40 °C) Catalytic Hydrogenation	35
	 Ran. Copolymer (150 °C)		23.9 MPa	660%	25%		
5	 (147 °C)	 (-60 °C)	28 MPa	652%	39.5 %	Anionic PLZ (CHx, 40 °C) Catalytic Hydrogenation	38

polymerized by this method contains 75 to 79 % of syndiotactic repeating units and has a glass transition temperature higher than 120 °C³⁹ (**Table 1.2**, no. 6).

Other methacrylate derivatives, such as poly(ethyl methacrylate) (PEMA, $T_g \sim 90^\circ\text{C}$), poly(tert-butyl methacrylate) (PtBMA, $T_g \sim 116^\circ\text{C}$) and poly(isobornyl methacrylate) (PIBMA, $T_g \sim 202^\circ\text{C}$), also could be anionic polymerized by similar methods⁴⁰. Resulting triblock copolymers with polybutadiene as the rubbery matrix displayed high ultimate stress at break and strain at break over 500 %. Notice that when PIBMA was used as the rigid block, triblock copolymers exhibited 600 % strain at break with ultimate tensile stress of 2.2 MPa even when the temperature was 150 °C.⁴¹ Tuning UST from 130 °C to 149 °C was possible by randomly copolymerizing IBMA with MMA with different feed ratios.⁴⁴ UST of styrenic TPEs were enhanced by incorporating MMA as the minor component (13 wt%) in linear PMMA-PS-PB-PS-PMMA pentablock terpolymers TPEs (32 MPa ultimate stress, 900 % strain at break)^{45,46} (**Table 1.2**, no. 7-9).

The above mentioned TPEs systems contained polybutadiene as the elastic block. In all acrylic TPEs where poly(alkyl acrylate) was used as the soft block, TPEs have better UV and oxidation resistance due to the lack of unsaturation.⁴⁷⁻⁵⁵ A typical all acrylic TPE, PMMA-PnBA-PMMA triblock copolymers, was prepared by transesterification of PMMA-poly(tert-butyl acrylate)-PMMA precursor which was synthesized by sequential anionic polymerization of MMA, tert-butyl acrylate and MMA in THF at -78°C .^{47,48} By keeping

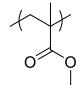
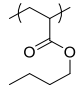
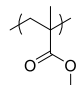
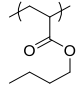
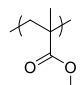
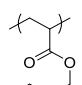
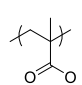
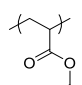
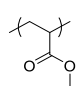
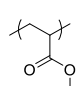
Table 1.2: Mechanical properties of ABA triblock copolymer type TPEs prepared by anionic polymerization in polar solvent

No	Hard Segment (T_g , °C)	Soft Segment (T_g , °C)	Mechanical Properties			Synthetic Methods	Ref
			Stress / MPa	Strain / %	wt %		
6	 (120 °C)	 (-62 °C)	34.0 MPa	890%	36%	Anionic PLZ (CHx/ether, 25 °C) Anionic PLZ (CHx/THF, -78 °C)	39, 42
7	 (90 °C)	 (-60 °C)	18.7 MPa	1120%	35%	Anionic PLZ (CHx/ether, 25 °C) Anionic PLZ (CHx/THF, -78 °C)	40, 41
	 (116 °C)		24.4 MPa	1080%	29%		
	 (132 °C)		32.0 MPa	835%	38%		
	 (160 °C)		35.0 MPa	650%	42%		
8	 Ran. Copolymer (130 - 149 °C)	 (-58 °C)	24.0 MPa	1000%	34%	Anionic PLZ (CHx/ether, 25 °C) Anionic PLZ (CHx/THF, -78 °C)	44
			27.0 MPa	1000%	31%		
			30.0 MPa	1100%	24%		
9	 Block Copolymer (118 °C)	 (-60 °C)	32.0 MPa	900%	13% (PMMA) 25% (PS)	Anionic PLZ (CHx/ether, 25 °C) Anionic PLZ (CHx/THF, -78 °C)	45, 46

the molecular weight of PnBA at 100 kg/mol and varying the weight percentage of PMMA from 9.1 % to 50 %, the ultimate tensile strength was increased from 1.8 MPa to 16.1 MPa where the elongation at break decreased from 1016 % to 228 %.⁴⁸ (**Table 1.3**, no. 10) Difunctional atom transfer radical polymerization (ATRP) initiator was employed to prepare PMMA-PnBA-PMMA triblock copolymers without transalcoholysis.⁴⁹ Tong compared mechanical properties of two different PMMA-PnBA-PMMA triblock copolymers synthesized by anionic polymerization and ATRP with similar molecular weight and composition. The sample prepared by anionic polymerization showed much higher initial stress, modulus with ultimate stress of 8.6 MPa and strain at break of 700 %. The sample prepared by ATRP, however, broke at 400 % of strain with ultimate stress of 4.1 MPa⁵⁰ (**Table 1.3**, no. 11). The reason will be discussed later in **section 1.2.4**.

The mechanical properties of all acrylic TPEs are generally inferior to styrenic TPEs due to phase blending and high entanglement molecular weight (M_e) of poly(alkyl acrylate) (M_e for PB is 1,700 g/mol whereas M_e for PnBA is 28,000 g/mol).⁵¹ Longer alkyl substitution enhanced the strength of phase separation with PMMA but also increased the M_e and decreased strain at break. The glass transition temperature decreased as the length of alkyl substitution increased.^{52,53} By using different alcohols during transalcoholysis, all acrylic TPEs with poly(ethyl acrylate), poly(n-propyl acrylate) and poly(isooctyl acrylate) as the elastic middle block were synthesized.⁵⁴ With similar composition (22 wt% of

Table 1.3: Mechanical properties of ABA triblock copolymer type TPEs – all acrylic polymers

No.	Hard Segment (T_g , °C)	Soft Segment (T_g , °C)	Mechanical Properties			Synthetic Methods	Ref.
			Stress / MPa	Strain / %	wt %		
10			1.8 MPa	1016%	9.1%	Anionic PLZ (THF, -78 °C) Transalcoholysis (PTSA, 150 °C)	48
			14.7 MPa	610%	28.6%		
			16.1 MPa	228%	50.0%		
11			8.6MPa	700%	24.2%	Anionic PLZ (THF, -78 °C) Transalcoholysis (PTSA, 150 °C)	50
							
12			7.1MPa	480%	22.2%	Anionic PLZ (THF, -78 °C) Transalcoholysis (PTSA, 150 °C)	54,55
			15.2MPa	680%	21.1%		
			16.4MPa	390%	22.8%		

PMMA) and overall molecular weight, all acrylic TPEs with poly(isooctyl acrylate) as the middle block showed the highest ultimate stress (16.2 MPa) but lowest strain at break (390 %) compared to TPEs with other middle blocks.⁵⁵ (**Table 1.3**, no. 12)

A third anionic polymerization strategy to improve UST is to use *rigid conjugated diene monomers* such as 1,3-cyclohexadiene (CHD) as the glassy block. One feature of anionic polymerization of conjugated dienes is that the microstructure of the resulting polymer varies with different initiation systems. 1,3-cyclohexadiene demonstrated controlled anionic polymerization behavior with three different initiation systems: n-BuLi/tetramethylethylenediamine (TMEDA), n-BuLi/1,2-dimethoxyethane (DME), or sec-BuLi/1,4-diazabicyclo[2.2.2]-octane (DABCO).^{56,57} Resulting poly(1,3-cyclohexadiene) (PCHD) has 55 %, 75 % and 90 % of 1,4-addition respectively. T_g of these polymers decreased from 155°C to 110 °C as the percentage of 1,2-microstructure was decreased. PCHD-PB-PCHD⁵⁸ triblock copolymer with 30 wt% of PCHD exhibited 10.2 MPa ultimate stress with a relatively low strain at break of 290 %. This might be due to side reactions during anionic polymerization of CHD. By partial hydrogenation of PB without saturated PCHD, ultimate stress increased to 14.0 MPa with better strain at break of 570 %, which indicated a stronger physical crosslinking. The end block PCHD of this triblock copolymer was completely hydrogenated into polycyclohexane, a polyolefin with

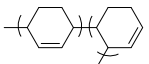
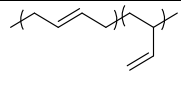
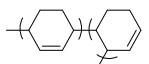
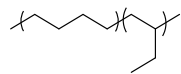
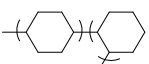
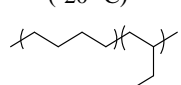
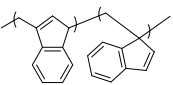
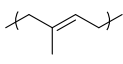
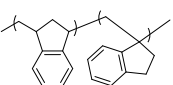
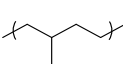
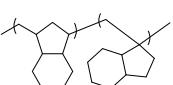
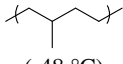
T_g above 231°C.⁵⁹ The completely hydrogenated triblock copolymers displayed 10.0 MPa tensile stress at 600 % strain without breaking. (**Table 1.4**, no. 13)

1.2.2 Polymers prepared by cationic polymerization:

The late 1960s witnessed the rapid development of styrenic thermoplastic elastomers from research in laboratories to commercial products. S-TPEs suffered from two major disadvantages: (1) The upper service temperature limited many advanced applications of S-TPEs. (2) Polydiene middle block's lack of tolerance to strong UV and oxidation. Hydrogenation to saturate polydienes improves the resistance of S-TPEs to UV. However, tertiary protons introduced after hydrogenation lacked stability to strong oxidation reagents.⁶⁴

A renaissance in living cationic polymerization²⁵ advanced many research towards TPEs with better UV/oxidation stability and higher UST. Many cationically synthesized TPEs used polyisobutylene (PIB) as the elastic middle block due to its softness and chemical resistance. Triblock copolymer PS-PIB-PS prepared by sequential living cationic polymerization through a difunctional initiator displayed an ultimate tensile stress of 26 MPa, which was competitive with commercial Kraton SIS TPEs.^{65,66} The molecular weight of PIB should targeted between 40,000 to 160,000 g/mol in order to promote tensile properties. Phase separation was observed between PS and PIB when the M_n of PS was

Table 1.4: Mechanical properties of ABA triblock copolymer type TPEs based on hydrogenated polymers

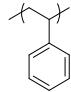
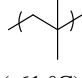
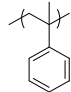
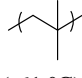
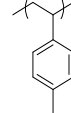
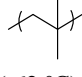
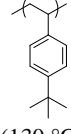
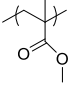
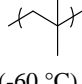
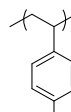
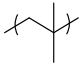
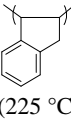
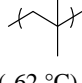
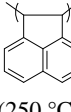
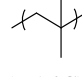
No	Hard Segment (T_g , °C)	Soft Segment (T_g , °C)	Mechanical Properties			Synthetic Methods	Ref.
			Stress / MPa	Strain / %	wt %		
13	 (140 °C)	 (-60 °C)	10.2 MPa	290%	30%	Anionic PLZ (CHx, 40 °C) Catalytic Hydrogenation	58
	 (140 °C)	 (-20 °C)	14.0MPa	570%	30%		
	 (200 °C)	 (-20 °C)	10.8MPa>	600%>	30%		
14	 (145 °C)	 (-56 °C)	14.3 MPa	1390%	20%	Anionic PLZ (benzene, r.t.) Catalytic Hydrogenation	62, 63
	 (125 °C)	 (-48 °C)	11.2 MPa	750%	20%		
	 (135 °C)	 (-48 °C)	16.8 MPa>	510%>	20%		

above 5000 g/mol. Other triblock copolymers with PIB as the elastic middle block and glassy end block of polystyrene derivatives, such as poly(α -methyl styrene),^{67,68,69,70} poly(*p*-methyl styrene)⁷¹ and poly(*tert*-butyl styrene),⁶⁹ were also synthesized by living cationic polymerization. PMMA-PIB-PMMA triblock copolymer was prepared by a cationic/anionic mechanism switching process.⁷² All these triblock copolymers demonstrated similar stress-strain behavior compared to TPEs developed by anionic polymerization with polydienes as the rubbery matrix. (**Table 1.5**, no. 15-18)

One feature that distinguishes cationic polymerization from anionic polymerization is the ability to control the polymerization of high T_g monomers such as *p*-chlorostyrene (*p*CS),⁷¹ indene (ID)^{69,73} and acenaphthylene (ACP).⁷⁴ Triblock copolymers using P*p*CS (T_g , 129 °C), PID (T_g , 225 °C) or PACP (T_g , 250 °C) as the hard segment and PIB as the soft segment were successfully prepared by cationic polymerization and showed stress-strain behavior similar to typical TPEs. Notice that P*p*CS is a polar polymer with weather and flame resistance. Indene is potentially a very cost effective monomer for high temperature applications. (**Table 1.5**, no. 19-21)

Alkyl vinyl ethers are another unique group of monomers polymerized by living cationic polymerization. Hydrolysis of cationically synthesized poly(*tert*-butyl vinyl ether) (PtBVE) produced well defined poly(vinyl alcohol) (PVA).⁷⁵ As a widely used water

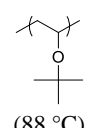
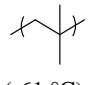
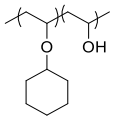
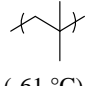
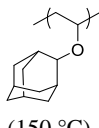
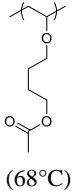
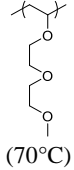
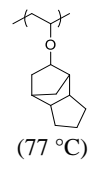
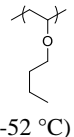
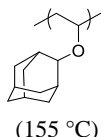
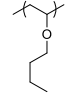
Table 1.5: Mechanical properties of ABA triblock copolymer type TPEs synthesized by cationic polymerization

No.	Hard Segment (T_g , °C)	Soft Segment (T_g , °C)	Mechanical Properties			Synthetic Methods	Ref.
			Stress / MPa	Strain / %	wt %		
15	 (89 °C)	 (-61 °C)	26MPa	760%	25.1%	Cationic PLZ (CH ₃ Cl/MCH _x , -80 °C)	65
16	 (180°C)	 (-61 °C)	24.5MPa	370%	44.7%	Cationic PLZ (CH ₃ Cl/MCH _x , -80 °C)	70
			11.5MPa	830%	22%		
17	 (110 °C)	 (-62 °C)	15.1MPa	560%	32%	Cationic PLZ (CH ₃ Cl/MCH _x , -80 °C)	71
	 (130 °C)		18.1MPa	400%	50%		
18	 (108 °C)	 (-60 °C)	14.5MPa	650%	34%	Cationic PLZ (CH ₃ Cl/MCH _x , -80 °C) Anionic PLZ (CH _x , 40 °C)	72
19	 (123 °C)	 (-61 °C)	21MPa	460%	38%	Cationic PLZ (CH ₃ Cl/MCH _x , -80 °C)	71
			10MPa	1200%	30%		
20	 (225 °C)	 (-62 °C)	15.7MPa	600%	20.5%	Cationic PLZ (CH ₃ Cl/MCH _x , -80 °C)	73
			20.5MPa	400%	40%		
21	 (250 °C)	 (-61 °C)	14.7MPa	793%	13%	Cationic PLZ (CH ₃ Cl/MCH _x , -80 °C)	74

soluble polymer in coating and textiles, semicrystalline PVA has a T_g of 80 °C and T_m of 208 °C which makes it a candidate for TPEs with oil resistance. PVA-PIB-PVA triblock copolymer could be prepared by direct hydrolysis of PtBVE-PIB-PtBVE. However, mechanical properties were not measured since the resulting polymers had very limited solubility and were largely degraded by thermal processing. Cyclohexyl vinyl ether (CHVE) could be statistically copolymerized with tert-butyl vinyl ether by living cationic polymerization initiated from difunctional polyisobutylene living cation. Hydrolysis of the resulting triblock copolymers yielded P(CHVE-stat-VA)-PIB-P(CHVE-stat-VA)⁷⁶ containing statistical copolymer of PCHVE and PVA as the rigid phase. With 22 wt% of P(CHVE-stat-VA), polymers broke at 830 % strain with ultimate stress of 11.5 MPa. (Table 1.6, no. 22-23)

Similar to poly(alkyl acrylate), the T_g of poly(alkyl vinyl ether) could also be tuned with alkyl substituents of different lengths.⁷⁷ With poly(n-butyl vinyl ether) (PnBVE, T_g , ~ -55 °C) as the elastic block, ABA-type triblock copolymer with (PTCVE, T_g ~ 77 °C),⁷⁷ poly(tricyclodecyl vinyl ether)⁷⁸ and poly(2-adamantyl vinyl ether) (PADVE, T_g ~ 155 °C) as glassy blocks were synthesized by living cationic polymerization.⁷⁹ Despite the similarity of monomer structures, microphase separation was observed by transmission electron microscopy (TEM). All of these vinyl ether TPEs showed relatively low strain at break (<355 %) and ultimate stress (<5.55 MPa), possibly because of high entanglement

Table 1.6: Mechanical properties of ABA triblock copolymer type TPEs – all vinyl ether polymers

No.	Hard Segment (T_g , °C)	Soft Segment (T_g , °C)	Mechanical Properties			Synthetic Methods	Ref.
			Stress / MPa	Strain / %	wt %		
22	 (88 °C)	 (-61 °C)	15.11MPa	800%	31%	Cationic PLZ (CH ₃ Cl/MCHx, -80 °C)	75
			9.16MPa	1300%	22%		
23	 (88 °C)	 (-61 °C)	24.5MPa	370%	44.7%	Cationic PLZ (CH ₃ Cl/MCHx, -80 °C) Hydrolysis	76
			11.5MPa	830%	22%		
24	 (150 °C)	 (68 °C)	1.35MPa	116%	30.7%	Cationic PLZ (Toluene, 0 °C)	77
		 (70 °C)	0.74MPa	92%	27.6%		
25	 (77 °C)	 (-52 °C)	2.4MPa	90%	24.4%	Cationic PLZ (Toluene, 0 °C)	78
26	 (155 °C)	 (-52 °C)	5.55MPa	245%	30%	Cationic PLZ (Toluene, 0 °C)	79
			1.52MPa	355%	17.2%		

molecular weight of PnBVE. All vinyl ether triblock copolymers with poly(6-acetoxyhexyl vinyl ether) and poly (2-(2-methoxyethoxy)ethyl vinyl ether) as elastic blocks showed excellent CO₂ separation ability with modest mechanical properties (**Figure 1.3**).⁷⁷ (**Table 1.6**, no. 24-26)

1.2.3 Polymers prepared by metal catalyzed ring opening polymerization:

Poly(lactide) (PLA, $T_g \sim 60^\circ\text{C}$) is an amorphous biodegradable polymer synthesized by metal catalyzed ring opening polymerization (ROP) from racemic D,L-lactide whereas isotactic poly(L-lactide) (PLLA) and poly(D-lactide) (PDLA) are semicrystalline polymers ($T_m \sim 170^\circ\text{C}$). Blends of PLLA and PDLA can form stereocomplex crystals which further improves chemical resistance with higher melting temperature ($T_m \sim 203^\circ\text{C}$).⁸⁰

In the early research stage about incorporating PLA as the end block for ABA triblock copolymers for TPE applications, difunctional hydroxyl terminated PI,⁸¹ PIB,⁸² polydimethylsiloxane (PDMS)⁸³ and poly(ethylene-co-propylene)⁸⁴ were used as the initiators. These elastic middle block were prepared by either living anionic or cationic polymerization followed by termination with hydroxyl functionality. TPEs based on these systems received limited success with relative low stress and strain at break (**Table 1.7**, no. 27-30).

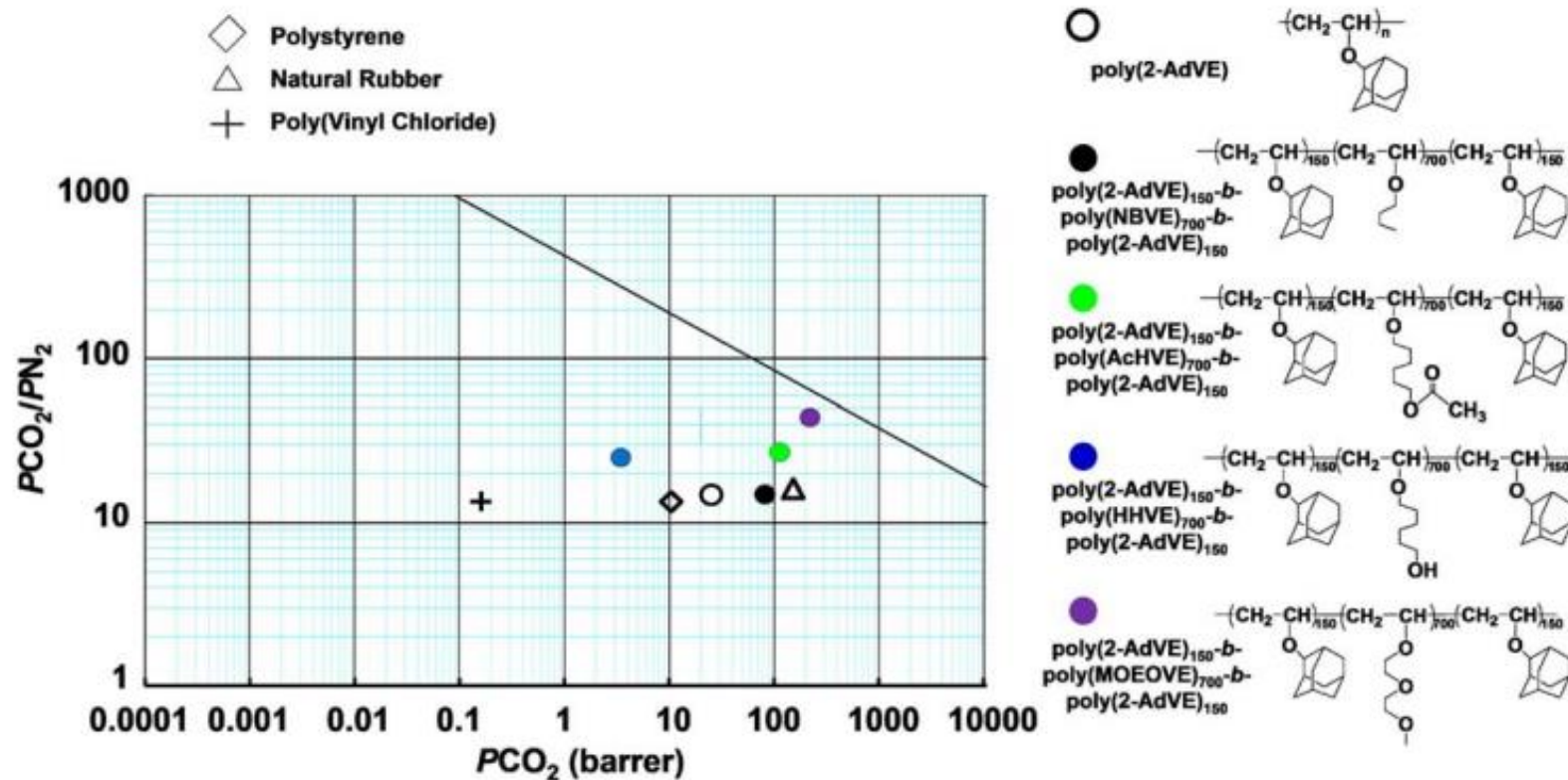
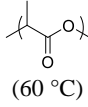
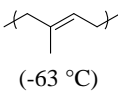
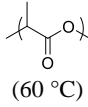
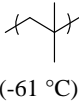
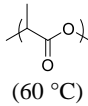
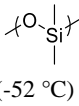
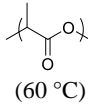
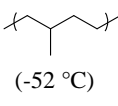


Figure 1.3: CO₂ separation plots for poly(6-acetoxihexyl vinyl ether) and poly (2-(2-methoxyethoxy)ethyl vinyl ether) based triblock copolymers together with commodity polymers [polystyrene, natural rubber, and poly(vinyl chloride)] for comparison.⁷

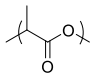
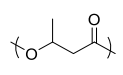
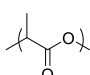
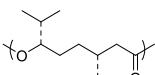
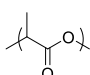
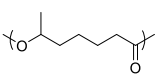
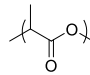
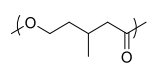
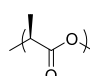
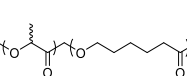
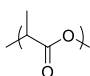
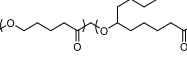
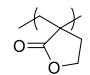
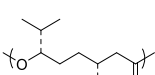
Table 1.7: Mechanical properties of ABA triblock copolymer type TPEs synthesized by ring opening polymerization with PLA as the glassy segment.

No.	Hard Segment (T_g , °C)	Soft Segment (T_g , °C)	Mechanical Properties			Synthetic Methods	Ref.
			Stress / MPa	Strain / %	wt %		
27	 (60 °C)	 (-63 °C)	3.1 MPa	200%	18 vol%	Anionic PLZ (Toluene, 25 °C) Metal Catalyzed ROP (Toluene, 125 °C)	81
			9.2 MPa	650%	28 vol%		
			10.1 MPa	450%	40 vol%		
28	 (60 °C)	 (-61 °C)	N/A	N/A	N/A	Cationic PLZ (CH ₃ Cl/MCH _x , -80 °C) ROP (THF)	82
29	 (60 °C)	 (-52 °C)	N/A	N/A	N/A	Metal Catalyzed ROP (Toluene, 125 °C)	83
30	 (60 °C)	 (-52 °C)	2.98MPa	215%	45%	Anionic PLZ	84
						Catlytic Hydrogenation Metal Catalyzed ROP (Toluene, 125 °C)	

Preparing polymers from renewable resource materials instead of from petroleum resources has been a lasting goal of chemists for many decades. Monomers including 3-hydroxybutyrate (HA), menthide (MD), 6-methyl- ϵ -caprolactone (MCL), ϵ -caprolactone (CL), β -methyl- δ -valerolactone (MCL), ϵ -decalactone (DL) potentially could be produced from sustainable resources.⁸⁵ These monomers undergo metal catalyzed ring opening polymerization (ROP), yielding biodegradable elastic polymers.^{86,87} Since ROP generated polymers with hydroxyl functionality on both ends, the resulting polymers could be directly used as macroinitiators for lactide, producing various types of biodegradable ABA triblock copolymer TPEs. When poly(3-hydroxybutyrate) (PHA)⁸⁸ was used as elastic block, TPEs had strain at break lower than 200 %. Using polymenthide^{89,90} (PM) as elastic block, the strain at break could be largely improved to 960 % compared to PHA system but ultimate stress was decreased to 1.7 MPa even with 40 vol% of PLA. This low tensile stress might be due to the overall molecular weight not being high enough for strong phase separation. With 30 vol% of poly(6-methyl- ϵ -caprolactone)⁹¹ (PMCL) as the elastic block, 1880 % strain at break was achieved with 10.2 MPa ultimate stress (**Table 1.8**, no. 31-33).

Very recently, Xiong⁹² developed an economically viable strategy to prepare β -methyl- δ -valerolactone (MCL) through an artificial biosynthetic approach (**Figure 1.4**). Ring opening polymerization of MCL generated elastic amorphous aliphatic polyester with T_g of -52 °C. Excellent tensile properties were obtained by utilizing PMCL as the elastic block with PLA as the hard segment. With 32 vol% of PLA, PLA- PMCL-PLA triblock

Table 1.8: Mechanical properties of ABA triblock copolymer type TPEs synthesized by ring opening polymerization with sustainable recourse

No	Hard Segment (T_g , °C)	Soft Segment (T_g , °C)	Mechanical Properties			Synthetic Methods	Ref
			Stress / MPa	Strain / %	wt %		
31	 (50 ~ 80 °C)	 (-2 °C)	10MPa	200%	44%	Metal Catalyzed ROP (Toluene, 100 °C)	88
32	 (44 °C)	 (-26 °C)	1.7MPa	960%	40.7%	Metal Catalyzed ROP (Toluene, 100 °C)	89
33	 (45 °C)	 (-43 °C)	10.2MPa	1880%	30%	Metal Catalyzed ROP (Toluene, 110 °C)	91
			14.2MPa	1360%	34%		
34	 (45 °C)	 (-52 °C)	25MPa	1725%	32vol %	Metal Catalyzed ROP (Toluene, 110 °C)	92
35	 (T_m , 152 °C)	 (-30°C)	17MPa	2800%	20%	Metal Catalyzed ROP (Toluene, 110 °C)	93
			21MPa	1900%	33%		
36	 (45 °C)	 (-63 °C)	9.9MPa	2100%	17vol %	Metal Catalyzed ROP (Toluene, 110 °C)	94
			13.5MPa	1690%	21vol %		
			18MPa	1200%	32vol %		
37	 (170 ~190 °C)	 (-21 °C)	4.1MPa	1600%>	6vol %	Metal Catalyzed ROP (Toluene, 135 °C)	97
			10.6MPa	800%	15vol %		
			13.0MPa	730%	20vol %	ATRP (DMF, 65 °C)	

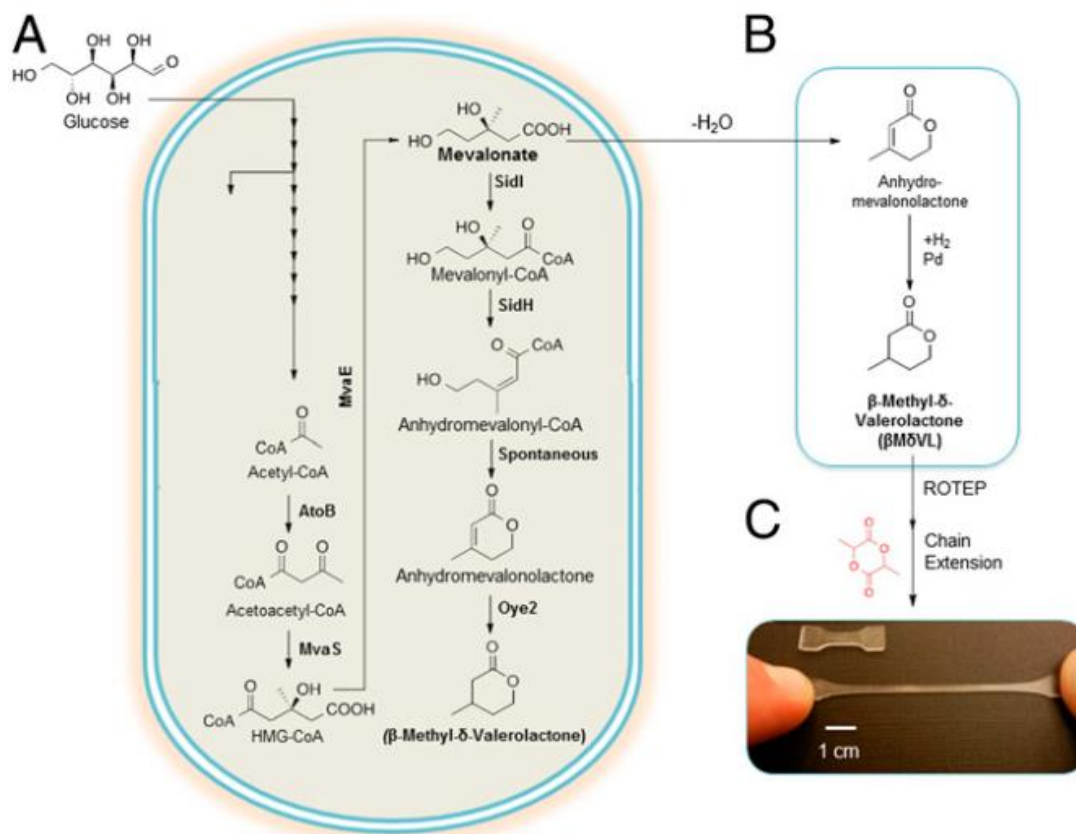


Figure 1.4: (a) Total biosynthetic pathway for the production of MVL. (b) A semisynthetic route to produce MVL from mevalonate. (c) Conversion of MVL to an elastomeric triblock polymer that can be repeatedly stretched to 18 times its original length without breaking.⁹²

PMCL-PLA triblock copolymer displayed 1725 % strain at break with ultimate stress of 25 MPa, which is competitive with commercial Kraton polymer based on petroleum resources (**Table 1.8**, no. 34).

As a low T_g semicrystalline polymer, poly(ϵ -caprolactone) (PCL, $T_g \sim -60$ °C, $T_m \sim 60$ °C) is a biodegradable material with great potential for medical applications. Copolymerizing ϵ -caprolactone with ϵ -decalactone or lactide created amorphous elastic polymers suitable for TPE applications.^{93,94} Statistical copolymer constructed from ϵ -caprolactone and D-lactide had a T_g of -30 °C. With 20 wt% of isotactic poly(L-lactide) (PLLA) as the glassy block, triblock copolymers showed exceptionally high strain at break of 2800 % and decent ultimate stress of 17 MPa.⁹³ By varying volume fraction of the hard segment PLA from 17 % to 32 %, TPEs based on random copolymer of ϵ -caprolactone / ϵ -decalactone as soft segment demonstrated tunable ultimate stress from 9.9 MPa to 18 MPa with strain at break from 1200 % to 2100 %⁹⁴ (**Table 1.8**, no. 35-36).

Incorporating biodegradable PLA ($T_g \sim 60$ °C) enabled TPEs for many biomedical applications. However, high temperature applications are largely limited due to the low T_g of PLA. Poly(α -methylene- γ -butyrolactone) (PMBL) is a rigid thermoplastic⁹⁵ with a T_g of about 195 °C. The renewable monomer MBL was derived from tulipalin A and subjected to radical polymerization⁹⁶. After converting di-hydroxyl terminated poly(menthene) into difunctional atomic transfer radical polymerization initiator, PMBL-PM-PMBL⁹⁷ triblock type TPEs for high temperature application were prepared. Ultimate tensile stress ranging

from 3.9 MPa to 13 MPa and strain at break ranging from 730 % to 1800 % were achieved based on different volume fractions of PMBL (**Table 1.8**, no. 37).

1.2.4 Polymers prepared by controlled radical polymerization techniques:

Starting from the late 1990s, tremendous progress has been achieved in the field of controlled radical polymerization such as atomic transfer radical polymerization (ATRP), reversible addition-fragmentation chain-transfer polymerization (RAFT) and nitroxide mediated radical polymerization (NMRP).⁹⁸ These techniques open up various opportunities to prepare functionalized polymers with predictable molecular weight, narrow molecular weight distribution and complicated macromolecular architectures.⁹⁹ Controlled polymerization was achieved for many monomers such as acrylonitrile,¹⁰⁰ acrylamide¹⁰¹ and vinyl amide,¹⁰² which cannot be controllably polymerized by anionic or cationic mechanisms.

Many block, star, grafted and brush polymers with different functionalities have been prepared by ATRP.¹⁰³ However, ABA type block copolymers synthesized by ATRP have received limited success for TPE applications mainly due to two reasons: (1) broad distribution of hard block reduces the strength of phase separation, (2) unavoidable diblock copolymer mixture in triblock copolymers acted as plasticizer diminishing the phase boundary.^{39,48} Significantly lower tensile stress and strain were observed for PMMA-PnBA-PMMA triblock copolymers prepared by ATRP compared with triblock copolymers

prepared by anionic polymerization followed by tansalcoholysis.⁴⁸ The copolymerization of methyl methacrylate with α -methylene- γ -butyrolactone as glassy block was necessary to improve tensile properties of triblock copolymers with poly(n-butyl acrylate) as elastic block.¹⁰⁴ However, the ultimate stress was still lower than 3.2 MPa with strain at break of 650 % (**Table 1.9**, no. 38).

Poly[2,5-bis[(n-hexogycarbonyl)]styrene] (PMPCS) is a mesogen-jacked liquid crystalline polymer with a T_g of about 120 °C. As a new type of rod-coil-rod TPE based on PMPCS and PnBA, tensile tests showed 1050 % strain at break with 3.2 MPa ultimate stress.¹⁰⁵ Different from PMPCS, poly2,5-bis[(n-hexogycarbonyl)]styrene (PHCS) is an amorphous polymer with a T_g of about -10 °C due to long chain alkyl substitution at the 2- and 5- positions of styrene. Poly(4-vinylpyridine) (P4VP) is a high T_g polymer that can complex with Zn^{2+} (**Figure 1.5**). Tuning stress-strain properties, glass transition temperature and morphology of TPEs based on P4VP-PHCS-P4VP was achieved by adding different amounts of $Zn(ClO_4)_2$ ¹⁰⁶ (**Table 1.9**, no. 39-40).

In order to minimize undesired chain transfer and termination reactions, controlled radical polymerization needs to maintain a very low radical concentration. This increases reaction time compared to conventional free radical and ionic polymerization.¹⁰⁷ Radical segregation effect introduced by (mini)emulsion polymerization in heterogeneous system, on the other hand, reduced the reaction time and suppressed radical termination.^{108,109} Combining emulsion polymerization with RAFT, PS-PnBA-PS triblock copolymers with

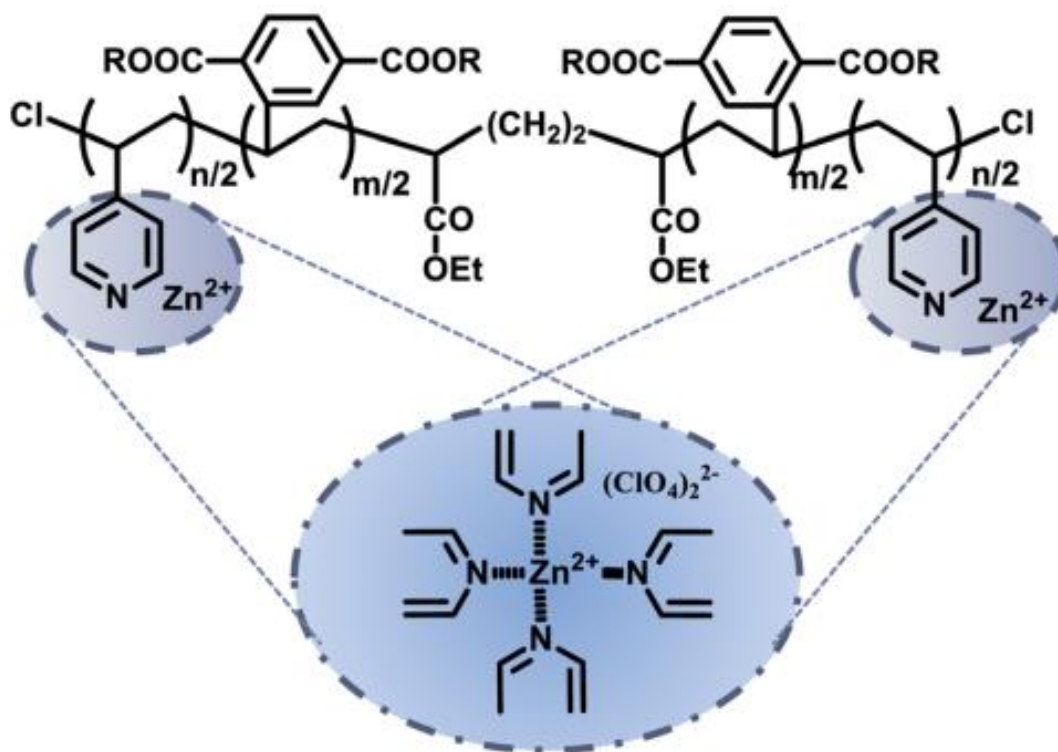
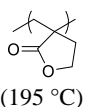
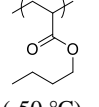
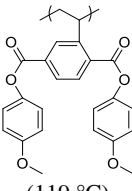
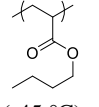
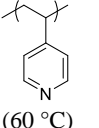
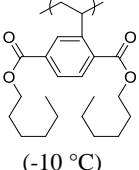


Figure 1.5: Illustration of a Zn²⁺/VHV hybrid via metal-ligand complexation.¹⁰⁵

Table 1.9: Mechanical properties of ABA triblock copolymer type TPEs synthesized by ATRP

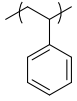
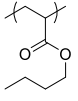
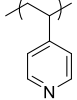
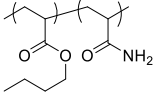
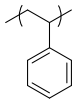
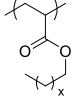
No.	Hard Segment (T_g , °C)	Soft Segment (T_g , °C)	Mechanical Properties			Synthetic Methods	Ref.
			Stress / MPa	Strain / %	wt %		
38	 (195 °C)	 (-50 °C)	0.5MPa	310%	13.8%	ATRP (DMF, 65°C)	104
39	 (119 °C)	 (-45 °C)	3.2MPa	1050%	37.58%	ATRP (Chlorobenzene, 65°C)	105
40	 (60 °C)	 (-10 °C)	6.6MPa	400%	17%	ATRP (Chlorobenzene, 65°C)	106

different molecular weight and composition were prepared in shorter reaction time.¹¹⁰ By varying weight percentage of PS from 20.2 % to 71.5 %, ultimate tensile strength was in the range from 3.0 MPa to 12.5 MPa and strain at break was in the range from 90 % to 1300 %. It was also found that by using a poly[styrene-alt-(maleic anhydride)] (PSM) as a macro-chain transfer agent in emulsion polymerization for PS-PnBA-PS¹¹¹, ultimate stress increased whereas strain at break decreased as the percentage of PSM increased. Another TPEs based on PS and poly(lauryl acrylate) were prepared by a solution of RAFT polymerization process.¹¹² Ultimate stress was lower than 1 MPa and strain at break was lower than 280 %. An interesting ABA triblock copolymer was prepared by RAFT polymerization based on P4VP as a hard segment and random copolymer of PnBA and poly(acrylamide) (PAM) as the elastic block. The PAM moiety in the middle block crosslinked the elastic domain through hydrogen bonding association.¹¹³ (**Table 1.10**, no. 41-43)

1.2.5 Polymers prepared by metathesis polymerization techniques:

Polyolefins represent almost two-thirds of global consumption of plastic and elastomer products. Ethylene and propylene are the two main feedstocks for polyolefins due to their low cost and availability. Linear polyethylene (PE), as well as isotactic and syndiotactic polypropylene (*i*-PP and *s*-PP) are semicrystalline polymers and could be employed as the hard segment for TPE applications. Atactic polypropylene (*a*-PP) and

Table 1.10: Mechanical properties of ABA triblock copolymer type TPEs synthesized by RAFT polymerization

No.	Hard Segment (T_g , °C)	Soft Segment (T_g , °C)	Mechanical Properties			Synthetic Methods	Ref.
			Stress / MPa	Strain / %	wt %		
41	 (95 °C)	 (-45 °C)	3.2MPa	1300%	20.2%	RAFT (H ₂ O, 70°C)	111
			7.0MPa	620%	36.1%		
			10.3MPa	520%	46.1%		
42	 (106 °C)	 (-23 °C)	3.2MPa	1050%	37.58%	ATRP (Chlorobenzene, 65°C)	113
43	 (60 °C)	 (-10 °C)	6.6MPa	400%	17%	ATRP (Chlorobenzene, 65°C)	112

poly(ethylene-co-propylene) (PEP) are amorphous soft polymers and suitable for TPE's elastic segment.¹¹⁴

In 1959, Natta already proposed a possible TPE structure based on *i*-PP as the hard segment and *a*-PP as the soft segment.¹¹⁵ After almost half a century, in 2006, two different groups reported two kinds of TPEs based on ethylene and/or propylene monomers synthesized by living coordination polymerization (LCP). Sita¹¹⁶ used a specifically designed zirconium/borate complex for programmable stereomodulated living Ziegler-Natta polymerization. Simply by adjusting the zirconium/borate ratio and disrupting propylene feeding during the polymerization, diblock, triblock and tetrablock copolymers of *a*-PP and *i*-PP were prepared with 40 wt% of *i*-PP.

Coates¹¹⁷ prepared a nickel catalyst that produced *i*-PP at -60 °C and *a*-PP at 0 °C. Simply by changing the reaction temperature, *i*-PP-*b*-*a*-PP-*b*-*i*-PP triblock and *i*-PP-*b*-*a*-PP-*b*-*i*-PP-*b*-*a*-PP-*b*-*i*-PP pentablock copolymers were prepared. The same group used titanium catalysts to prepare *s*-PP-*b*-PEP-*b*-*s*-PP triblock copolymers. The resulting triblock copolymer exhibited 80 MPa ultimate stress with 500 % strain at break. Very recently, Sita¹¹⁸ reported another triblock TPEs based on poly(1,3-methylenecyclohexane) (PMCH) and *a*-PP. Triblock copolymers of PMCH-*b*-*a*-PP-*b*-PMCH were prepared by LCP with hafnium catalysts (**Figure 1.6**). Interestingly, the rigid block PMCH was prepared by ring closing of 1,6-heptadiene, and the resulting polymer PMCH was micro-phase separated with *a*-PP (**Table 1.11**, no. 44-46).

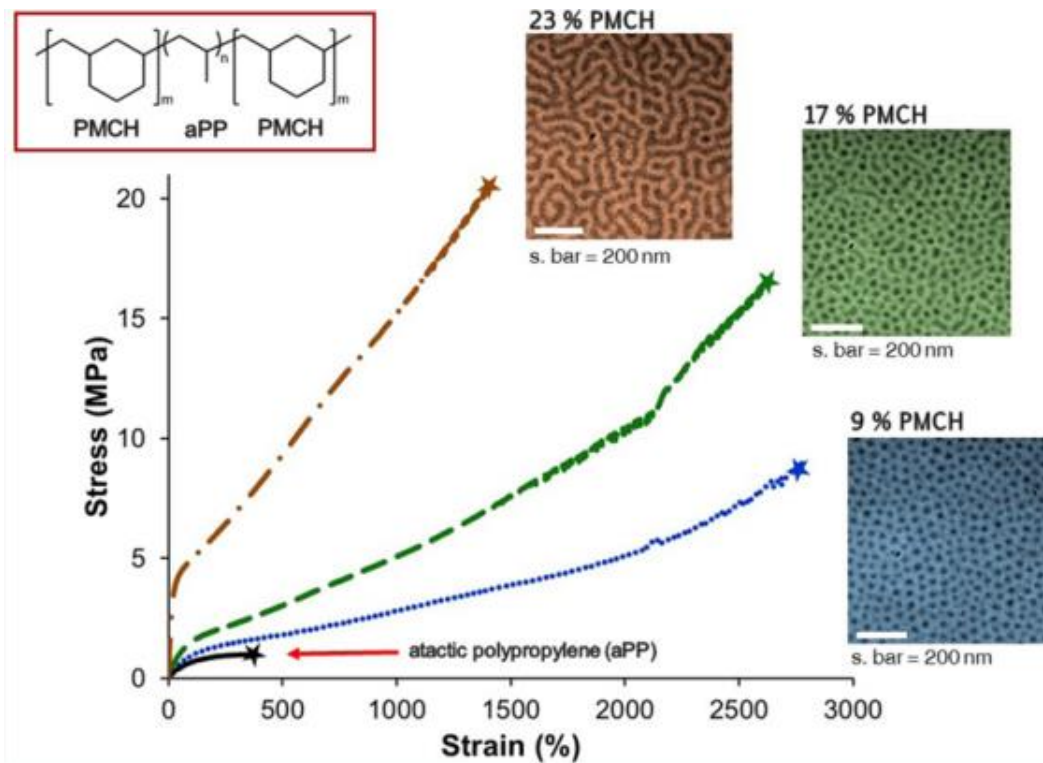
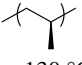
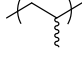
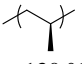
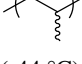
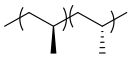
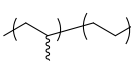
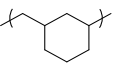
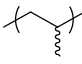


Figure 1.6: Triblock TPEs based on PMCH and a-PP.¹¹⁸

Table 1.11: Mechanical properties of ABA triblock copolymer type TPEs synthesized by coordination polymerization

No	Hard Segment (T _g , °C)	Soft Segment (T _g , °C)	Mechanical Properties			Synthetic Methods	Ref
			Stress / MPa	Strain / %	wt %		
44	 (T _m , 130 °C)	 (-45 °C)	18.5MPa	1227%	40%	LCP (Toluene, -10°C)	116
45	 (T _m , 130 °C)	 (-44 °C)	40MPa	1800%	24% (Triblock)	LCP (Toluene, 0°C/-60°C)	117
	 (T _m , 134 °C)	 (-57 °C)	240MPa	2250%	24% (Pentablock)		
46	 (60 °C)	 (-10 °C)	8.9MPa	2773%	9vol%	LCP (Toluene, 0°C/-60°C)	118
			16.4MPa	2631%	17vol%		
			20.3MPa	1390%	23vol%		

1.3 Star branched polymers for TPEs:

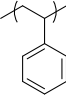
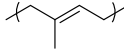
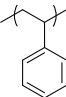
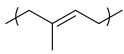
Star branched polymers are polymers with more than two arms radiating from the same core. If these arms have different chemical composition or molecular weight, the star polymer is named miktoarm (mixed-arm) star polymer. Generally, star polymers are prepared by two methods: (1) “Arm-first” where polymer arms are synthesized first and coupled onto a core decorated with appropriate reaction sites. (2) “Core first”, where polymer arms are grown from a multi-functional initiator.^{119,120}

When more than two PS-*b*-PI diblock copolymers are connected at the same core through the end of PI end blocks, with proper composition, such (PS-*b*-PI)_x star branched polymers displayed mechanical properties similar to SIS linear triblock TPEs. By using an arm-first divinylbenzene linking strategy, Fetters¹²¹ prepared polystyrene-polydiene star block copolymers with number of arms up to 29. They found these star polymers had superior tensile properties compared to linear triblock copolymers of similar composition. The enhancement of tensile strength saturated when the number of arms was more than six. Morphological analysis indicated for the same molecular weight, multi-arm star polymers had smaller PS domains size as compared with linear polymers¹²². Thus, star polymers had more condensed physical crosslinks per unit volume, which attributed to their higher tensile strength. Another reason for better tensile strength was that the core in star polymers acted as permanent crosslinks due to covalent chemical linkage. Besides better tensile stress of star polymers, the intrinsic viscosity of star polymers were lower than their linear

analogues. PS/PI and PS/PB diblock star copolymer TPEs are now commercially available under the trade name Kraton[®] (**Table 1.12**, no. 47).

Confirmed by both experiments¹²³ and theory¹²⁴, the morphological dependence of block copolymers could be decoupled from chemical composition by varying chain architecture. Progress in self-consistent field theory (SCFT)¹²⁵ facilitated the ability to design TPEs based on nonlinear architectures such as miktoarm star polymer with superior mechanical properties.¹²⁶ For SIS triblock copolymer, over 36 vol% of PS component leads to lamellar morphology which is unfavorable for TPE applications (**Figure 1.7**).¹²⁷ For A(BA[′])₄ miktoarm star polymer with one A block and 4 BA[′] block emanating from the same core, Fredrickson¹²⁶ predicted a stable morphology, of cylindrical A phase hexagonally dispersed in B matrix with volume fraction of A polymer up to 70 %. As for experiments, miktoarm star polymer S(IS[′])₃ with 50 vol% of PS achieved stable cylindrical morphology.¹²⁸ High volume fraction of PS enabled this new types of TPE with a higher modulus, strength toughness and recoverable elasticity. While SIS[′] with 50 vol% of PS yield at low elongation indicated its thermoplastic nature (**Table 1.12**, no. 48). By blending with PS homopolymers, a new stiff TPE (modulus was 99.2 MPa) with aperiodic “bricks and mortar” mesophase morphology was achieved with up to 82 wt% of PS.¹²⁹ Using similar miktoarm star polymer by blending with PS, Lynd created lamellar morphology with up to 97 wt% of PS.¹³⁰

Table 1.12: Mechanical properties of star-branched polymer type TPEs synthesized by anionic polymerization

No.	Hard Segment (T _g , °C)	Soft Segment (T _g , °C)	Mechanical Properties			Architecture	Synthetic Methods	Ref.
			Stress / MPa	Strain / %	wt %			
47			33.8MPa	1110%	29%	SIS Linear	Anionic PLZ	121
			37.3MPa	1110%	29%	(SI) ₄ Star		
			39.2MPa	1030%	32%	(SI) ₇ Star		
			39.7MPa	1100%	33%	(SI) ₂₂ Star		
48			12.6MPa	742%	40vol %	S(IS ⁺) ₃	Anionic PLZ	127
			11.3MPa	496%	50vol %			
			19.96MPa	294%	70vol %			

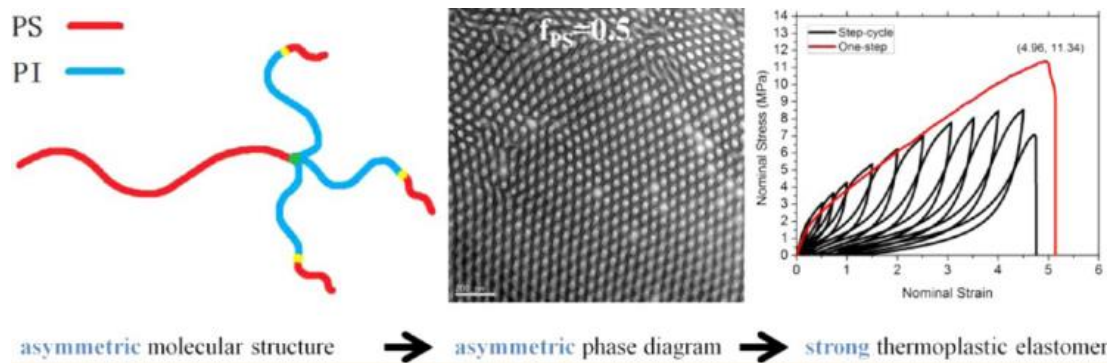


Figure 1.7: S(IS)₃ miktoarm star copolymer type TPEs.¹²⁸

For the “core-first” strategy: developing multifunctional anionic initiators received limited success mainly because of the poor solubility of such initiators in hydrocarbon solvents.¹³¹ However multifunctional initiators for cationic polymerization are possible. (PpCS-PIB)₈ eight arms star polymers were prepared through a calix[8]arene core with eight initiation sites.¹³² (PMMA-PIB)₃ three arms star polymers were prepared by a trifunctional cationic initiator followed by ATRP of MMA.¹³³ For the “arm-first” strategy: at the end of living cationic polymerization, vinyl functionality was introduced by reacting the living cation of PS-PIB⁺ and PID-PIB⁺ with allyltrimethylsilane. The vinyl end functionality further reacted with Si-H on cyclosiloxane by Pt catalyzed hydrosilylation and produced star polymers of (PS-PIB)_n and (PID-PIB)_n based on different numbers of Si-H on cyclosiloxane.^{134,135,136} Similar to arm first divinylbenzene linking strategy for anionic polymerization, 1,4-cyclohexane dimethanol divinyl ether was applied as the linking agent for arm first cationic polymerization to prepare star polymers with poly(2-

admantyl vinyl ether) as hard segment and poly(n-butyl vinyl ether) as elastic segment.⁷⁹ (**Table 1.13**, no. 49-53).

By using tri-functional ATRP initiator for “core first” strategy, three arms star polymers with PMMA,¹³⁷ polyacrylonitrile (PAN),¹³⁸ and PS¹³⁹ as glassy segment, PnBA as elastic segment were prepared for TPE properties evaluation. As an all acrylic TPE, three arm star (PMMA-PnBA)₃ with 36 % of PMMA showed 11 MPa ultimate stress with 545 % strain at break. (PAN-PnBA)₃ star polymers displayed ultimate tensile stress from 6.3 MPa to 12.7 MPa as the strain at break in the range from 382 % to 700 %. Phase separation between PAN and PnBA was retained when the temperature was below 250 °C. As temperature was further raised up to 280 °C, the PAN domain started to crosslink chemically, and the storage modulus of these materials dropped when temperature was close to 300 °C. With multifunctional ATRP initiator of 10 and 20 initiation sites, 10 arms and 20 arms PMBL/PnBA star polymers were prepared for high temperature TPE applications.¹⁴⁰ The highest ultimate tensile stress achieved was 7.8 MPa. Strain at break was lower than 140 % (**Table 1.14**, no. 54-57).

1.4 Grafted polymers for TPEs:

As an important class of commercial polymeric materials, graft copolymers are composed of a polymer backbone with polymer side chains attached to it. Grafted polymers can be prepared by three strategies: (1) “Grafting onto”, where both polymer backbone and

Table 1.13: Mechanical properties of star-branched polymer type TPEs synthesized by cationic polymerization

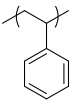
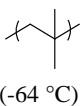
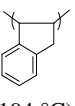
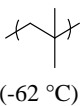
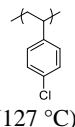
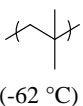
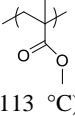
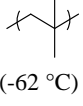
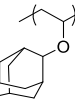
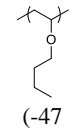
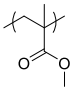
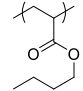
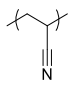
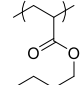
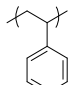
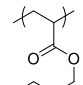
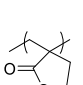
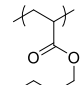
No.	Hard Segment (T _g , °C)	Soft Segment (T _g , °C)	Mechanical Properties			Architecture	Synthetic Methods	Ref.
			Stress / MPa	Strain / %	wt %			
49	 (95 °C)	 (-64 °C)	18.1MPa	540%	23%	(PS-PIB) ₅ Star	Cationic PLZ	134,135
			20.2MPa	550%	23%	(PS-PIB) ₁₆ Star		
			21.1MPa	560%	23%	(PS-PIB) ₂₁ Star		
50	 (194 °C)	 (-62 °C)	12.7MPa	545%	23%	(PID-PIB) ₅ Star	Cationic PLZ	136
			16.8MPa	550%	23%	(PID-PIB) ₂₁ Star		
51	 (127 °C)	 (-62 °C)	22-27MPa	400-650%	23-31%	(PpCS-PIB) ₈ Star	Cationic PLZ	132
52	 (113 °C)	 (-62 °C)	22.5MPa	125%	31.7%	(PMMA-PIB) ₃ Star	Cationic PLZ ATRP	133
53	 (165 °C)	 (-47 °C)	6.9MPa	330%	21.1%	(PADVE-PnBVE) ₈₀ Star	Cationic PLZ	79

Table 1.14: Mechanical properties of star-branched polymer type TPEs synthesized by ATRP

No	Hard Segmen t (T _g , °C)	Soft Segmen t (T _g , °C)	Mechanical Properties			Architecture	Synthetic Methods	Ref
			Stress / MPa	Strain / %	wt %			
54	 (131 °C)	 (-51 °C)	11MPa	545%	36%	(PMMA- PnBA) ₃ Star	ATRP	137
55	 (105 °C)	 (-50 °C)	6.8MPa	700%	11%	(PAN- PnBA) ₃ Star	ATRP	138
			6.3MPa	440%	15%			
			12.7MPa	382%	22%			
56	 (117 °C)	 (-21 °C)	2.35MPa	700%	20.5 %	(PS-PnBA) ₃ Star	ATRP	139
57	 (117 °C)	 (-21 °C)	7.8MPa	140%	24.2 %	(PMBL- PnBA) ₁₀ Star	ATRP	140

side chain are pre-synthesized and then through the end functionalities on side chain and in-chain functionality on backbone, side chains are grafted onto the polymer backbones. (2) “Grafting from”, where multifunctional polymer backbones serve as the macroinitiator and initiated the polymerization of side chain monomers to graft from the backbone. (3) “Grafted through” or “macromonomer” approaches”, where polymer side chains having a polymerizable end group are synthesized, and those macromonomers are subsequently polymerized to form the backbone creating graft polymer.^{141,142,143,144}

By using anionic polymerization followed by polycondensation, Mays and co-workers prepared a series of grafted polymers with regular spaced trifunctional, tetrafunctional and hexafunctional junction points where PI was the backbone and PS was the side chain.^{145,146} Structure-property relationship of these grafted polymers were elucidated by characterizing morphology^{147,148} and mechanical properties^{149,150,151} of grafted polymers with different compositions (14 to 23 vol% of PS) and architectures (trifunctional, tetrafunctional and hexafunctional junction points). From their research, multigraft polymers with tetrafunctional junction points showed 1550 % strain at break which is 500% higher than that for the commercial product Kraton 1102. This superelasticity is a consequence of having the PI backbone anchored by multiple PS physical crosslinks (**Figure 1.8**). Both tetra- and hexafunctional multigraft polymers displayed higher elasticity than commercial TPE's like Kraton or Styroflex. Polymers with

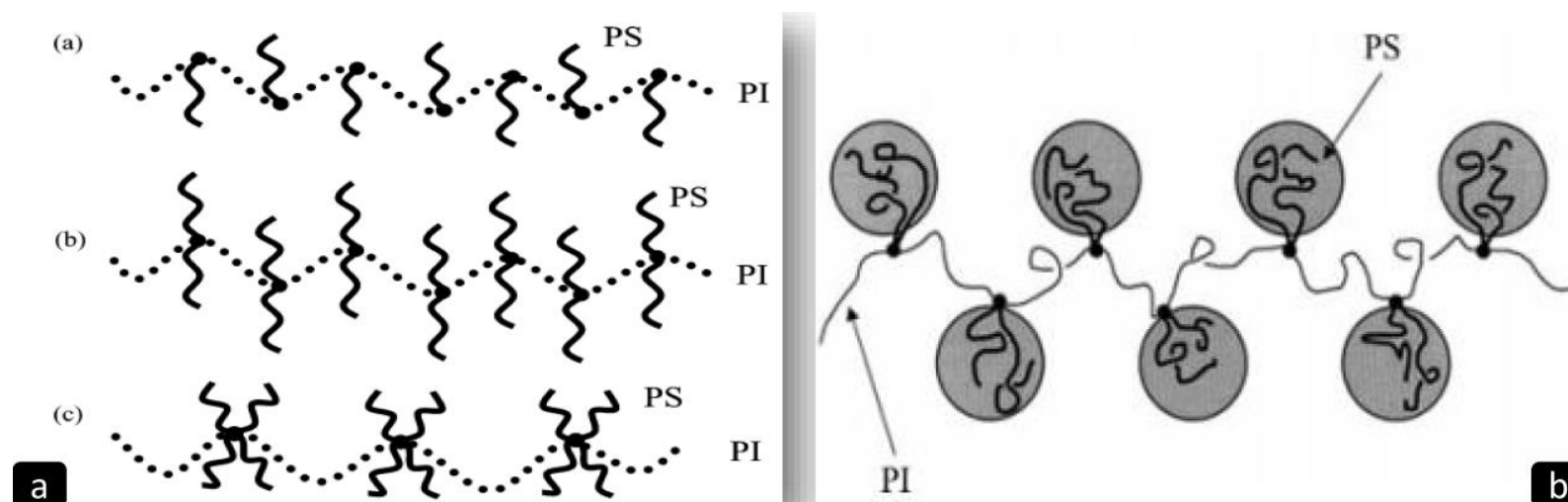


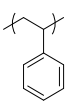
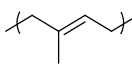
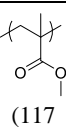
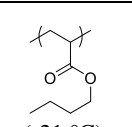
Figure 1.8: a). Illustration of multigrafted copolymers based on PI backbone and PS branches. b). Chain conformation of multigrafted copolymers in microphase-separated state.¹⁴³

more functionalities at one junction point had higher tensile stress and modulus (**Table 1.15**, no. 58).

Inspired by this work, the same group prepared graft all acrylic TPEs based on PMMA side chain and PnBA backbone.¹⁵² The PMMA macromonomers were synthesized by living anionic polymerization and copolymerized with nBA by RAFT polymerization. Similar to other linear and star all acrylic TPEs, low modulus and stress was found in PnBA-g-PMMA graft polymers due to high M_e of PnBA and phase blending between PMMA and PnBA. Zhang and Mays further extended the versatilities of graft polymer architecture by a cost efficient process combining (mini)emulsion polymerization with anionic polymerization or ATRP to prepare trifunctional and tetrafunctional grafted copolymers with PS or PMMA as side chain, PI or PnBA as the backbone.^{153,154,155,156} However, mechanical properties of these materials from tensile test were not presented (**Table 1.15**, no. 59).

Polyhedral oligomeric silsesquioxanes (POSS) are silicon containing organic-inorganic materials.¹⁵⁷ Hybrid materials with silicone combines thermal /oxidative resistance from inorganic materials and processability of organic materials.¹⁵⁸ Copolymerizing ethylene and propylene with ethyl-POSS-norbornene by coordination polymerization produced random terpolymers of ethylene-propylene-silsesquioxane.¹⁵⁹ High stress (>10 MPa) was observed for these silica containing TPEs. Similar research conducted by Bazan¹⁶⁰, which copolymerized ethylene with 5-norbornene-2-bromo-2-

Table 1.15: Mechanical properties of grafted polymer type TPEs synthesized by anionic polymerization

No	Side Chain (T_g , °C)	Backbone (T_g , °C)	Mechanical Properties			Architecture*	Synthetic Methods	Ref
			Stress / MPa	Strain / %	wt %			
58			6.39MPa	1386%	17vol %	MG-3-17-3.7	Anionic PLZ	149
			14.15MPa	1550%	14vol %	MG-4-14-3.5		
			14.63MPa	1373%	21vol %	MG-6-21-5.2		
59			0.05MPa	>500%	26%	MG-3-26-9.2	Anionic PLZ	152
			0.55MPa	450%	22%	MG-3-22-5.3	RAFT	

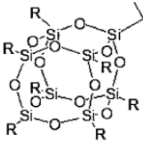
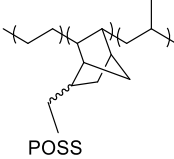
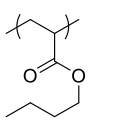
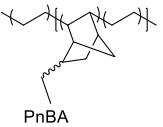
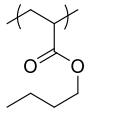
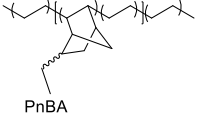
*MG-n-m-x, n is the number of functionality of then junction point, m is the weight percentage of hard segment, x is the average number of junction points.

methylpropanoate (NBMP) which yielded a PE backbone with randomly distributed 2-bromo-2-methylpropanoate as ATRP initiator. Further grafting n-Butyl acrylate by ATRP produced PE-g-PnBA TPEs with 15 MPa ultimate stress and 490 % strain at break. The same group further prepared PE-b-(PE-co-PNBMP)-b-PE, a triblock copolymer with PE at both end and macroinitiator in the middle block.¹⁶¹ Graft polymers showed ultimate tensile stress of 27 MPa with 1310 % strain at break (**Table 1.16**, no. 60-62).

Traditionally there are two types of macromolecular architectures that form a continuous rubbery matrix and suitable for TPEs: (1) linear and star polymers with glassy end (out) block and elastic middle (inner) block (architecture I); (2) graft polymers with elastic backbone and rigid side chain (architecture II). Tang and Wang¹⁶² proposed a reversed graft architecture with elastic side chain grafted on rigid backbone (architecture III, **Figure 1.9**). Notice that in architecture III, the backbone does not necessarily need to be a glassy polymers. Rigid polymers and inorganic materials such as cellulose,^{162,163,164,165} carbon nanotubes^{166,167} and even iron magnetic particles¹⁶⁸ could be used as backbone.

In order to validate the effectiveness of architecture III, ATRP-initiator-functionalized rigid cellulose was prepared with different number of initiation sites.¹⁶² MMA and nBA was randomly copolymerized on the cellulose backbone in DMF at 70 °C. Compared with linear, star and grafted all acrylic TPEs, architecture III type all acrylic TPEs displayed higher ultimate stress (11.1 MPa) with modest strain at break (550 %). Another reason for high stress was attributed to the hydrogen bonding between the carbonyl

Table 1.16: Mechanical properties of grafted polymer type TPEs synthesized by ring opening metathesis polymerization

No	Side Chain	Backbone	Mechanical Properties			Synthetic Methods	Ref
			Stress / MPa	Strain / %	wt %		
60		 POSS	10.2MPa	723%	21%	Coordination PLZ	159
			13.4MPa	448%	30%		
			19.3MPa	450%	36%		
61		 PnBA	15MPa	490%	11%	Coordination PLZ ATRP	160
			3MPa	780%	28%		
			0.9MPa	1170%	29%		
62		 PnBA	20MPa	2000%	72%	Coordination PLZ ATRP	161

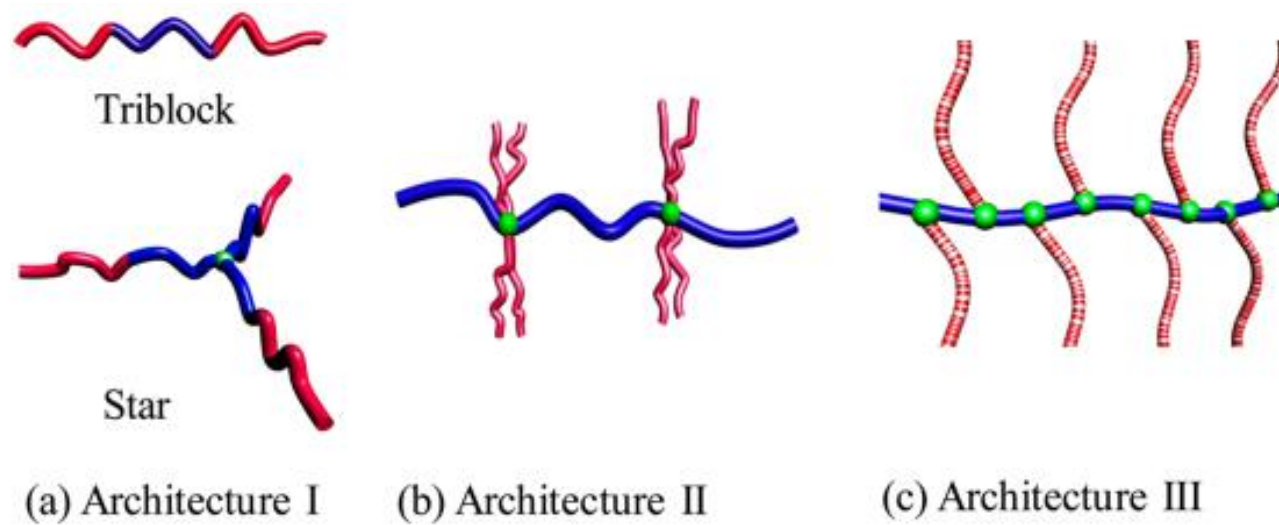


Figure 1.9: Illustration of TPES' architecture¹⁶²

group on acrylic side chains and hydroxyl groups on cellulose. Microphase separation was observed between all acrylic side chain and cellulose backbone. Sustainable TPEs with monomers derived from rosin and fatty acids were prepared by the same strategy.¹⁶⁴

Grafting polyisoprene onto the backbone of cellulose was achieved by Wang,¹⁶³ and the resulting materials could mimic mechanical properties of human skin (**Figure 1.10**).¹⁶⁵ Different from cellulose-g-(PnBA-co-PMMA), for which only one T_g corresponding to (PnBA-co-PMMA) was reported, two distinguishable T_g s were observed through dynamic mechanical analysis in cellulose-g-PI. (**Table 1.17**, no. 63-65). By replacing cellulose with functionalized carbon nanotubes (CNT) and Fe₃O₄ nanoparticles (NPs), TPEs with type III architecture were successfully prepared. When carbon nanotubes¹⁶⁶ were used as the rigid segment, 1.7 % of CNT loading increased the ultimate tensile stress from 2.4 MPa to 7.8 MPa. Strain at break was reduced from 951 % to 520 %. TPEs with Fe₃O₄ showed recyclability under magnetic field.¹⁶⁸ (**Table 1.17**, no. 66-67)

1.5 Perspective:

The past 60 years has witnessed rapid development of thermoplastic elastomers from discoveries in the laboratory to widely applied commodities involved in everyone's daily life. Starting from the 21 century, progress made in different polymerization techniques has advanced new types of TPEs with various chemical compositions and

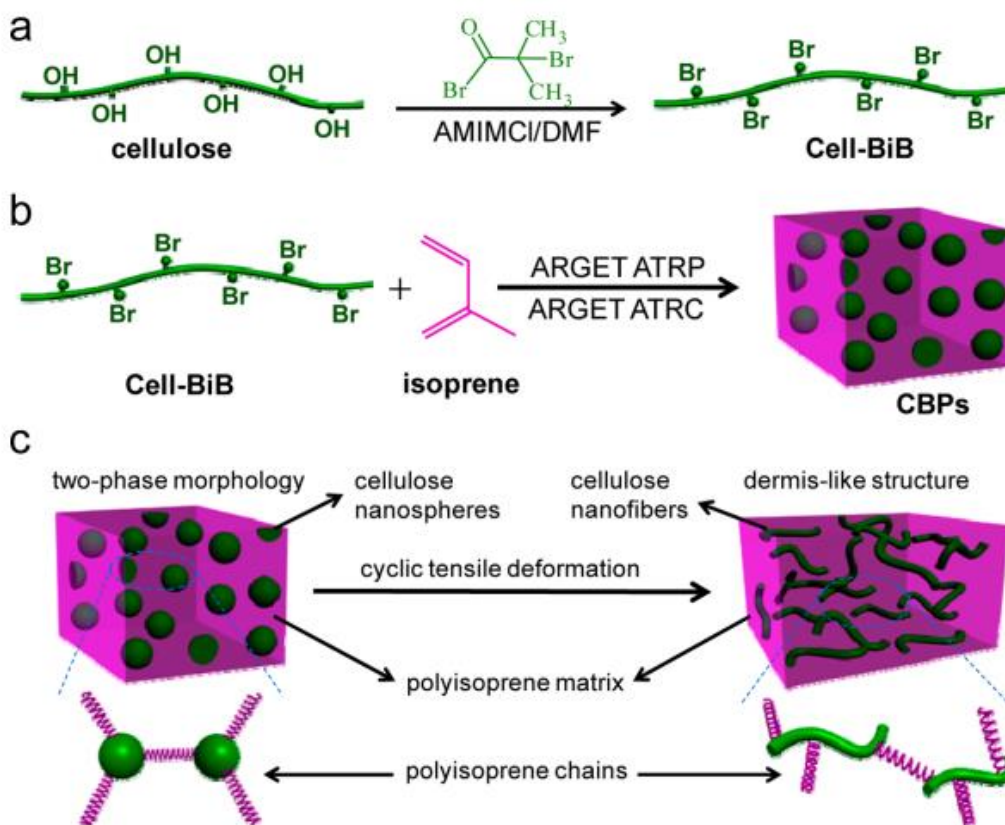
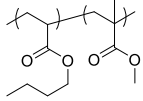
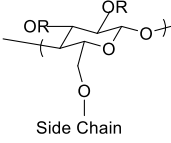
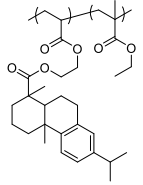
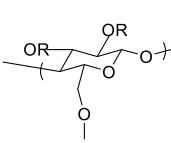
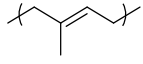
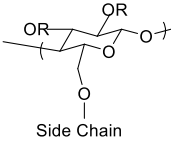
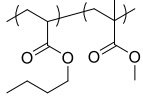
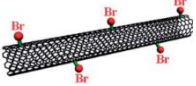
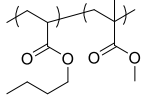
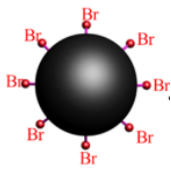


Figure 1.10: Design concept and synthesis of nanostructured elastomers mimicking the mechanical properties of human skin. (a) ATRP macroinitiator, (b) Cross-linked brush polymers were synthesized and self-assembled into two-phase morphology. (c) Two phase morphology of CBPs can be reconfigured into that close to the skin microstructure model.¹⁶³

Table 1.17: Mechanical properties of grafted polymer type TPEs based on architecture III

No	Side Chain	Backbone	Mechanical Properties			Synthetic Methods	Ref
			Stress / MPa	Strain / %	wt %		
63		 Side Chain	2.3MPa	1000%	39.6%	ATRP	162
			6.6MPa	660%	47.5%		
			11.1MPa	550%	54.8%		
64		 Side Chain	0.25MPa	1000%	20%	ATRP	164
			2.0MPa	500%	30%		
65		 Side Chain	9.7MPa	160%	4.3%	ATRP	165
			32MPa	60%	20.6%		
66		 Carbon Nanotube	2.4MPa	951%	0%	ATRP	166
			7.8MPa	520%	1.7%		
			9.9MPa	293%	3.8%		
67		 Fe ₃ O ₄ Nano particle	3.5MPa	921%	1.3%	ATRP	168
			9.0MPa	641%	2.8%		
			14.6MPa	458%	1.3%		

macromolecular architectures. However, each polymerization technique has both merits and weakness.

Kraton styrenic thermoplastic elastomers are the most commercially successful polymeric materials synthesized by living anionic polymerization. The disadvantage of S-TPEs is obvious: low service temperature and poor UV/oxidation resistance. All acrylic TPEs show better chemical resistance, however, the mechanical properties of these materials are much lower than those of S-TPEs.

Cationic polymerization was used to prepare PIB based TPEs showing higher service temperature with better chemical resistance. The problem for cationic polymerization is the low polymerization temperature, which is not favorable for industrial applications. Low polymerization temperature also limited large scale production of (methyl) acrylate based TPEs by anionic polymerization.

Metal catalyzed ring opening polymerization produced biodegradable polymers from sustainable resources. However, most metal catalyzed ROP need toxic tin as the catalyst. Atomic transfer radical polymerization needs to reduce the radical concentration in order to control the polymerization. Polymers prepared by ATRP generally contain residual metal catalyst. Terminating the reaction at low conversion is necessary for block polymers preparation by ATRP.

Well defined PI-g-(PS)_n (n=1,2,3) showed great mechanical properties competitive with Kraton products. However, these anionically prepared polymers required laborious

synthetic procedures. As one of the most favorable polymerization techniques in industry, emulsion polymerization offers many benefits: polymers with high weight average molecular could be prepared quickly in water as the reaction medium. Particles of polymers could be directly applied for coating and painting without purification. Recent research using macromonomer approaches to synthesize PI-g-PS by a combination of anionic polymerization and emulsion polymerization opens up opportunities to prepare thermoplastic elastomers by a cost efficient strategy. However, the PS macromonomer was prepared by anionic polymerization. Living anionic polymerization required oxygen and moisture free environment in order to retain the reactivity of chain end anion. Thrilling opportunities are waiting if PS macromonomer could be prepared by all emulsion process with more than one branch points in the same macromonomer.

References:

- [1]. Bonart, R. *Polymer* **1979**, 20 (11), 1389-1403.
- [2]. Spontak, R. J.; Patel, N. P. *Current Opinion in Colloid & Interface Science* **2000**, 5 (5-6), 333-340.
- [3]. Shanks, R. A., General purpose elastomers: Structure, chemistry, physics and performance. In *Advances in Elastomers I*, Springer: 2013; pp 11-45.
- [4]. Walker, B. M.; Rader, C. P., *Handbook of thermoplastic elastomers*. Van Nostrand Reinhold New York: 1979.
- [5]. Drobny, J. G., *Handbook of thermoplastic elastomers*. Elsevier: 2014.
- [6]. Bhowmick, A. K.; Stephens, H., *Handbook of elastomers*. CRC Press: 2000.
- [7]. Fakirov, S., *Handbook of condensation thermoplastic elastomers*. John Wiley & Sons: 2006.
- [8]. Legge, N. R.; Holden, G.; Schroeder, H., Thermoplastic elastomers: a comprehensive review. *Carl Hanser Verlag, Kolbergerstr. 22, D-8000 Munchen 80, FRG, 1987. 574* **1987**.
- [9]. Matuszak, M. P., Production of isooctanes from cyclopropane and isobutane. U.S. Patent 2,632,031.: 17 Mar. 1953.
- [10]. Langerak, E. O.; Prucino, L. J.; Remington, W. R., Elastomers from polyalkylene ether glycol reacted with arylene diisocyanate and water. Patent No. 2,692,873. : 1954.

- [11]. S., S. C., Simulated vulcanizates of polyurethane elastomers. U.S. Patent 2,871,218, : 1959.
- [12]. Geoffrey, H.; Ralph, M., Block polymers of monovinyl aromatic hydrocarbons and conjugated dienes. U.S. Patent No. 3,265,765: 1966.
- [13]. Hsieh, H. Q., R. P., *Anionic polymerization: principles and practical applications*. . CRC Press: : 1996.
- [14]. Handlin, D. L. T., S.; Wright, K., Applications of Thermoplastic Elastomers Based on Styrenic Block Copolymers In *Macromolecular Engineering: Precise Synthesis, Materials Properties, Applications*, Matyjaszewski, K. G., Y.; Leibler, L., Eds. , Ed. Wiley-VCH: 2007; Vol. 4, pp 2001-2031.: 2007.
- [15]. Szwarc, M., "Living" polymers. **1956**.
- [16]. Hirao, A.; Goseki, R.; Ishizone, T. *Macromolecules* **2014**, *47* (6), 1883-1905.
- [17]. Orlov, Y., Polymer thermodynamics: Leverage modeling results for industrial applications. In *Polymer Reaction Engineering IX*, E. Vivaldo-Lima, U. J. D., BASF; F. Zaldo-Garcia, CP-COMEX; J. Tsavalas,, Ed. ECI Symposium Series,: Univ. of New Hampshire Eds, , 2015.
- [18]. Drolet, F.; Fredrickson, G. H. *Physical Review Letters* **1999**, *83* (21), 4317.
- [19]. Iwao, T., Polymer solutions: An introduction to physical properties. New York: Wiley: 2002.

- [20]. Quirk, R. P., *Applications of anionic polymerization research*. American Chemical Society; Distributed by Oxford University Press: 1998.
- [21]. [http://www.grandviewresearch.com/industry-analysis/thermoplastic-elastomers-](http://www.grandviewresearch.com/industry-analysis/thermoplastic-elastomers-market)market Thermoplastic Elastomers (TPE) Market Analysis By Product (Styrenic Block Copolymers (SBC, SBS, SIS, HSBC).
- [22]. Karl, M.; Richard, H., Composition of matter comprising polypropylene and an ethylene-propylene copolymer. U.S. Patent No. 3,262,992.: 1966.
- [23]. Coran, A. Y.; Patel, R. P., Elastoplastic compositions of butyl rubber and polyolefin resin. U.S. Patent No. 4,130,534.: 1978.
- [24]. Hadjichristidis, N.; Hirao, A., *Anionic Polymerization: Principles, Practice, Strength, Consequences and Applications*. Springer: 2015.
- [25]. Aoshima, S.; Kanaoka, S. *Chemical reviews* **2009**, *109* (11), 5245-5287.
- [26]. Matyjaszewski, K.; Tsarevsky, N. V. *Journal of the American Chemical Society* **2014**, *136* (18), 6513-6533.
- [27]. Khosravi, E.; Szymanska-Buzar, T., *Ring opening metathesis polymerisation and related chemistry: state of the art and visions for the new century*. Springer Science & Business Media: 2012; Vol. 56.
- [28]. Moad, G.; Rizzardo, E.; Thang, S. H. *Polymer* **2008**, *49* (5), 1079-1131.
- [29]. Hawker, C. J.; Bosman, A. W.; Harth, E. *Chemical Reviews* **2001**, *101* (12), 3661-3688.

- [30]. G. Holden, N. R. L., Styrenic Thermoplastic Elastomers. In *Thermoplastic Elastomers*, Holden, G., Ed. Carl Hanser Verlag GmbH & Co.; 1996.
- [31]. Morton, M.; McGrath, J. E.; Juliano, P. C. *Journal of Polymer Science Part C: Polymer Symposia*, Wiley Online Library: 1969; pp 99-115.
- [32]. Fetters, L. J.; Morton, M. *Macromolecules* **1969**, 2 (5), 453-458.
- [33]. Bolton, J. M.; Hillmyer, M. A.; Hoye, T. R. *ACS Macro Letters* **2014**, 3 (8), 717-720.
- [34]. Fetters, L.; Firer, E.; Dafaoui, M. *Macromolecules* **1977**, 10 (6), 1200-1207.
- [35]. Kobayashi, S.; Matsuzawa, T.; Matsuoka, S.-i.; Tajima, H.; Ishizone, T. *Macromolecules* **2006**, 39 (18), 5979-5986.
- [36]. Kobayashi, S.; Kataoka, H.; Ishizone, T.; Kato, T.; Ono, T.; Kobukata, S.; Ogi, H. *Macromolecules* **2008**, 41 (14), 5502-5508.
- [37]. Hucul, D. A.; Hahn, S. F. *Advanced Materials* **2000**, 12 (23), 1855-1858.
- [38]. Alfonzo, C. G.; Fleury, G.; Chaffin, K. A.; Bates, F. S. *Macromolecules* **2010**, 43 (12), 5295-5305.
- [39]. Yu, J. M.; Dubois, P.; Teyssié, P.; Jérôme, R. *Macromolecules* **1996**, 29 (19), 6090-6099.
- [40]. Yu, J. M.; Dubois, P.; Jérôme, R. *Macromolecules* **1996**, 29 (26), 8362-8370.
- [41]. Yu, J. M.; Dubois, P.; Jérôme, R. *Macromolecules* **1996**, 29 (23), 7316-7322.
- [42]. Bywater, S.; Worsfold, D. *Canadian Journal of Chemistry* **1967**, 45 (16), 1821-1824.

- [43]. Yu, Y.; Dubois, P.; Teyssié, P.; Jérôme, R. *Macromolecules* **1997**, *30* (15), 4254-4261.
- [44]. Yu, J.; Dubois, P.; Jérôme, R. *Macromolecules* **1997**, *30* (21), 6536-6543.
- [45]. Yu, J. M.; Dubois, P.; Jérôme, R. *Macromolecules* **1997**, *30* (17), 4984-4994.
- [46]. Yu, Y.; Dubois, P.; Jérôme, R.; Teyssié, P. *Journal of Polymer Science Part A: Polymer Chemistry* **1996**, *34* (11), 2221-2228.
- [47]. Varshney, S.; Kesani, P.; Agarwal, N.; Zhang, J.; Rafailovich, M. *Macromolecules* **1999**, *32* (1), 235-237.
- [48]. Tong, J.; Jérôme, R. *Polymer* **2000**, *41* (7), 2499-2510.
- [49]. Moineau, C.; Minet, M.; Teyssié, P.; Jérôme, R. *Macromolecules* **1999**, *32* (25), 8277-8282.
- [50]. Tong, J.-D.; Moineau, G.; Leclere, P.; Brédas, J.-L.; Lazzaroni, R.; Jérôme, R., *Macromolecules* **2000**, *33* (2), 470-479.
- [51]. Tong, J.-D.; Jérôme, R. *Macromolecules* **2000**, *33* (5), 1479-1481.
- [52]. Tong, J.-D.; Leclère, P.; Rasmont, A.; Brédas, J.-L.; Lazzaroni, R.; Jérôme, R. *Macromolecular Chemistry and Physics* **2000**, *201* (12), 1250-1258.
- [53]. Leclère, P.; Rasmont, A.; Brédas, J.-L.; Jérôme, R.; Aime, J.; Lazzaroni, R. In *Phase - separated microstructures in "all - acrylic " thermoplastic elastomers*, Macromolecular Symposia, Wiley Online Library: 2001; pp 117-137.

- [54]. Tong, J.; Leclère, P.; Doneux, C.; Brédas, J.-L.; Lazzaroni, R.; Jérôme, R. *Polymer* **2001**, *42* (8), 3503-3514.
- [55]. Chatterjee, D. P.; Mandal, B. M. *Macromolecules* **2006**, *39* (26), 9192-9200.
- [56]. Natori, I. *Macromolecules* **1997**, *30* (12), 3696-3697.
- [57]. Hong, K.; Mays, J. W. *Macromolecules* **2001**, *34* (4), 782-786.
- [58]. Imaizumi, K.; Ono, T.; Natori, I.; Sakurai, S.; Takeda, K. *Journal of Polymer Science Part B: Polymer Physics* **2001**, *39* (1), 13-22.
- [59]. Natori, I.; Imaizumi, K.; Yamagishi, H.; Kazunori, M. *Journal of Polymer Science Part B: Polymer Physics* **1998**, *36* (10), 1657-1668.
- [60]. Kosaka, Y.; Kitazawa, K.; Inomata, S.; Ishizone, T. *ACS Macro Letters* **2013**, *2* (2), 164-167.
- [61]. Kosaka, Y.; Kawauchi, S.; Goseki, R.; Ishizone, T. *Macromolecules* **2015**, *48* (13), 4421-4430.
- [62]. Wang, W., HighTemperature Thermoplastic Elastomers Synthesized by Living Anionic Polymerization in Hydrocarbon Solvent at Room Temperature. (Unpublished)
- [63]. Wang, W., Polybenzofulvene Based Thermoplastic Elastomer: Effects of Partial and Complete Hydrogenation. (Unpublished)
- [64]. Kennedy, J. P., Thermoplastic Elastomers by Carbocationic Polymerization. In *Thermoplastic Elastomers*, G. Holden, N. R. L., R. Quirk, H.E. Schroeder, Ed. Hanser Publishers: New York, 1996.

- [65]. Kaszas, G.; Puskas, J.; Kennedy, J.; Hager, W. *Journal of Polymer Science Part A: Polymer Chemistry* **1991**, *29* (3), 427-435.
- [66]. Cao, X.; Faust, R. *Macromolecules* **1999**, *32* (17), 5487-5494.
- [67]. Tsunogae, Y.; Kennedy, J. *Journal of Polymer Science Part A: Polymer Chemistry* **1994**, *32* (3), 403-412.
- [68]. Cao, X.; Sipos, L.; Faust, R. *Polymer Bulletin* **2000**, *45* (2), 121-128.
- [69]. Puskas, J.; Kaszas, G.; Kennedy, J.; Hager, W. *Journal of Polymer Science Part A: Polymer Chemistry* **1992**, *30* (1), 41-48.
- [70]. Li, D.; Faust, R. *Macromolecules* **1995**, *28* (14), 4893-4898.
- [71]. Kennedy, J.; Kurian, J. *Journal of Polymer Science Part A: Polymer Chemistry* **1990**, *28* (13), 3725-3738.
- [72]. Kennedy, J. P.; Price, J. L.; Koshimura, K. *Macromolecules* **1991**, *24* (25), 6567-6571.
- [73]. Kennedy, J.; MIDHA, S.; Tsunogae, Y. *Macromolecules* **1993**, *26* (3), 429-435.
- [74]. Fodor, Z.; Kennedy, J. *Polymer Bulletin* **1992**, *29* (6), 697-704.
- [75]. Zhou, Y.; Faust, R.; Chen, S.; Gido, S. P. *Macromolecules* **2004**, *37* (18), 6716-6725.
- [76]. Zhou, Y.; Faust, R.; Richard, R.; Schwarz, M. *Macromolecules* **2005**, *38* (20), 8183-8191.
- [77]. Hashimoto, T.; Imaeda, T.; Irie, S.; Urushisaki, M.; Sakaguchi, T. *Journal of Polymer Science Part A: Polymer Chemistry* **2015**, *53* (9), 1114-1124.

- [78]. Hashimoto, T.; Namikoshi, T.; Irie, S.; Urushisaki, M.; Sakaguchi, T.; Nemoto, T.; Isoda, S. *Journal of Polymer Science Part A: Polymer Chemistry* **2008**, *46* (5), 1902-1906.
- [79]. Imaeda, T.; Hashimoto, T.; Irie, S.; Urushisaki, M.; Sakaguchi, T. *Journal of Polymer Science Part A: Polymer Chemistry* **2013**, *51* (8), 1796-1807.
- [80]. Pan, P.; Inoue, Y. *Progress in Polymer Science* **2009**, *34* (7), 605-640.
- [81]. Frick, E. M.; Zalusky, A. S.; Hillmyer, M. A. *Biomacromolecules* **2003**, *4* (2), 216-223.
- [82]. Sipos, L.; Zsuga, M.; Deák, G. *Macromolecular rapid communications* **1995**, *16* (12), 935-940.
- [83]. Zhang, S.; Hou, Z.; Gonsalves, K. *Journal of Polymer Science Part A: Polymer Chemistry* **1996**, *34* (13), 2737-2742.
- [84]. Huang, Y.; Pan, P.; Shan, G.; Bao, Y. *RSC Advances* **2014**, *4* (89), 47965-47976.
- [85]. Belgacem, M. N.; Gandini, A., *Monomers, polymers and composites from renewable resources*. Elsevier: 2011.
- [86]. Ajellal, N.; Carpentier, J.-F.; Guillaume, C.; Guillaume, S. M.; Helou, M.; Poirier, V.; Sarazin, Y.; Trifonov, A. *Dalton Transactions* **2010**, *39* (36), 8363-8376.
- [87]. Hillmyer, M. A.; Tolman, W. B. *Accounts of chemical research* **2014**, *47* (8), 2390-2396.
- [88]. Hiki, S.; Miyamoto, M.; Kimura, Y. *Polymer* **2000**, *41* (20), 7369-7379.

- [89]. Wanamaker, C. L.; O'Leary, L. E.; Lynd, N. A.; Hillmyer, M. A.; Tolman, W. B. *Biomacromolecules* **2007**, *8* (11), 3634-3640.
- [90]. Wanamaker, C. L.; Bluemle, M. J.; Pitet, L. M.; O'Leary, L. E.; Tolman, W. B.; Hillmyer, M. A. *Biomacromolecules* **2009**, *10* (10), 2904-2911.
- [91]. Martello, M. T.; Hillmyer, M. A. *Macromolecules* **2011**, *44* (21), 8537-8545.
- [92]. Xiong, M.; Schneiderman, D. K.; Bates, F. S.; Hillmyer, M. A.; Zhang, K. *Proceedings of the National Academy of Sciences* **2014**, *111* (23), 8357-8362.
- [93]. Nakayama, Y.; Aihara, K.; Yamanishi, H.; Fukuoka, H.; Tanaka, R.; Cai, Z.; Shiono, T. *Journal of Polymer Science Part A: Polymer Chemistry* **2015**, *53* (3), 489-495.
- [94]. Schneiderman, D. K.; Hill, E. M.; Martello, M. T.; Hillmyer, M. A. *Polymer Chemistry* **2015**, *6* (19), 3641-3651.
- [95]. Suenaga, J.; Sutherlin, D. M.; Stille, J. K. *Macromolecules* **1984**, *17* (12), 2913-2916.
- [96]. Akkapeddi, M. K. *Polymer* **1979**, *20* (10), 1215-1216.
- [97]. Shin, J.; Lee, Y.; Tolman, W. B.; Hillmyer, M. A. *Biomacromolecules* **2012**, *13* (11), 3833-3840.
- [98]. Matyjaszewski, K.; Davis, T. P., *Handbook of radical polymerization*. Wiley Online Library: 2002.
- [99]. Matyjaszewski, K.; Tsarevsky, N. V. *Nature chemistry* **2009**, *1* (4), 276-288.
- [100]. Dong, H.; Tang, W.; Matyjaszewski, K. *Macromolecules* **2007**, *40* (9), 2974-2977.

- [101]. Thomas, D. B.; Sumerlin, B. S.; Lowe, A. B.; McCormick, C. L. *Macromolecules* **2003**, *36* (5), 1436-1439.
- [102]. Keddie, D. J. *Chemical Society Reviews* **2014**, *43* (2), 496-505.
- [103]. Matyjaszewski, K. *Science* **2011**, *333* (6046), 1104-1105.
- [104]. Mosnáček, J.; Yoon, J. A.; Juhari, A.; Koynov, K.; Matyjaszewski, K. *Polymer* **2009**, *50* (9), 2087-2094.
- [105]. Yi, Y.; Fan, X.; Wan, X.; Li, L.; Zhao, N.; Chen, X.; Xu, J.; Zhou, Q.-F. *Macromolecules* **2004**, *37* (20), 7610-7618.
- [106]. Liu, X.; Zhao, R.-Y.; Zhao, T.-P.; Liu, C.-Y.; Yang, S.; Chen, E.-Q. *RSC Advances* **2014**, *4* (35), 18431-18441.
- [107]. Braunecker, W. A.; Matyjaszewski, K. *Progress in Polymer Science* **2007**, *32* (1), 93-146.
- [108]. Butté, A.; Storti, G.; Morbidelli, M. *Macromolecules* **2001**, *34* (17), 5885-5896.
- [109]. Delaittre, G.; Charleux, B. *Macromolecules* **2008**, *41* (7), 2361-2367.
- [110]. Luo, Y.; Wang, X.; Zhu, Y.; Li, B.-G.; Zhu, S. *Macromolecules* **2010**, *43* (18), 7472-7481.
- [111]. Zhan, X.; He, R.; Zhang, Q.; Chen, F. *RSC Advances* **2014**, *4* (93), 51201-51207.
- [112]. Wang, S.; Vajjala Kesava, S.; Gomez, E. D.; Robertson, M. L. *Macromolecules* **2013**, *46* (18), 7202-7212.

- [113]. Hayashi, M.; Matsushima, S.; Noro, A.; Matsushita, Y. *Macromolecules* **2015**, *48* (2), 421-431.
- [114]. Vasile, C., *Handbook of polyolefins*. CRC Press: 2000.
- [115]. Natta, G. *Journal of polymer science* **1959**, *34* (127), 531-549.
- [116]. Harney, M. B.; Zhang, Y.; Sita, L. R. *Angewandte Chemie International Edition* **2006**, *45* (15), 2400-2404.
- [117]. Hotta, A.; Cochran, E.; Ruokolainen, J.; Khanna, V.; Fredrickson, G. H.; Kramer, E. J.; Shin, Y.-W.; Shimizu, F.; Cherian, A. E.; Hustad, P. D. *Proceedings of the National Academy of Sciences* **2006**, *103* (42), 15327-15332.
- [118]. Crawford, K. E.; Sita, L. R. *ACS Macro Letters* **2015**, *4*, 921-925.
- [119]. Hadjichristidis, N. *Journal of Polymer Science Part A: Polymer Chemistry* **1999**, *37* (7), 857-871.
- [120]. Khanna, K.; Varshney, S.; Kakkar, A. *Polymer Chemistry* **2010**, *1* (8), 1171-1185.
- [121]. Bi, L.-K.; Fetters, L. J. *Macromolecules* **1976**, *9* (5), 732-742.
- [122]. Bi, L.-K.; Fetters, L. *Macromolecules* **1975**, *8* (1), 90-92.
- [123]. Lai, C.; Russel, W. B.; Register, R. A.; Marchand, G. R.; Adamson, D. H. *Macromolecules* **2000**, *33* (9), 3461-3466.
- [124]. Milner, S. T. *Macromolecules* **1994**, *27* (8), 2333-2335.
- [125]. Vavasour, J.; Whitmore, M. *Macromolecules* **1993**, *26* (25), 7070-7075.

- [126]. Lynd, N. A.; Oyerokun, F. T.; O'Donoghue, D. L.; Handlin Jr, D. L.; Fredrickson, G. H. *Macromolecules* **2010**, *43* (7), 3479-3486.
- [127]. Bates, F. S.; Fredrickson, G. H. *Annual Review of Physical Chemistry* **1990**, *41* (1), 525-557.
- [128]. Shi, W.; Lynd, N. A.; Montarnal, D.; Luo, Y.; Fredrickson, G. H.; Kramer, E. J.; Ntaras, C.; Avgeropoulos, A.; Hexemer, A. *Macromolecules* **2014**, *47* (6), 2037-2043.
- [129]. Shi, W.; Hamilton, A. L.; Delaney, K. T.; Fredrickson, G. H.; Kramer, E. J.; Ntaras, C.; Avgeropoulos, A.; Lynd, N. A.; Demassieux, Q.; Creton, C. *Macromolecules* **2015**, *48* (15), 5378-5384.
- [130]. Shi, W.; Hamilton, A. L.; Delaney, K.; Fredrickson, G. H.; Kramer, E. J.; Ntaras, C.; Avgeropoulos, A.; Lynd, N. A. *Journal of the American Chemical Society* **2015**.
- [131]. Matmour, R.; Gnanou, Y. *Progress in Polymer Science* **2013**, *38* (1), 30-62.
- [132]. Jacob, S.; Kennedy, J. P. *Polymer Bulletin* **1998**, *41* (2), 167-174.
- [133]. Keszler, B.; Fenyvesi, G.; Kennedy, J. *Journal of Polymer Science Part A: Polymer Chemistry* **2000**, *38* (4), 706-714.
- [134]. Shim, J. S.; Asthana, S.; Omura, N.; Kennedy, J. P. *Journal of Polymer Science Part A: Polymer Chemistry* **1998**, *36* (17), 2997-3012.
- [135]. Shim, J. S.; Kennedy, J. P. *Journal of Polymer Science Part A: Polymer Chemistry* **1999**, *37* (6), 815-824.

- [136]. Shim, J. S.; Kennedy, J. P. *Journal of Polymer Science Part A: Polymer Chemistry* **2000**, *38* (2), 279-290.
- [137]. Dufour, B.; Koynov, K.; Pakula, T.; Matyjaszewski, K. *Macromolecular Chemistry and Physics* **2008**, *209* (16), 1686-1693.
- [138]. Dufour, B.; Tang, C.; Koynov, K.; Zhang, Y.; Pakula, T.; Matyjaszewski, K. *Macromolecules* **2008**, *41* (7), 2451-2458.
- [139]. Pakula, T.; Koynov, K.; Boerner, H.; Huang, J.; Lee, H.-i.; Pietrasik, J.; Sumerlin, B.; Matyjaszewski, K. *Polymer* **2011**, *52* (12), 2576-2583.
- [140]. Juhari, A.; Mosnáček, J.; Yoon, J. A.; Nese, A.; Koynov, K.; Kowalewski, T.; Matyjaszewski, K. *Polymer* **2010**, *51* (21), 4806-4813.
- [141]. Feng, C.; Li, Y.; Yang, D.; Hu, J.; Zhang, X.; Huang, X. *Chemical Society Reviews* **2011**, *40* (3), 1282-1295.
- [142]. Uhrig, D.; Mays, J. *Polymer Chemistry* **2011**, *2* (1), 69-76.
- [143]. Ito, S.; Goseki, R.; Ishizone, T.; Hirao, A. *Polymer Chemistry* **2014**, *5* (19), 5523-5534.
- [144]. Uhrig, D.; Schlegel, R.; Weidisch, R.; Mays, J. *European Polymer Journal* **2011**, *47* (4), 560-568.
- [145]. Iatrou, H.; Mays, J. W.; Hadjichristidis, N. *Macromolecules* **1998**, *31* (19), 6697-6701.
- [146]. Uhrig, D.; Mays, J. W. *Macromolecules* **2002**, *35* (19), 7182-7190.

- [147]. Beyer, F. L.; Gido, S. P.; Büschl, C.; Iatrou, H.; Uhrig, D.; Mays, J. W.; Chang, M. Y.; Garetz, B. A.; Balsara, N. P.; Tan, N. B. *Macromolecules* **2000**, *33* (6), 2039-2048.
- [148]. Duan, Y.; Thunga, M.; Schlegel, R.; Schneider, K.; Rettler, E.; Weidisch, R.; Siesler, H. W.; Stamm, M.; Mays, J. W.; Hadjichristidis, N. *Macromolecules* **2009**, *42* (12), 4155-4164.
- [149]. Weidisch, R.; Gido, S.; Uhrig, D.; Iatrou, H.; Mays, J.; Hadjichristidis, N. *Macromolecules* **2001**, *34* (18), 6333-6337.
- [150]. Staudinger, U.; Weidisch, R.; Zhu, Y.; Gido, S.; Uhrig, D.; Mays, J.; Iatrou, H.; Hadjichristidis, N. In *Mechanical properties and hysteresis behaviour of multigraft copolymers*, Macromolecular symposia, Wiley Online Library: 2006; pp 42-50.
- [151]. Schlegel, R.; Wilkin, D.; Duan, Y.; Weidisch, R.; Heinrich, G.; Uhrig, D.; Mays, J.; Iatrou, H.; Hadjichristidis, N. *Polymer* **2009**, *50* (26), 6297-6304.
- [152]. Goodwin, A. B.; Wang, W.; Kang, N.-G.; Wang, Y.; Hong, K.; Mays, J. W. *Industrial & Engineering Chemistry Research* **2015**.
- [153]. Wang, W.; Wang, W.; Lu, X.; Bobade, S.; Chen, J.; Kang, N.-G.; Zhang, Q.; Mays, J. *Macromolecules* **2014**, *47* (21), 7284-7295.
- [154]. Wang, W.; Wang, W.; Li, H.; Lu, X.; Chen, J.; Kang, N.-G.; Zhang, Q.; Mays, J. *Industrial & Engineering Chemistry Research* **2015**, *54* (4), 1292-1300.
- [155]. Li, H.; Wang, W.; Li, C.; Tan, J.; Yin, D.; Zhang, H.; Zhang, B.; Yin, C.; Zhang, Q. *Journal of colloid and interface science* **2015**, *453*, 226-236.

- [156]. Li, H.; Wang, W.; Tan, J.; Li, C.; Zhang, Q. *RSC Advances* **2015**, *5* (56), 45459-45466.
- [157]. Lichtenhan, J. D. *Comments on Inorganic Chemistry* **1995**, *17* (2), 115-130.
- [158]. Zheng, L.; Hong, S.; Cardoen, G.; Burgaz, E.; Guido, S. P.; Coughlin, E. B. *Macromolecules* **2004**, *37* (23), 8606-8611.
- [159]. Seurer, B.; Coughlin, E. B. *Macromolecular Chemistry and Physics* **2008**, *209* (12), 1198-1209.
- [160]. Schneider, Y.; Lynd, N. A.; Kramer, E. J.; Bazan, G. C. *Macromolecules* **2009**, *42* (22), 8763-8768.
- [161]. Coffin, R. C.; Schneider, Y.; Kramer, E. J.; Bazan, G. C. *Journal of the American Chemical Society* **2010**, *132* (39), 13869-13878.
- [162]. Jiang, F.; Wang, Z.; Qiao, Y.; Wang, Z.; Tang, C. *Macromolecules* **2013**, *46* (12), 4772-4780.
- [163]. Wang, Z.; Zhang, Y.; Jiang, F.; Fang, H.; Wang, Z. *Polymer Chemistry* **2014**, *5* (10), 3379-3388.
- [164]. Liu, Y.; Yao, K.; Chen, X.; Wang, J.; Wang, Z.; Ploehn, H. J.; Wang, C.; Chu, F.; Tang, C. *Polymer Chemistry* **2014**, *5* (9), 3170-3181.
- [165]. Wang, Z.; Jiang, F.; Zhang, Y.; You, Y.; Wang, Z.; Guan, Z. *ACS nano* **2014**, *9* (1), 271-278.

[166]. Jiang, F.; Zhang, Y.; Fang, C.; Wang, Z.; Wang, Z. *RSC Advances* **2014**, *4* (104), 60079-60085.

[167]. Jiang, F.; Zhang, Y.; Wang, Z.; Fang, H.; Ding, Y.; Xu, H.; Wang, Z. *Industrial & Engineering Chemistry Research* **2014**, *53* (52), 20154-20167.

[168]. Jiang, F.; Zhang, Y.; Wang, Z.; Wang, W.; Xu, Z.; Wang, Z. *ACS applied materials & interfaces* **2015**.

Chapter 2: Scope of the Dissertation

2.1 Research Motivation:

After Milkovich and Holden first patented SIS triblock copolymer type TPEs in 1965¹, for almost 50 years, one of the major research goals in the field of anionic polymerization for industrial application has been to produce high temperature thermoplastic elastomers that meet the following requirements:

1). The polymer needs to be synthesized in hydrocarbon solvent at mild temperature, since most of the anionic polymerization capability in industry is designed for synthesis of PS-PI-PS triblock copolymer type thermoplastic elastomers under inert atmosphere in cyclohexane at around 60 °C. TPEs based on methyl methacrylate derivatives showed higher upper service temperature; however, polymerization in THF at -78 °C would not be a favorable choice for large-scale production.^{2,3} Another reason to avoid using THF as the solvent is that polymerizing isoprene or butadiene in THF increases the presence of the 1,2-microstructure, which compromises the elasticity.

2). For high temperature applications, the upper service temperature of the thermoplastic elastomers needs to be higher than 100 °C. One potential application of high temperature TPEs is to replace or reduce the amount of carbon black in tire compounding as a rigid filler. Since polymer weigh less than carbon black, reducing the amount of carbon black in tire would produce tires with lower weight, thus better fuel economy. However, this application received limited success with SIS TPEs due to the low glass transition temperature of PS.

3). Building blocks in the triblock copolymers need to microphase separate in order to form an efficient physical crosslink structure that enhances the tensile properties. Thus, exploring new building blocks with above mentioned requirements to prepare thermoplastic elastomers with high upper service temperature is of great interest in the anionic polymerization community.

Benzofulvene is a rigid conjugated diene monomer recently discovered to undergo living anionic polymerization in both the hydrocarbon solvent benzene at room temperature and the polar solvent THF at -78°C and produce polymers with T_g above 145°C .^{4,5} (**Figure 2.1**) This high temperature polymer with living anionic polymerization ability in hydrocarbon solvent at room temperature triggered our attention to incorporate PBF as a rigid block for TPE applications, since most of the reactors for anionic polymerization in pilot plants are designed for mild temperature polymerization in hydrocarbon solvents. Thus, the first motivation in this dissertation is to *evaluate the possibility of preparing ABA triblock copolymers with polybenzofulvene as the glassy end blocks and polyisoprene as the elastic middle block for high temperature thermoplastic elastomer applications.*

Well-defined multi-grafted copolymers PI-g-(PS)_n (n=1,2,3) with polystyrene as the glassy side chain and polyisoprene as the elastic backbone, indeed, showed great mechanical properties competitive with or greater than Kraton products. Considering the fact that preparing these materials required complicated titration anionic polymerization

techniques and time consuming solvent/non-solvent fractionation,^{6,7} the second motivation is to *develop a cost effective strategy to prepare graft copolymers for thermoplastic elastic application.*

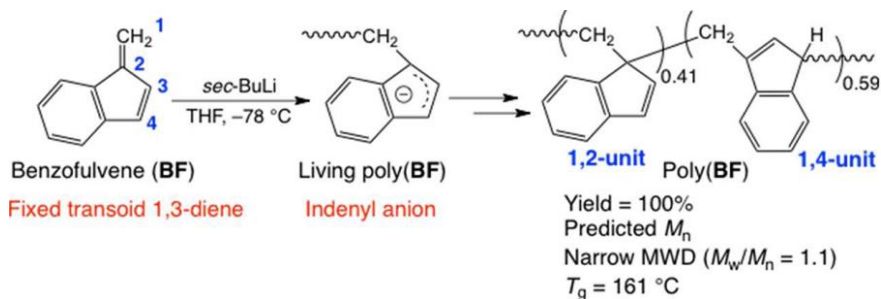


Figure 2.1: Anionic polymerization of benzofulvene⁴

2.2 Outline:

As **Chapter 1** summarized recent advances in the field of thermoplastic elastomers by using synthetic polymers, **Chapter 2** introduces the scope of the dissertation, and the rest of this thesis is arranged as follows:

Chapter 3 gives the overview of most experimental techniques with high vacuum lines used in this dissertation.

Chapter 4 describes the work of developing high temperature thermoplastic elastomers based on polybenzofulvene as the hard segment.

Chapter 5 describes further investigations into the effects of partial and complete hydrogenation on the properties of polybenzofulvene based TPEs.

Chapter 6 describes an economically viable method to prepare thermoplastic elastomers combining anionic polymerization and emulsion polymerization.

Chapter 7 concludes this thesis and provides future perspectives.

References:

- [1]. Geoffrey, H.; Ralph, M., Block polymers of monovinyl aromatic hydrocarbons and conjugated dienes. U.S. Patent No. 3,265,765: **1966**.
- [2]. Yu, J. M.; Dubois, P.; Jérôme, R. *Macromolecules* **1996**, 29 (26), 8362-8370.
- [3]. Yu, J. M.; Dubois, P.; Jérôme, R. *Macromolecules* **1996**, 29 (23), 7316-7322.
- [4]. Kosaka, Y.; Kitazawa, K.; Inomata, S.; Ishizone, T. *ACS Macro Letters* **2013**, 2 (2), 164-167.
- [5]. Kosaka, Y.; Kawauchi, S.; Goseki, R.; Ishizone, T. *Macromolecules* **2015**, 48 (13), 4421-4430.
- [6]. Iatrou, H.; Mays, J. W.; Hadjichristidis, N. *Macromolecules* **1998**, 31 (19), 6697-6701.
- [7]. Uhrig, D.; Mays, J. W. *Macromolecules* **2002**, 35 (19), 7182-7190.

Chapter 3: Experimental Techniques

3.1 High Vacuum Manifold:

Due to the high purity requirements for the monomers, additives and solvents involved in anionic polymerization and anion sensitivity to moisture and oxygen, a high vacuum manifold (**Figure 3.1**) with vacuum level less than 10^{-6} mbar is generally employed in order to preserve the anion reactivity, especially for the synthesis of macromolecules with complicated architectures. In a typical high vacuum manifold assembly, a mechanical pump provides rough vacuum lower than 10^{-4} mbar. By connecting the mechanical pump with a diffusion pump with refluxing oil or mercury, the vacuum level can be further decreased to 10^{-5} to 10^{-7} mbar which is suitable for reagent purification and anionic polymerization. Connecting a liquid nitrogen trap between diffusion pump and manifold is mandatory in order to condense volatile chemicals and prevent damaging refluxing fluid in diffusion pump. The main vacuum line is equipped with high vacuum valves connected with glass ports of different sizes on which to attach reactors and solvent cylinders onto the vacuum line. ^{1,2,3}

3.2 Anionic Polymerization by High Vacuum Techniques:

Considering the sensitivity of anions towards moisture, oxygen and other protonic impurities, purging the polymerization reactors with n-BuLi solution in hexane is generally recommended in pursuance of “living” anionic polymerization. Taking anionic polymerization of styrene as an illustration:

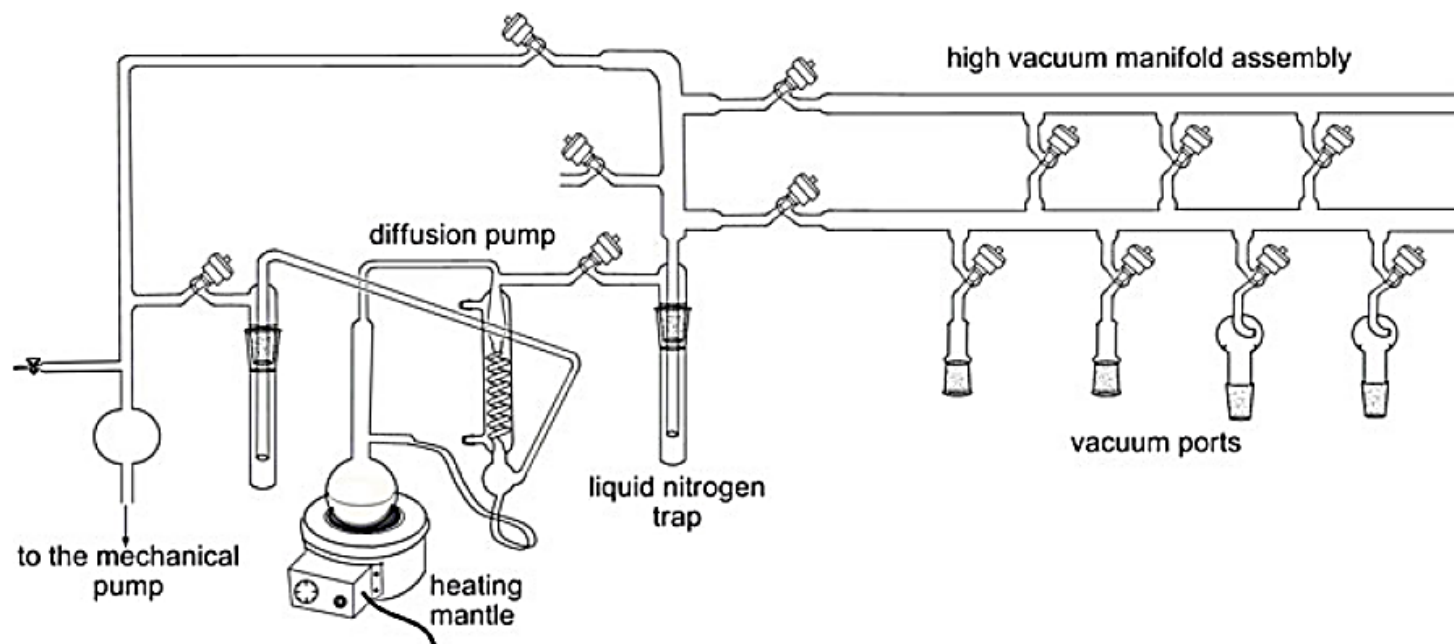


Figure 3.1: High vacuum manifold³

(1). Ampoules of monomer styrene (10 g), initiator *sec*-BuLi (0.5 mmol) and terminator methanol (1 ml) were assembled on a customized all glass apparatus and attached onto the high vacuum line (**Figure 3.2**).

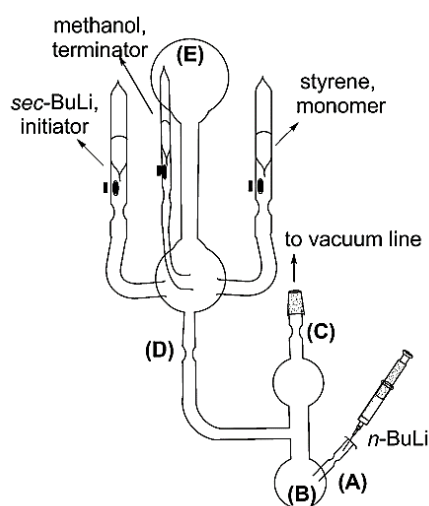


Figure 3.2: Glass apparatus for anionic polymerization of styrene³

(2). Upon checking for pinholes, 5 to 10 ml of *n*-BuLi (1.6 M in hexanes) was injected into the purging section (B) and sealed by a hand torch through a constriction (A). The reactor was separated from the constriction (C) after 125 ml of benzene was distilled into the reactor and degassed twice.

(3). The benzene and *n*-BuLi solutions were mixed and decanted over the entire apparatus in order to remove any contaminations in the glass apparatus. Flask (B) was kept

in a warm water bath after all washing solution was transferred into flask (B). The remaining n-BuLi on the glass surface was washed off by refluxing benzene over the entire apparatus by using liquid nitrogen and a towel.

(4). The apparatus was placed in a horizontal position as shown in **Figure 3.3**. All benzene was distilled from the purging section (B) using a warm water bath to main reactor (E) in an ice bath. The purging section was removed through constriction D after 100 ml of benzene was transferred into E.

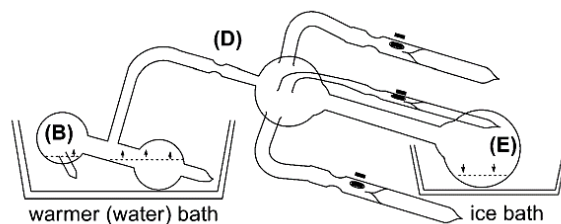


Figure 3.3: Distill benzene in anionic polymerization apparatus³

(5). The reactor was placed in a reversed vertical position with pure benzene in the main reactor (E) (**Figure 3.4**). The styrene ampoule was first ruptured and mixed with benzene. The color of the solution turned orange immediately when sec-BuLi was introduced into the solution. After 8 h, methanol was introduced into the reactor to terminate the reaction.

(6). After termination the polymer solution in benzene was poured into a large excess of methanol. The precipitation was filtered and dried in the vacuum oven at 40 °C for 24 h to remove residual solvent.

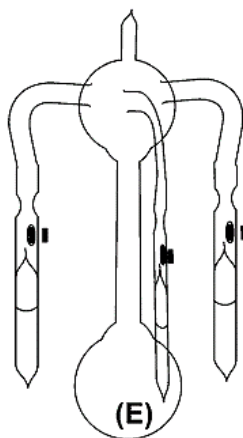


Figure 3.4: Final reactor for anionic polymerization³

3.3 Synthesizing anionic initiator:

The most commonly used anionic initiator *sec*-BuLi was prepared by reacting lithium metal with *sec*-BuCl in hexane. The following procedure is used with high vacuum techniques (**Figure 3.5**):

(1). After checking for pinholes in the customized glass apparatus, the lithium metal was transferred into (A) under inert atmosphere and the apparatus is connected to the vacuum line. 5 to 10 ml of *n*-BuLi was injected into the reactor through septum (B) and

afterwards the vacuum level was restored. Constriction (C) was sealed by using a hand torch under high vacuum.

(2). The apparatus was separated from the manifold through constriction (D) after the desired amount of hexane was distilled into the reactor (E). The entire apparatus was washed with a hexane/n-BuLi mixture and the purging section was separated from the main reactor through constriction (I) after the desired amount of hexane was distilled into the main reactor (F). (Washing procedure was similar to that used in polymerization of styrene.)

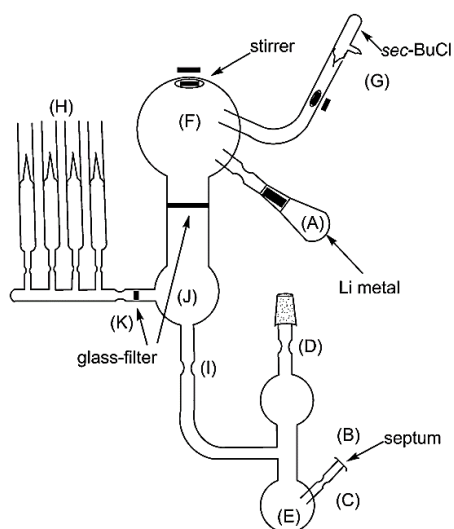


Figure 3.5: Glass apparatus to prepare sec-BuLi ³

(3). Sec-BuCl was slowly distilled into lithium/hexane mixture at 0 °C under magnetic stirring and the reactor was kept in the ice bath for 15 h.

(4). Unreacted lithium was separated with *sec*-BuLi solution in hexane through the glass filter. The initiator solution was finally transferred into pre-calibrated ampoules (H) and stored at -30 °C.

Additives like *sec*-BuOLi in hexane and other initiators such as *n*-BuLi solution in hexane or (1,3-phenylene)bis(3-methyl-1-phenylpentylidene) dilithium initiator in benzene could be prepared by similar procedures.

References:

- [1]. Hadjichristidis, N.; Iatrou, H.; Pispas, S.; Pitsikalis, M. *Journal of Polymer Science Part A: Polymer Chemistry* 2000, 38 (18), 3211-3234.
- [2]. Uhrig, D.; Mays, J. W. *Journal of Polymer Science Part A: Polymer Chemistry* 2005, 43 (24), 6179-6222.
- [3]. Ratkanthwar, K.; Hadjichristidis, N.; Mays, J., *High Vacuum Techniques for Anionic Polymerization*. In *Anionic Polymerization*, Springer: 2015; pp 19-59.

**Chapter 4: High Temperature Thermoplastic Elastomers Synthesized by Living
Anionic Polymerization in Hydrocarbon Solvent at Room Temperature**

Abstract: Here we present the synthesis and characterization of a new class of high temperature thermoplastic elastomers comprised of polybenzofulvene-polyisoprene-polybenzofulvene (FIF) triblock copolymers. All copolymers were prepared by living anionic polymerization in benzene at room temperature. Homopolymerization and effects of additives on the glass transition temperature (T_g) of polybenzofulvene (PBF) were also investigated. Among all triblock copolymers studied, FIF with 14 vol% of PBF exhibited a maximum stress of 14.3 ± 1.3 MPa and strain at break of 1394 ± 66 % from tensile tests. The stress-strain curves of FIF-10 and 14 were analyzed by a statistical molecular approach using a non-affine tube model to estimate the thermoplastic elastomer behavior. Dynamic mechanical analysis showed that the upper service temperature of FIF is 145°C . Microphase separation of FIF triblock copolymers was observed by small angle X-ray scattering, even though long range order was not achieved under the annealing conditions employed. In addition, the microphase separation of the resulting triblock copolymers was examined by atomic force microscopy.

Keywords: Thermoplastic elastomers, anionic polymerization, high temperature, block copolymer

4.1 Introduction:

Since its discovery and after thriving for almost 60 years,¹ living anionic polymerization has played a critical role in academic and industrial fields of polymer research because well-defined polymers with predictable molecular weight, narrow molecular weight distributions (PDI), and linear to complex macromolecular architecture can be prepared by this technique.^{2,3} Additionally, living anionic polymerization can produce polymers with negligible impurities in quantitative yields and with short production times under industrially relevant conditions. Therefore, anionic polymerization remains more favorable for commercialization as compared to other controlled polymerization techniques.^{4,5}

Styrenic thermoplastic elastomers (STPEs), prepared by living anionic polymerization in hydrocarbon solvents at mild temperatures, are largely used in the fields of paving, roofing, footwear and medical tubing.⁶ Such materials are A-B-A type triblock copolymers consisting of 1,4-polyisoprene ($T_g \sim -56^\circ\text{C}$) or 1,4-polybutadiene ($T_g \sim -90^\circ\text{C}$) as the rubbery B block that is physically cross-linked by glassy A blocks of polystyrene (PS, $T_g \sim 100^\circ\text{C}$) on both ends. The triblock copolymers of polystyrene-*b*-polyisoprene-*b*-polystyrene (SIS), designed first by Milkovich and Holden,⁷ were targeted to improve the green strength and hot tear properties of polyisoprene for production of synthetic rubber

tires in large volume. However, this application failed and other advanced consumptions of STPEs are still largely limited by the glass transition temperature of PS.⁸ When the service temperature is approaching 100 °C, softening of the PS domains weakens the physical cross-link leading to a sharp drop in tensile strength.

Many strategies and alternative monomers have been developed in order to improve the upper service temperature (UST) of TPEs. High T_g polymers such as poly(α -methyl styrene) ($T_g \sim 173^\circ\text{C}$)⁹, or poly(α -methyl *p*-methyl styrene) ($T_g \sim 183^\circ\text{C}$)¹⁰ could be used as an alternative glassy block to replace PS. However, the bulkiness introduced by the methyl group at the α position leads to low ceiling temperatures ($<6^\circ\text{C}$), requiring low polymerization temperatures (-78°C) in polar solvents such as THF in order to achieve quantitative yield. PS derivatives with bulky pendent group at the para position, such as poly(*tert*-butyl styrene) (PtBS, $T_g \sim 130^\circ\text{C}$)¹¹ or poly(*p*-admentyl styrene) (P-AdmS, $T_g \sim 203^\circ\text{C}$)¹² could also increase the UST of TPEs. However, the lipophilic nature introduced by these pendent groups caused phase blending with polydienes and reduced tensile strength. Catalytic hydrogenation to fully saturate PS into poly(vinylcyclohexane) (PVCH, $T_g \sim 147^\circ\text{C}$)^{13,14} produced TPEs with higher UST and better thermal stabilities but these conditions will hydrogenate polydienes at the same time. The additional cost as well as the

complete hydrogenation has limited the development of this approach, especially in applications where unsaturated polydienes are required.

As another approach, anionic polymerization of methyl methacrylate^{15,16} and other methacrylates^{17,18} in THF at -78°C was performed by initiating methacrylate monomer from a difunctional polydiene anion. Since polymerization of butadiene or isoprene in polar solvents will form less cis-1,4 microstructure, and thus dramatically increase the T_g , the difunctional polydiene anion needs to be synthesized in a hydrocarbon solvent. Due to the low polymerization temperature and high cost, this approach is not suitable for large scale industrial application. The various TPEs synthesized by other living/controlled polymerization techniques also showed limited industrial applications. The cationic polymerization to produce high T_g polymers¹⁹⁻²³ has same limitation due to the polymerization temperature. On the other hand, high service temperature TPEs prepared by controlled radical polymerization such as atom transfer radical polymerization, required longer reaction time and pre-termination to control the polymerization, and generally contained metal catalyst.^{24,25}

In this study, we present the synthesis and characterization of A-B-A triblock copolymer type thermoplastic elastomers, with polyisoprene as the elastic B block and polybenzofulvene with a T_g of 145°C ,²⁶⁻²⁸ as the glassy A block, via anionic

polymerization. FIF triblock copolymers with four different compositions were prepared by living anionic polymerization in benzene at room temperature. The tensile testing of FIF samples was carried out to obtain stress-strain curves and the mechanical properties are compared with Kraton D1112P SIS. Based on tensile testing, the optimal chemical composition of FIF for use as a TPE was investigated. Atomic force microscopy (AFM) and small angle X-ray scattering (SAXS) were used to confirm the micro-phase separation between PI and PBF. The effect of additives on the T_g of PBF is also presented.

4.2 Experimental Section:

4.2.1 Materials: Isoprene (Fisher, >99%), *n*-BuLi (Fisher, 2.5M in hexanes), 2-chlorobutane (Fisher, >99%), hexane (Fisher, >99.5%), methanol (Fisher, ≥ 99.9), benzene (Aldrich, ≥ 99.9), cyclohexane (Fisher, >99%), 2-butanol (Aldrich, >99%) were purified according to high vacuum techniques reported previously.³⁰ *Sec*-BuLi was prepared by reacting 2-chlorobutane with Li metal under vacuum. 1,2-Dimethoxyethane (DME, Aldrich, >99.9%) was distilled over CaH₂, potassium dispersion two times and diluted with anhydrous benzene. 1,4-Diazabicyclo[2.2.2]octane (DABCO, Aldrich, >99%) was sublimated three times under high vacuum and diluted with anhydrous benzene. Tetramethylethylenediamine (TMEDA, Aldrich, $\geq 99\%$) was distilled over CaH₂, potassium/sodium alloy and diluted with cyclohexane. Lithium (Aldrich, >99%, granular),

sodium (Aldrich, >99.9%, cubes), potassium (Aldrich, >98%, chunks), indene (TCI, 95%), paraformaldehyde (Aldrich, 95%, powder), potassium tert-butoxide (TCI, 1.0 M in tetrahydrofuran), Ethylmagnesium bromide (Aldrich, 3.0 M in diethyl ether), 1,3-bis(1-phenylvinyl)benzene (PEB, donated by Dow Chemical, >95%), butylhydroxytoluene (BHT, Aldrich, >99%), were used as received. The solution of *sec*-BuLi and *sec*-BuOLi in hexane and the solution of (1,3-phenylene)bis(3-methyl-1-phenylpentylidene) dilithium initiator in benzene were prepared according to reported procedure and diluted into desired concentration.³⁰ Generally, the solution of DLI in benzene was prepared by addition of 2.2 equivalents of *sec*-BuLi (27.06mmol) into 1,3-bis(1-phenylvinyl)benzene (12.3mmol, 3.47g) in hexane (300ml). Since DLI is insoluble in hexane, as the reaction proceeded DLI was precipitated inside the reactor. After removing hexane by filtration, the resulting red solid was diluted with benzene and calibrated by conducting a polymerization with isoprene and measuring the molecular weight of the resulting polymer. Benzofulvene monomer was synthesized based on the literature²⁶, diluted with anhydrous benzene (0.3 to 0.5M), and ampulized under high vacuum condition. All ampoules of monomer, initiator, and additives were stored at -30 °C.

4.2.2 Anionic polymerization of BF monomer: All anionic polymerizations were carried out under high vacuum condition (10^{-6} torr) with purged all glass apparatus

equipped with break seals. In a typical polymerization, the solution of BF (7.03 mmol, 0.900 g) in benzene was introduced into the solution of *sec*-BuLi (0.0235 mmol) in hexane and the solution of polymer was quenched with degassed methanol after 1h. All polymers were precipitated into large excess of methanol, filtered, and dried. After complete drying, 0.5 wt% of BHT as the antioxidant was added into polymer. The characterization of PBF was performed by $^1\text{H-NMR}$, size exclusion chromatography (SEC) and differential scanning calorimetry (DSC). The yield of PBF was quantitative.

4.2.3 Anionic polymerization of BF monomer in the presence of additives: The solution of DME (0.121 mmol) in benzene was introduced into the solution of *n*-BuLi (0.0121 mmol) in hexane at 0 °C using an ice bath and kept at 5 °C. The solution of BF (1.54 mmol, 0.197 g) in benzene was added to the initiation system. After complete polymerization over 1 h, the solution of polymer was quenched with degassed methanol and the purification was performed as described above. For anionic polymerizations of BF monomer in the presence of other additives, similar addition and purification procedure was employed. When *sec*-BuOLi was used as the additive, the polymerization was carried out at room temperature.

4.2.4 Diblock copolymerization of BF and isoprene: For the synthesis of PI-*b*-PBF diblock copolymer, the typical procedure of sequential block copolymerization was

performed. The solution of isoprene monomer (20.58 mmol, 1.4g) in benzene (20 ml) was first introduced into the solution of *sec*-BuLi (0.0668 mmol) in hexane (3 ml). The solution of BF monomer (2.51 mmol, 0.321 g) in benzene (5 ml) was added to the solution of living polyisoprene in benzene after 12h. The solution of diblock copolymer in benzene was terminated by adding degassed methanol after 1 h. The resulting diblock copolymer of PI-*b*-PBF was precipitated into large excess of methanol with 0.5wt% of BHT as the antioxidant, filtered, and dried in vacuum drying oven for 24 h.

4.2.5 Triblock copolymerization of isoprene and BF: In a typical polymerization procedure, DLI and *sec*-BuOLi were first mixed in benzene followed by addition of isoprene. After complete consumption of isoprene, as monitored by SEC over 5 days, BF monomer (5.75 mmol, 0.737 g) was introduced into the solution of living polyisoprene (0.0614 mmol, 4.36 g) in benzene and the resulting solution of this triblock copolymer was terminated with degassed methanol after 8h. All FIF triblock copolymers were precipitated into large excess of methanol with 0.5 wt% of IRGANOX[®] B 225 as the long-term thermal stabilizer. Precipitates were filtered and dried in vacuum oven for 48h.

4.2.6 Preparation of samples: For tensile tests, a solution of 2 g of polymer in 80 ml of toluene was stirred overnight at room temperature and casted into glass bowls with inner diameter of about 90 mm and evaporated slowly over 7 days. Upon removing residual

solvent from the films, all samples were annealed at 70°C under vacuum (10^{-1} torr) and stamped into dog bone shaped specimens (type 5A, ISO 527/2) with film thickness around 0.2-0.3 mm. For dynamic mechanical analysis, polymer solutions were casted into smaller PTFE dishes resulting film thicknesses of 0.5-0.6 mm. For the measurement of small angle X-ray scattering, it was first tried to anneal solvent casted samples at 170 °C for 24 h under N₂ in order to achieve a thermodynamically equilibrated morphology. However, all samples of PI and PBF were thermally cross-linked as evidenced by SEC trace. Thus, all samples were annealed at 155 °C for 12 h under dynamic vacuum. No noticeable cross-linking polymers with high molecular weights were detected by SEC. For atomic force microscopy, the solution of triblock copolymer FIF in toluene with concentration of 2 mg/ml was prepared and spin casted on freshly cleaned mica substrate. The film of triblock copolymer was then annealed at 155°C for 12 h under dynamic vacuum.

4.2.7 Measurements: ¹H- and ¹³C-NMR were measured on a Varian Mercury 500 instrument using deuterated chloroform (CDCl₃) for homopolymers of PBF and using deuterated tetrahydrofuran (THF-*d*₈) for block copolymers of PI-*b*-PBF and PBF-*b*-PI-*b*-PBF (FIF). Molecular weight (MW) and molecular weight distribution (MWD) were measured by size exclusion chromatography in THF at 40 °C with flow rate of 1.0 ml/min using a Polymer Labs GPC-120 SEC equipped with four detectors of a Polymer Labs

refractometer, a Precision Detector PD2040 (two angle static light scattering detector), a Precision Detector PD2000DLS (dynamic light scattering detector), and Viscotek 220 differential viscometer. The column set installed is the Polymer Labs PLgel; 7.5x300 mm; 10 μm ; 500, 1×10^4 , 1×10^6 , and 1×10^7 Å. Glass transition temperature were measured by a TA Instruments Q-2000 differential scanning calorimeter (DSC) from -80 °C to 200 °C at a heating rate of 10 °C/min with a 5 minute isothermal hold at the maximum and minimum temperatures. Reported glass transition temperatures were based on the second heating scans. Thermal stability was examined using a TA instruments Q-50 TGA. A 5-10 mg sample was placed on platinum pan and equilibrated at 30 °C. The temperature was ramped from 30-800 °C at a rate of 10 °C/min under nitrogen atmosphere. Tensile tests were performed with a Zwick/Roell Z050 at the cross-head speed of 15 mm/ min, clamping distance of 50 mm and measuring distance of 15 mm. A multiXtens extensometer was applied to obtain the displacement. For each polymer sample three tensile specimens were tested. Small angle X-ray scattering profiles were obtained from a Rigaku S-Max 3000 using Ni-filtered Cu K α radiation (wavelength is 1.54 Å) operated at 40 kV, 200 mA with pinholes collimation system located 87.52 cm from the sample. Atomic force microscopy (AFM) measurements were performed with Asylum Cypher in tapping mode in air. The probe used for AFM measurement is HiRes-C19/Cr-Au (MikroMasch) with 1 nm radius and 65 kHz resonance.

4.3 Results and Discussion:

4.3.1 Anionic polymerization of BF and glass transition temperature of PBF:

Anionic polymerization of benzofulvene was first carried out in benzene at room temperature (RT) with *sec*-BuLi as an initiator as shown in **Table 4.1**. Controlled molecular weights in the range from 4.8 to 86.4 kg/mol and narrow molecular weight distribution (MWD < 1.16) were achieved until M_n was around 80 kg/mol (**Table 4.1**, runs 1-7, **Figure 4.1**). However, the polymerization of BF targeting 200 kg/mol, as shown in **Table 4.1**, run 8, was uncontrolled and exhibited a bimodal distribution. The calculated M_n of 200 kg/mol was not in good agreement with the observed M_n of 175.2 kg/mol. In contrast to polymerization of BF in THF as previously reported,²⁶ the yellow BF solution in benzene turns to pale yellow in 2 min after mixing with *sec*-BuLi solution in hexane and the polymerization was complete within 1 h (**Table 4.1**, run 1-5). Longer reaction times were required for higher target molecular weights. All polymers were recovered in quantitative yield. The glass transition temperature of PBF increased from 127.0°C and stabilized around 153°C as the M_n was increased from 4.5 kg/mol to 86.4 kg/mol.

Table 4.1 Anionic polymerization of BF in benzene in the absence of additives:

Run	Sample ID	BF (mmol)	Initiator (mmol)	Time (h)	M _n (kg/mol)		M _w /M _n ^c	T _g (°C) ^d
					Calcd ^a	Obsd ^b		
1	PBF-5	3.92	0.111	0.5	4.5	4.8	1.16	127.0
2	PBF-10	1.56	0.0211	0.5	9.5	12.0	1.09	145.7
3	PBF-15	2.34	0.0203	0.5	14.8	14.6	1.08	147.5
4	PBF-20	3.90	0.0255	0.5	19.6	18.9	1.06	151.2
5	PBF-40	7.03	0.0235	1	38.3	42.3	1.08	152.2
6	PBF-60	8.59	0.0183	2	60.1	60.6	1.12	153.4
7	PBF-80	10.16	0.0163	2	79.8	86.4	1.11	153.1
8	PBF-200	16.41	0.0105	6	200	175.2	1.45 ^e	163.5

^a M_n(Calcd) = (MW Monomer) × [BF] / [Initiator]. ^b M_n(Obsd) was characterized by SEC equipped with triple detectors: refractive index (RI), light scattering (LS) and viscometer detectors. ^c M_w/M_n was calculated by SEC with polystyrene standard in THF. ^d T_g was measured by DSC on the second heating scans. ^e Bimodal.

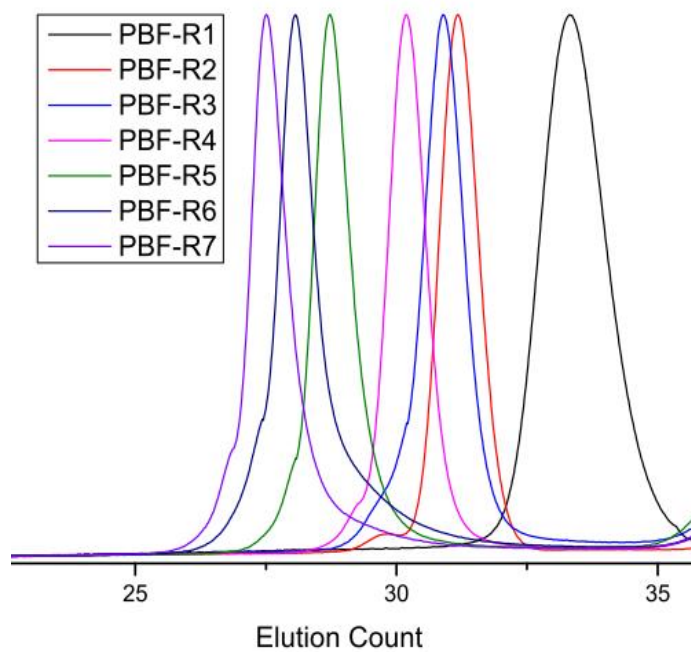


Figure 4.1 SEC curve of PBF synthesized in benzene at room temperature with *sec*-BuLi. (Denote: PBF is polybenzofulvene and R1 to R7 is run 1 to run 7 in Table 4.1)

4.3.2 Effects of additives on glass transition temperature: One feature of anionic polymerization of diene monomers is that different polar additives can change the reactivity of the propagating anion and lead to polymers with different microstructures, i.e. tunable 1,2- and 1,4-addition.⁴ Different from conventional additives which are small molecules added to compound during processing, the terminology “additives” used in this paper are chemicals added during the polymerization to change the microstructure of resulting polymers. Generally, glass transition temperatures (T_g) of polydienes such as polybutadiene and polyisoprene increase as the percentage of 1,2-addition is increased relative to that of 1,4-addition in the polymer chain. For the anionic polymerization of 1,3-cyclohexadiene, controlled polymerization behavior was observed when additives such as 1,4-diazabicyclo[2.2.2]octane (DABCO), tetramethylethylenediamine (TEMEDA) and dimethoxyethane (DME) and were used during the polymerization. The percentage of 1,2-addition in the resulting PCHD was 10%, 28% and 45% with respect to these three additives. The glass transition temperature increased as the percentage of 1,2-addition increased²⁹⁻³⁰. Different from isoprene or butadiene, benzofulvene is a relative bulky monomer like 1,3-cyclohexadiene. Thus, the same initiation systems used in tailing microstructure of 1,3-cyclohexadiene were employed in this research to study the effects of additives on the homo-polymerization behavior of PBF and the T_g of resulting polymers.

Additives used in this work are listed in **Figure 4.2** and results of anionic polymerization are summarized in **Table 4.2**. The anionic polymerization of BF using DME as additive was performed with *n*-BuLi around 5 °C and produced well-defined PBF with controlled molecular weight and narrow MWD (MWD < 1.16) (run 9 and 10 in **Table 4.2**). The additive *sec*-BuOLi (lithium *sec*-butoxide) (run 13, 14 in **Table 4.2**) was utilized for anionic polymerization of BF at RT with *sec*-buLi as the initiator and the MW and MWD were controlled like anionic polymerization with DME. For the anionic polymerization of isoprene and butadiene, it has been observed that *sec*-BuOLi has less effects on polydiene microstructure and T_g compare to the polymerization without any additives. PBF prepared by using *sec*-BuOLi showed lower $T_g = 142.3^\circ\text{C}$ and 153.1°C which is similar to polymerization without any additives. Other polymerizations using as additives either 1,4-diazabicyclo[2.2.2]octane (DABCO) or tetramethylethylenediamine (TEMEDA) were carried out at RT but both polymerizations were uncontrolled since broad MWDs were obtained and multimodal curves were observed in SEC. Among the polymerizations using various additives, 12% and 86% yield was obtained using the TEMEDA and DABCO system respectively, while other polymerizations demonstrated almost quantitative yield.

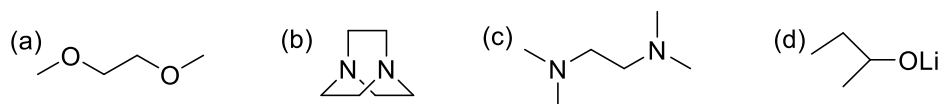


Figure 4.2 Additives for anionic polymerization of BF in benzene: (a) DME, (b) DABCO, (c) TMEDA, and (d) *sec*-BuOLi for anionic polymerization of BF.

Figure 4.3 showed the relationship of glass transition temperature of these homopolymers with molecular weight and type of additive. As the molecular weight of PBF (run 1 to run 8 in **Table 4.1**) increased from 4.8k to 175.2k, T_g increased from 127.0 to 163.5 °C gradually but molecular weight has a slight effect on T_g as seen in the plot with black squares in **Figure 4.3**. On the other hand, a type of additive was significantly dominant to the T_g of PBF as shown in **Table 4.2** and **Figure 4.3** because T_g of PBF, changed by polymerization condition using a different type of additive, is attributed to microstructure of 1,2- and 1,4-addition. The PBF, prepared via anionic polymerization with an additive of DME, has highest T_g of above 190 °C (**Figure 4.3**, red circles) because this PBF has almost 99% of 1,2-addition microstructure which was analyzed by NMR spectra. Especially, the PBF with 39.0 kg/mol synthesized using DME exhibited higher T_g of 198.7 °C than 191.5 °C of PBF with 15.9 kg/mol. The PBF synthesized with an additive of DABCO also has high T_g of 187 °C but M_n and MWD of PBF was uncontrolled. The uncontrollable PBF was synthesized in the presence of TMEDA but this polymer showed similar T_g of 155.2 °C to the T_g of PBF synthesized without additive (run 4 to run 7 in

Table 4.2 Anionic Polymerization of BF in benzene in the presence of additives.

Run	Sample ID	BF (mmol)	Initiator (mmol)	[Additive] [Initiator]	Mn (kg/mol)		M _w /M _n ^c	Yield (%)	T _g (°C) ^d
					Calcd ^a	Obsd ^b			
9	PBF_DME_16	1.54	0.0121	10	16.3	15.9	1.10	99%	191.5
10	PBF_DME_40	3.08	0.0099	10	40.0	39.0	1.12	98%	198.7
11	PBF_DABCO_20	3.18	0.0201	3	20.3	28.5	1.86 ^e	86%	187.0
12	PBF_TMEDA_20	3.40	0.0220	1	19.8	12.2	2.35 ^e	12%	155.2
13	PBF_sec-BuOLi_7	3.16	0.0554	10	7.3	6.9	1.16	99%	142.3
14	PBF_sec-BuOLi_23	4.05	0.0228	10	22.7	23.1	1.10	99%	153.1

^a M_n(Calcd) = (MW Monomer) × [BF] / [Initiator]. ^b M_n(Obsd) was characterized by SEC equipped with triple detectors: refractive index (RI), light scattering (LS) and viscometer detectors, dn/dc of PBF was 0.227. ^c M_w/M_n was calculated by SEC with polystyrene standard in THF. ^d T_g was measured by DSC on the second heating scans. ^e Multimodal. Initiator: *n*-BuLi (run 9,10) and *s*-BuLi (run 11 to 14).

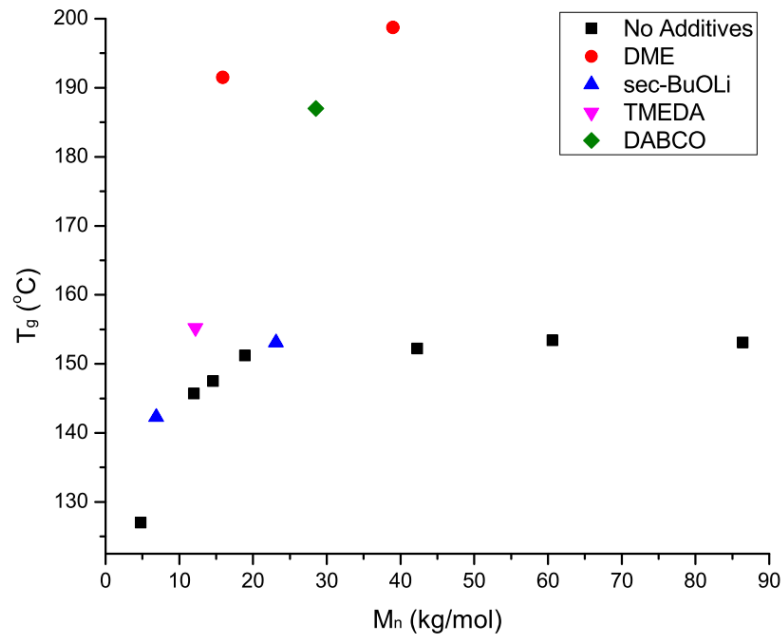


Figure 4.3 T_g versus M_n of PBF synthesized with different additives: DME (red cycle), sec-BuOLi (blue triangle), TMEDA (pink triangle), DABCO (green square) and no additives (black square).

Table 4.1). PBF synthesized with *sec*-BuOLi followed the same increasing trend of PBF prepared without additives.

4.3.3 NMR analysis of PBF synthesized without additive and with DME as the additive: In order to analyze the microstructure of PBF, we tracked chemical shifts of three different carbons: C_x for quaternary carbon in 1,2-addition, C_y for methylene carbon in between 1,2- and 1,4- addition and C_z for tertiary carbon of 1,4-addition. According to previous report, there were four possible dimers in polybenzofulvene if stereoregularity was not taken into consideration: h-1,4-1,4-t; h-1,4-1,2-t; h-1,2-1,4-t and h-1,2-1,2-t. Here, h means head and t means tail in the structure (**Figure 4.4**). In **Figure 4.5**, signal at 57 ppm was assigned to C_x in both PBF-10 and PBF-DME-16 since this signal was only observed in ^{13}C -NMR. Signals at 46 ppm and 48 ppm for PBF-10 (a and b in **Figure 4.5**) were assigned to C_z since these signals were observed in both ^{13}C -NMR and positive phase in DEPT-135. Integration from quantitative ^{13}C -NMR of C_x and C_z showed 26% of 1,2-addition in PBF-10. Surprisingly, C_z signal was not observed in PBF-DME-16 and only C_y signal was observed from 25 ppm to 50 ppm. Thus, the microstructure in PBF-DME-16 was dominated by 1,2-addition.

4.3.4 Diblock Copolymerization of BF with Isoprene: In order to synthesize A-B-A type triblock copolymers of polybenzofulvene-*b*-polyisoprene-*b*-polybenzofulvene (PBF-*b*-PI-*b*-PBF) with PI as elastic block (B) and PBF as glassy block (A), the relative

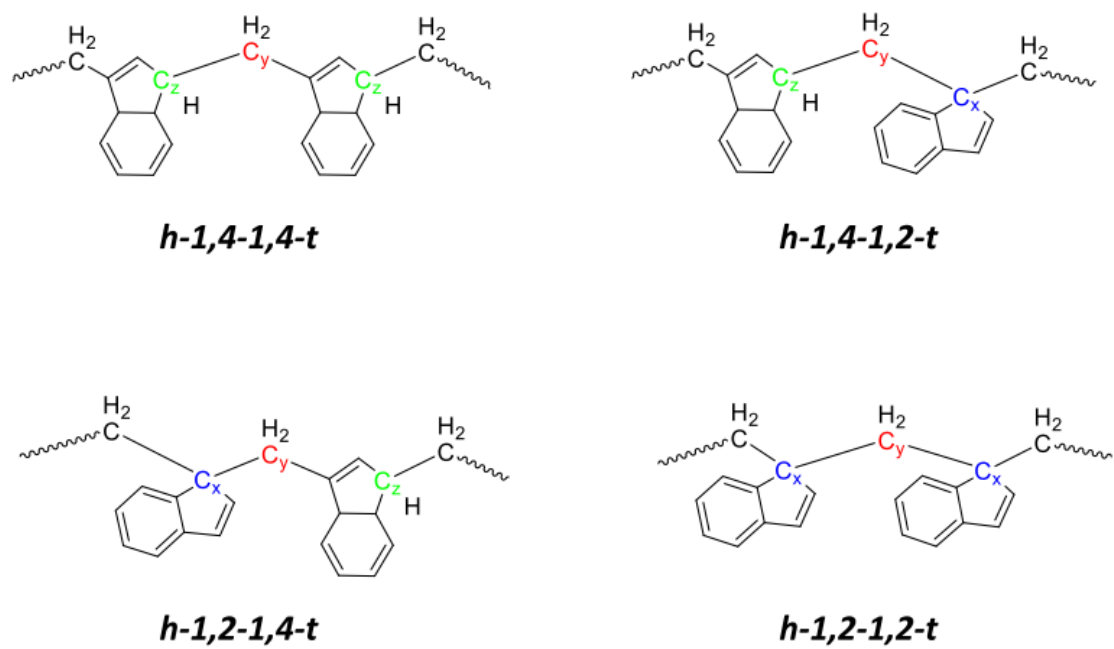


Figure 4.4 Possible dimers of PBF

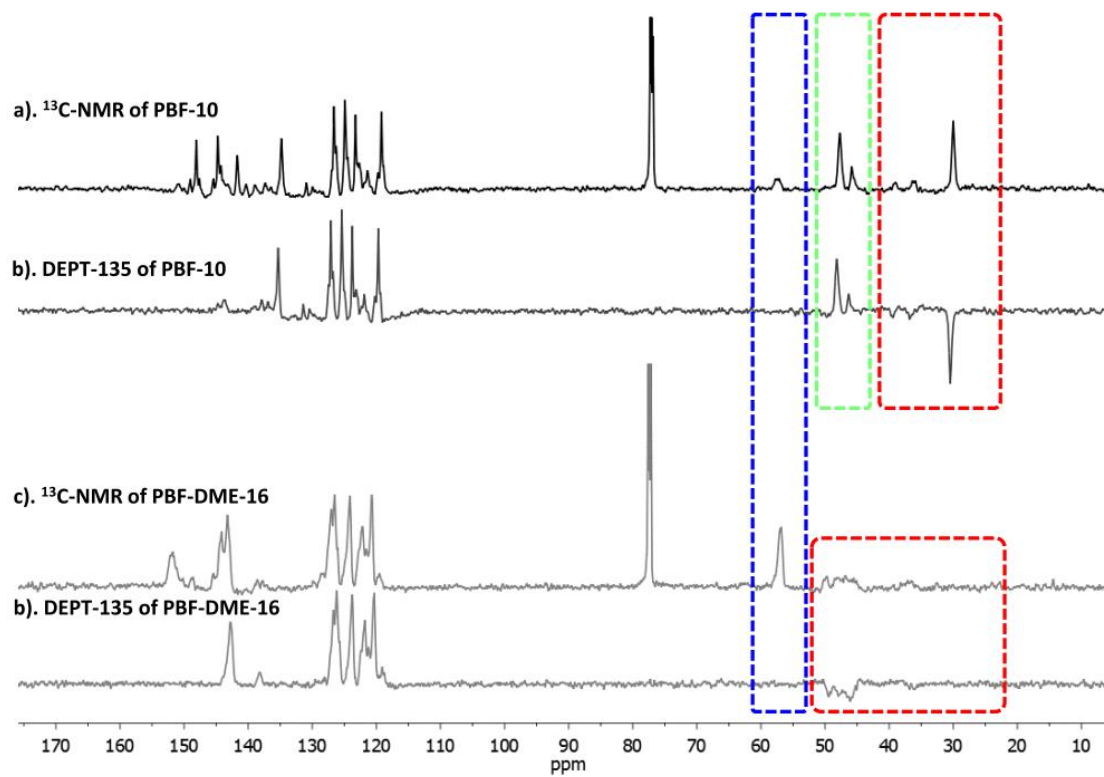


Figure 4.5 ^{13}C -NMR of PBF: a) ^{13}C -NMR of PBF-10, b) DEPT of PBF-10, c) ^{13}C -NMR of PBF-DME-16, d) DEPT of PBF-DME-16

reactivity of isoprene and benzofulvene in benzene was investigated, firstly by synthesizing diblock copolymers of PI-*b*-PBF and PBF-*b*-PI via sequential anionic polymerization with a mono-directional initiator of *sec*-BuLi. Based on the previous report that benzofulvene could be initiated by enolated living poly(methyl methacrylate) lithium anion in THF,²⁶ the well-defined PI-*b*-PBF diblock copolymer was prepared successfully by sequential anionic polymerization with quantitative yield, controlled MW, and narrow MWD (run 15 in **Table 4.3, Figure 4.6**). On the other hand, the opposite sequential addition of BF as the first monomer and isoprene as the second monomer for the block copolymerization produced only homopolymer of PBF and no block copolymers of PBF-*b*-PI. This indicated the electrophilicity of the BF monomer is higher than that of isoprene monomer and the nucleophilicity of living polyisoprene is higher than that of living polybenzofulvene. Thus, isoprene monomer could not be initiated by the polybenzofulvenyl lithium anion (run 16 in **Table 4.3**). This result of crossover initiation between isoprene and benzofulvene monomer is consistent with previous publication.

4.3.5 Triblock Copolymerization of BF with Isoprene: For the above reasons, neither sequential anionic polymerization using BF monomer as first monomer nor anion coupling reaction using polybenzofulvenyl lithium anion could be used to prepare polybenzofulvene-*b*-polyisoprene-*b*-polybenzofulvene (FIF) triblock copolymers. To synthesize FIF triblock copolymers with four different compositions (**Scheme 4.1**), a new

Table 4.3 Diblock Copolymerization of isoprene and benzofulvene.

Run	Sample ID	Initiator (mmol)	Monomer (mmol)		First Homopolymer (kg/mol)			Diblock Copolymer (kg/mol)		
			1st	2ed	Calcd ^a	Obsd ^b	M _w /M _n	Calcd ^c	Obsd ^b	M _w /M _n ^d
15	PI-b-PBF	0.0668	Isoprene 20.58	BF 2.51	21.0	21.2	1.05	25.8	25.6	1.12
16	PBF-b-PI	0.0334	BF 3.34	Isoprene 18.5	12.8	13.6	1.09	50.5	13.6	1.09

^a M_n(Calcd) = (MW Monomer) × [Isoprene] / [Initiator]. ^b M_n(Obsd) was characterized by SEC equipped with triple detectors: refractive index (RI), light scattering (LS) and viscometer detectors. ^c M_n(Calcd) = (MW Monomer) × [BF] / [Initiator]. ^d M_w/M_n was calculated by SEC with polystyrene standard in TH

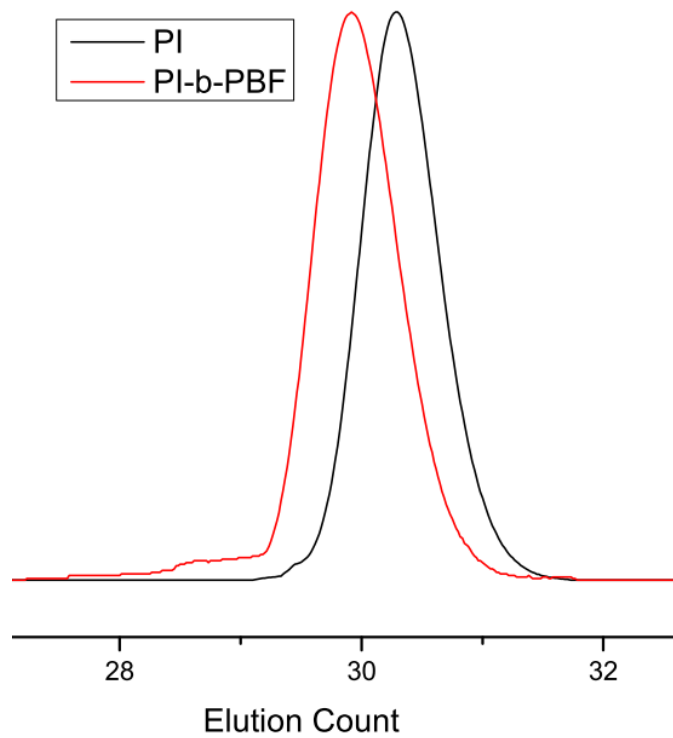
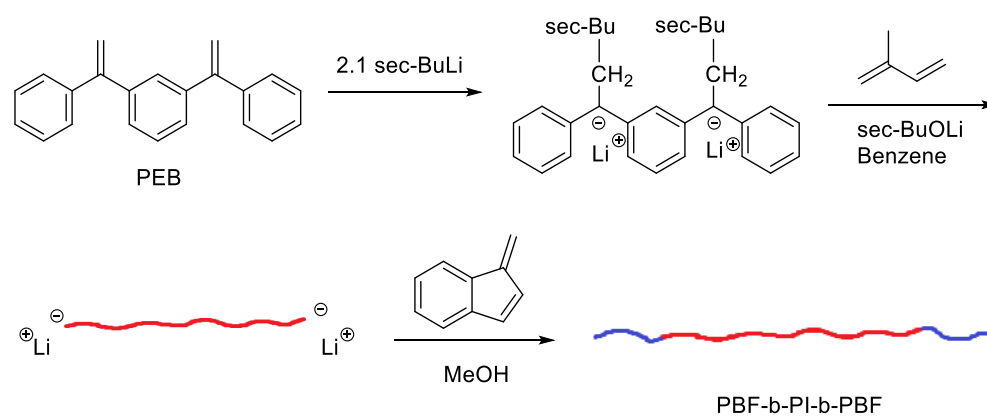


Figure 4.6 SEC curve of PI and PI-*b*-PBF diblock copolymer.



Scheme 4.1 DLI approach to synthesize FIF triblock copolymer

approach involving the initiation system of difunctional lithium initiator (DLI)/*sec*-BuOLi (molar ratio = 10), prepared in benzene at room temperature, was employed. FIF with 9.5 vol% (FIF-10), 13.6 vol% (FIF-14), 22.0 vol% (FIF-22) and 30.9 vol% (FIF-31) PBF were prepared by this DLI approach (**Table 4.4**). In FIF-10, 22 and 31 (run 17-19), the M_n of PI is 76.6 kg/mol, whereas FIF-14 (run 20) has 87.6 kg/mol of PI M_n . All resulting triblock copolymers have narrow MWDs and predicted molecular weight, which were confirmed by SEC (**Figure 4.7**) and $^1\text{H-NMR}$ (**Figure 4.8**). Using FIF-22 as an example (**Figure 4.8**), signals of 6.75ppm to 7.60 ppm, 4.95ppm to 5.25ppm, and 4.55ppm to 5.80ppm in the $^1\text{H-NMR}$ spectra corresponds to aromatic proton (H_a) in PBF block, 1,4-addition proton (H_b) in PI block, and 3,4-addition proton (H_c) in PI block, respectively. According to the analysis of $^1\text{H-NMR}$ spectra, it was confirmed that PI block in FIF triblock copolymers has 93% of 1,4-addition. The volume percentage of PBF presented in FIF was calculated based on integration $^1\text{H-NMR}$ with the density of PBF homopolymers of 1.146 g/cm³ as well as on SEC as listed in **Table 4.4**. The density of polyisoprene used in this paper was 0.926 g/cm³.

4.3.6 Dynamic Mechanical Analysis (DMA): The UST of FIF triblock copolymers was examined by dynamic mechanical analysis. As the temperature was ramped from -100°C to 200°C with frequency of 10 rad/s, the first a relaxation process α_{PI} was observed at -54 °C which corresponds to the T_g of rubbery material PI. As evidence of the increasing of

Table 4.4 Composition of FIF triblock copolymers.

run	Sample ID	PI kg/mol		FIF kg/mol		PBF kg/mol	ϕ_{PBF} %	
		M_n^a	M_w/M_n^b	M_n^a	M_w/M_n^b	M_n^c	NMR	SEC
17	FIF-10	76.7	1.08	87.8	1.08	5.6	9.5	10.1
18	FIF-22	76.7	1.08	98.2	1.10	10.7	22.0	19.1
19	FIF-31	76.7	1.08	106.0	1.09	20.0	30.9	30.1
20	FIF-14	87.6	1.11	110.6	1.14	11.5	13.6	12.8

^a M_n of PI and FIF was characterized by SEC equipped with triple detectors: refractive index (RI), light scattering (LS) and viscometer detectors. ^b M_w/M_n was calculated by SEC with polystyrene standard in THF. ^c M_n of PBF was calculated from $(M_{n,\text{FIF}} - M_{n,\text{PI}}) / 2$.

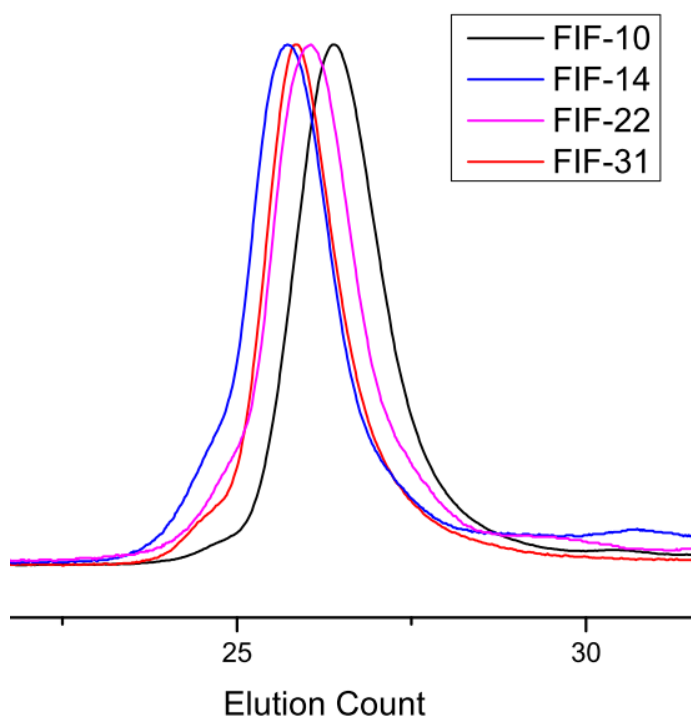


Figure 4.7 SEC curve of FIF triblock copolymers.

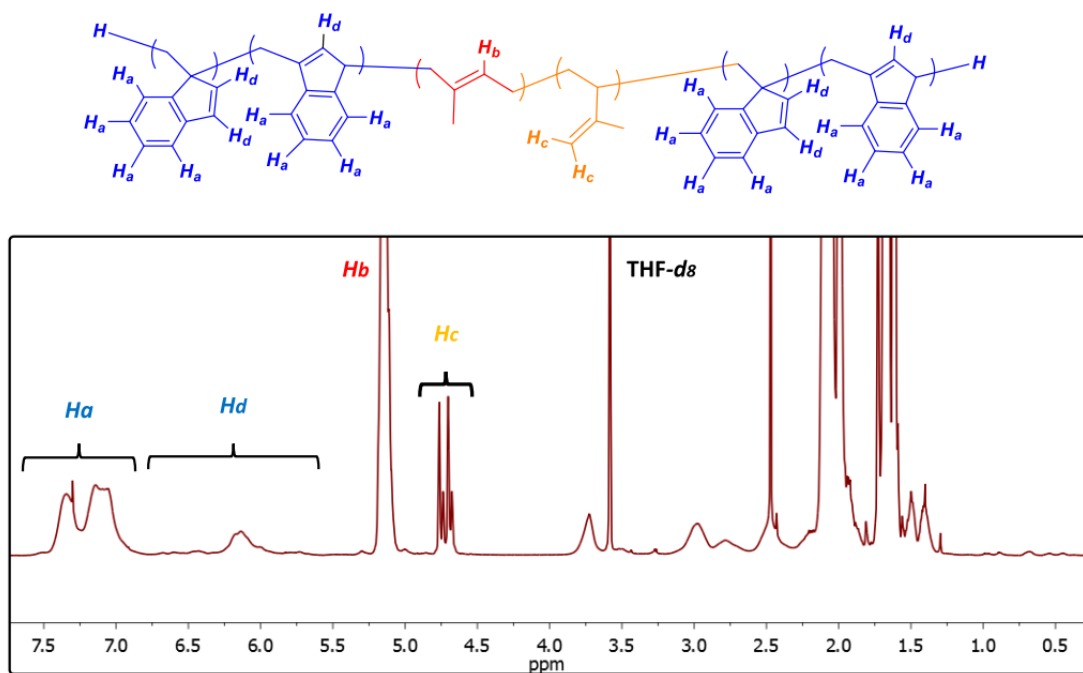


Figure 4.8 $^1\text{H-NMR}$ of FIF-22 measured in $\text{THF-}d_8$.

upper service temperature (**Figure 4.9. a**), the storage modulus of FIF-14, 22 and 31 starts to drop when the ramping temperature approaches 143 °C, indicating the existence of a second relaxation process α_{PBF} corresponding to the softening of the of the PBF component. Accordingly, the temperature where this happens were consist with the T_g of PBF measured by DSC. The storage modulus G' of different samples in the plateau range between the glass transition temperatures of both component was expectedly increased as the volume percentage of PBF was increased. This change in G' is accompanied by an increase in the loss modulus in the range between both T_g 's (**Figure 4.9 b**) indicating the occurrence of a larger fraction of interfacial material with increasing PBF content. Note that a broad additional relaxation process with a maximum at about 30°C was observed for samples with higher PBF contents (FIF-22, 31). This is a clear hint that there are not only pure PI and PBF phases but also a lot of interphase containing isoprene and BF units. A direct consequence of this additional intermediate relaxation peak in $G''(T)$ in samples with larger PBF volume fraction is the increasing slope dG'/dT in the storage modulus.

4.3.7 Stress-strain behavior of FIF triblock copolymers: After confirming the UST, the tensile strength of FIF triblock copolymers was tested. It was found that the Young's modulus (E), tensile stress (σ) and strain at break (ϵ_B) could be tuned based on the volume fraction of PBF (**Table 4.5**). The rather low Young's Modulus for FIF-10 and FIF-14 gives indications for a non-continuous hard phase in the rubbery matrix. Specifically,

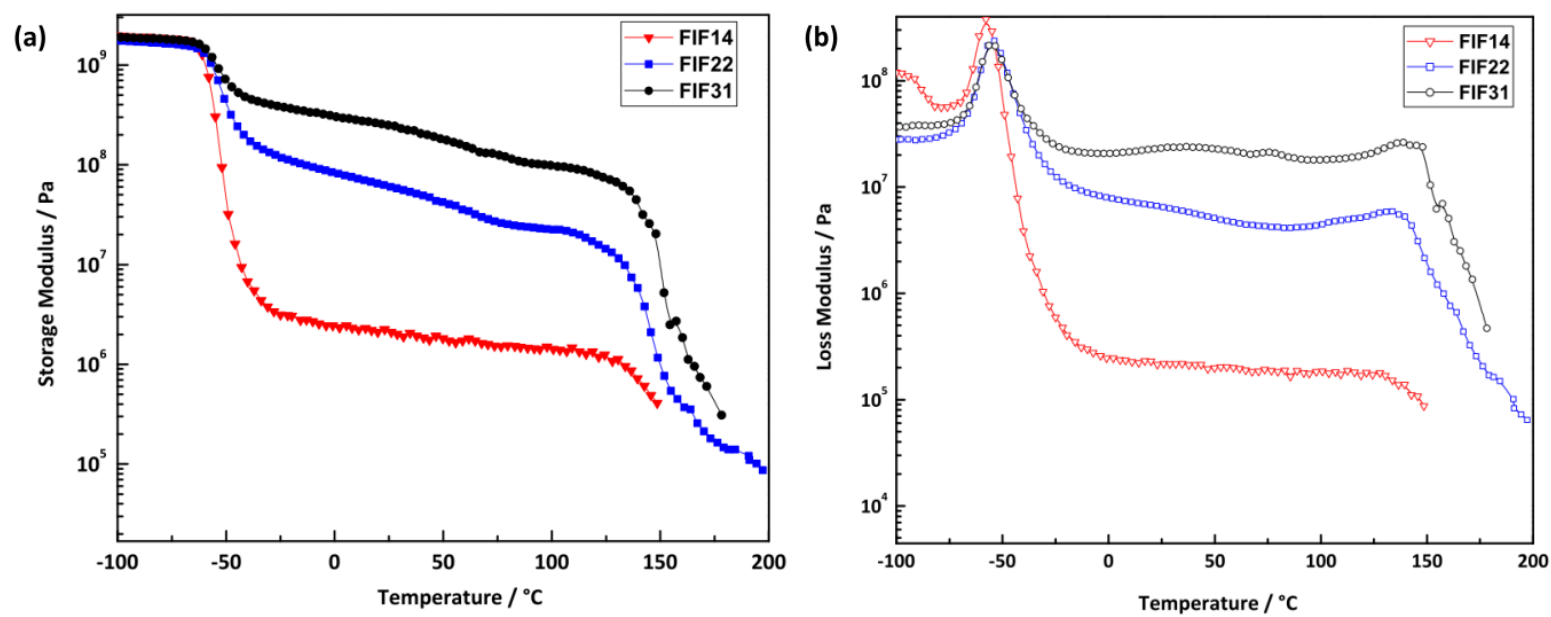


Figure 4.9 DMA of FIF triblock copolymers: (a) Storage Modulus vs. Temp. and (b) Loss Modulus vs. Temp.

Table 4.5 Mechanical property parameters of FIF

Sample ID	Tensile Test			Non-affine Tube Model			
	E / [N/mm ²]	σ_M / [MPa]	ε_B / [%]	G_c / [kPa]	G_e / [kPa]	n	fit range
FIF-10	2.8 ± 0.2	1.91 ± 0.30	855.3 ± 143.1	$151,3 \pm 3,8$	321 ± 22.9	644 ± 39	1 - 7.8
FIF-14	2.6 ± 0.2	$14,3 \pm 1.3$	1394 ± 65.7	240 ± 25	352 ± 15	346 ± 8	1 - 11
FIF-22	16.4 ± 0.4	1.52 ± 0.03	160.3 ± 27.8				
FIF-31	246.0 ± 11.5	5.28 ± 0.03	30.8 ± 2.5				

FIF-14 displayed highest strain at break of $1394.4 \pm 65.7\%$ and best tensile strength of 14.3 ± 1.3 MPa (**Figure 4.10**) among all samples. These tensile properties were competitive with Kraton D1112P, a commercial SIS triblock copolymer used in sealants, coating, adhesives and other elastomer modification. (For Kraton D1163P, ultimate tensile strength is 10.34 MPa, strain at break is 1400 %) ²⁹. The typical TPEs behavior of FIF-14 was demonstrated with efficient physical crosslink between main chains in the system of FIF.

Statistical molecular analysis with a non-affine tube model was used to fit the stress-strain curve of FIF-10 and FIF-14 in order to estimate modulus corresponding to chemical cross links (G_c), entanglements (G_e) and number of segments between two successively trapped entanglements ($n = n_e/T_e$).³¹ Three types of failure characteristics observed for the FIF-polymers: i) FIF-10 shows an elastomeric behavior at the beginning but no strain hardening is found. This gives rise to the assumption that the physical cross links are less effective here: there is no sufficient interaction between the PBT-grafts within the domains so that they are pulled out easily. ii) For FIF-14 a strain hardening region is clearly observed indicating that the higher molecular weight of the PBF-grafts effectively hinders stress induced reptation of the PI-chains. This results in a stronger cross-link network in FIF-14 (**Table 4.5**). However at high strains, deviations between model and experimental data can be observed for FIF-14, indicating that physical cross links become weak resulting plastic deformation (**Figure 4.11**). iii) FIF-22 and FIF-31 are showing rather thermoplastic

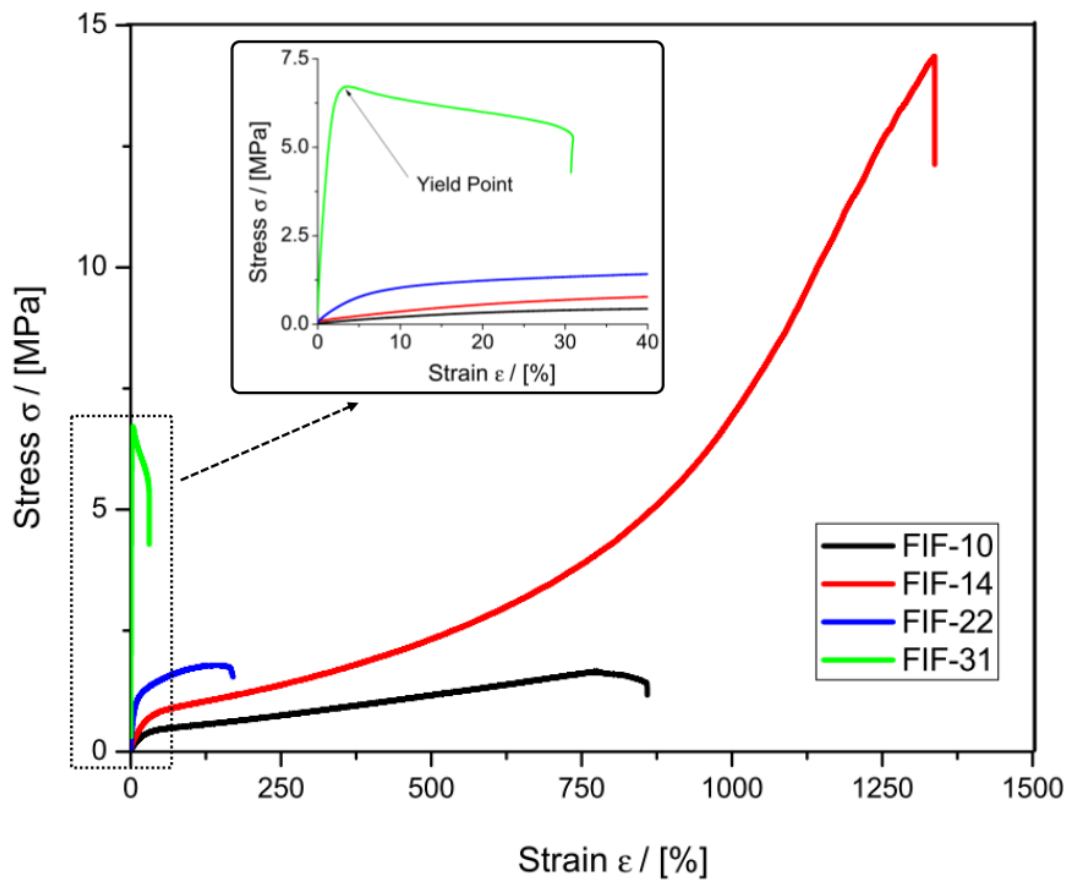


Figure 4.10 Stress-strain curve of FIF triblock copolymers

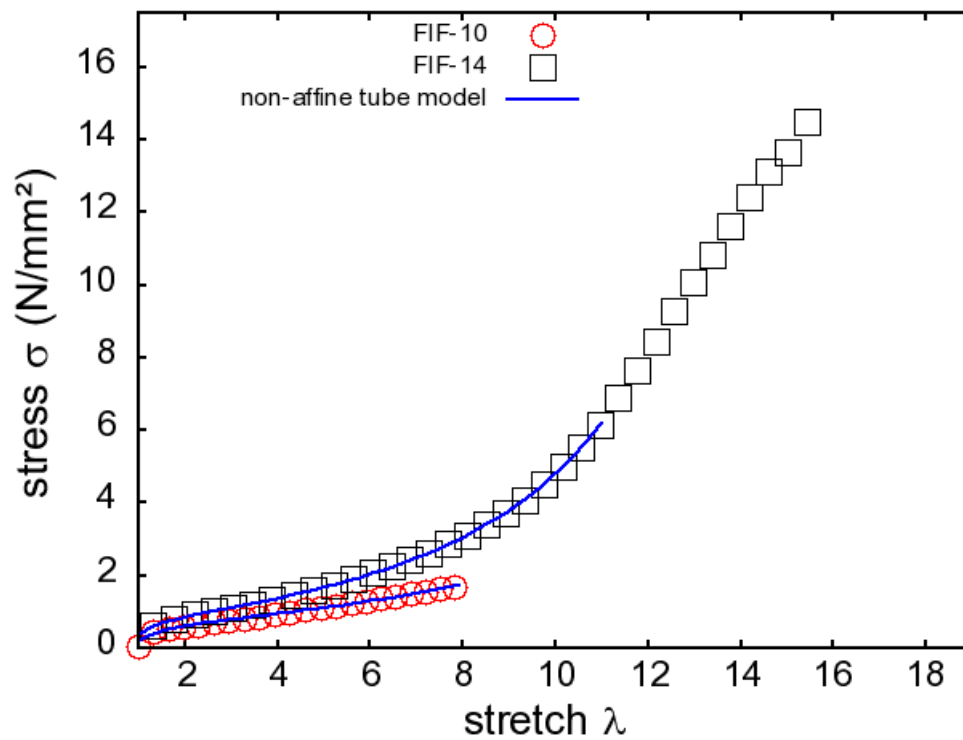


Figure 4.11 Non-affine tube model analysis of FIF triblock copolymers

behavior with higher Young's Modulus and lower strain at break, letting us assume that a continuous hard phase (either cylindrical or lamellae PBT domains) is formed. Further evidence for this assumption is the appearance of a yield point for FIF-31 at 3.5% strain and 5.3 MPa.

The parameters of the non-affine tube model for FIF-10 and FIF-14 are shown in **Table 4.5**. For both modulus values, G_c and G_e , an increase becomes apparent when comparing FIF-10 and FIF-14. G_c is increasing by about 60% and G_e by 10% only. This difference becomes reasonable, when considering the PI backbone molecular weight of FIF-10 and FIF-14, influencing the PI entanglement density. Because of the chosen synthesis conditions $M_{w,PI}$ is similar, resulting in minor changes of G_e . The more pronounced increase of G_c is due to the larger amount of hard phase in FIF-14. The parameter represents the amount of physical resolvable hard domains acting like chemical cross links. Larger G_c values correspond to steeper slopes in the Gaussian region of the stress-strain curve. The parameter n represents the number of statistical segments between two successively trapped entanglements in the model and shows large values if the upturn of the stress-strain curve occurs at high elongations. In this case, n correlates to the PI backbone molecular weight between two glassy grafts. Discussing this parameter makes sense only if the stress-strain curves are showing such an upturn, which is not the case for

FIF-10. There, the load-bearing capacity of the cross-links is too small. For FIF-14, n can be considered as more significant.

4.3.8 Microphase separation behavior: The micro-phase separation behavior between PBF and PI in FIF triblock copolymers was investigated by SAXS and AFM measurements. In the SAXS measurements (**Figure 4.12**), micro-phase separation between PBF and PI was observed but without long range order. None of the reflection pattern (q/q^*) of FIF-10, 14, 22 and 31 matched with Bragg reflection for the morphology of any A-B-A type block copolymer.³² A broad secondary peak was observed at approximately $3.3 q^*$ after the maximum primary peak q^* for FIF-10, 14 and 22. Since in these experiments, all samples were annealed at 155°C for 12h in order to prevent thermo-crosslinking of unsaturated carbon-carbon double bond in FIFs. The annealing condition might be insufficient for glassy PBF domains to reorganize into ordered lattice for SAXS pattern. Generally, in order to achieve a thermodynamically equilibrium morphology, annealing temperature needs to be 20 to 30 °C higher than glass transition temperature. From the DSC measurement (**Figure 4.13**), the T_g of PBF was not observed for FIF-10 and FIF-14. This indicated certain level of phase blending might also occurred between PBF and PI, which could also contributed to disordered SAXS profiles.

Since OsO_4 and RuO_4 have no selectivity over unsaturated carbon-carbon double bond presented in both PBF and PI blocks, we were not able to obtain enough TEM contrast

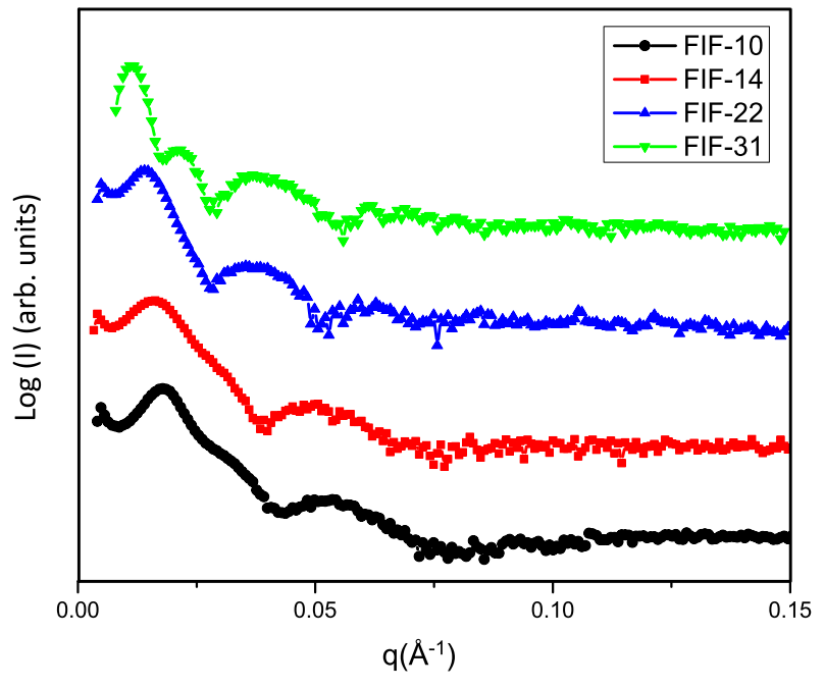


Figure 4.12 SAXS data for FIF triblock copolymers

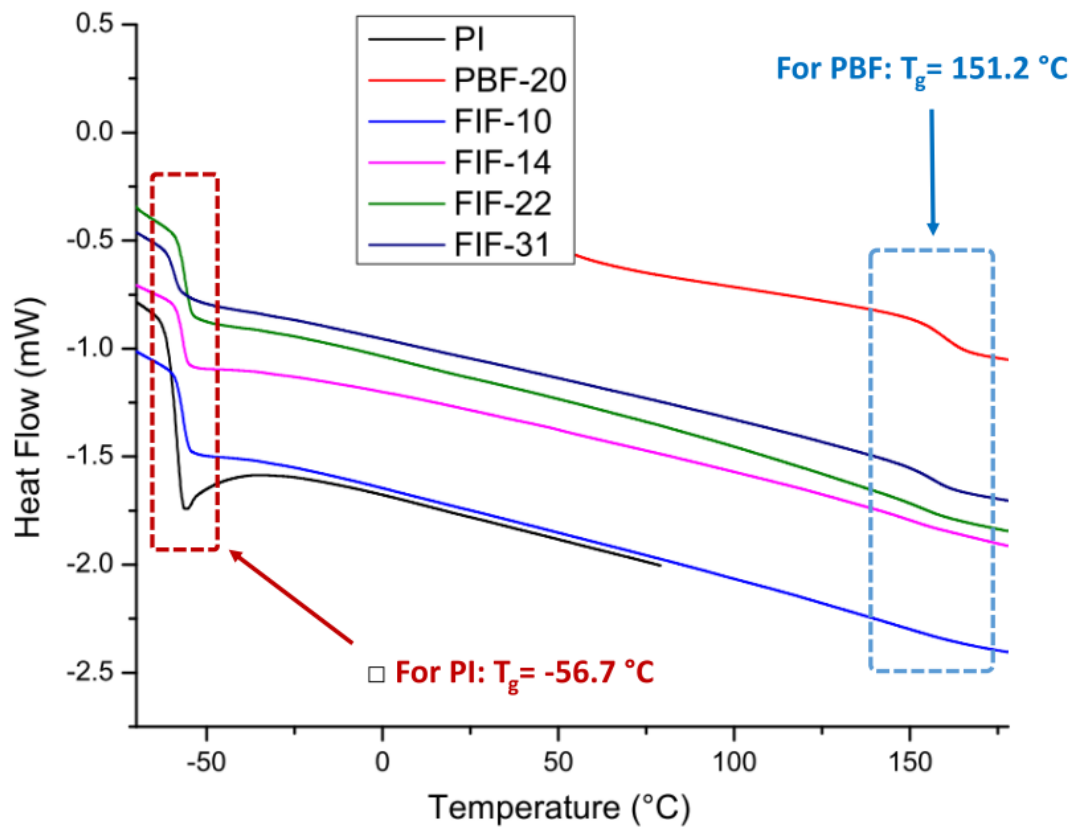


Figure 4.13 DSC measurement of FIF triblock copolymers, PBF-20 and polyisoprene homopolymers.

for study of the material morphology in a bulk. In order to visualize the morphology and micro-phase separation behavior between PBF and PI, non-contact mode, phase contrast and force modulation AFM (**Figure 4.14**) was employed. The measurements of FIF-10 (a-1) and FIF-14 (b-1) showed a relative smooth morphology on a scale of $500\text{nm} \times 500\text{nm}$. From comparison of morphology (a-1 and b-1) and phase contrast (a-2 and b-2) it is clearly seen, that phase shift doesn't follow topological structure of the surface. It means that observed contrast on the phase images mostly reflects difference in elastic and adhesive properties between PI and PBF blocks. A mixture of spherical and cylindrical worm-like structures was a main architecture ensemble observed in both FIF-10 and FIF-14.

4.4 Conclusions:

In summary, FIF triblock copolymers with four different compositions were prepared by living anionic polymerization in benzene at room temperature. Dynamical mechanical analysis indicates that the upper service temperature of FIF copolymers is around $145\text{ }^{\circ}\text{C}$. Tensile testing of sample FIF-14 (with 14 vol% of PBF) displayed a maximum stress of $14.3 \pm 1.3\text{ MPa}$ with strain at break of $1394 \pm 66\%$. SAXS profile showed microphase separation of PBF and PI without long range order. Atomic force microscopy (AFM) in tapping mode and force modulation mode confirmed the phase separation behavior. The different type of additives used for anionic polymerization

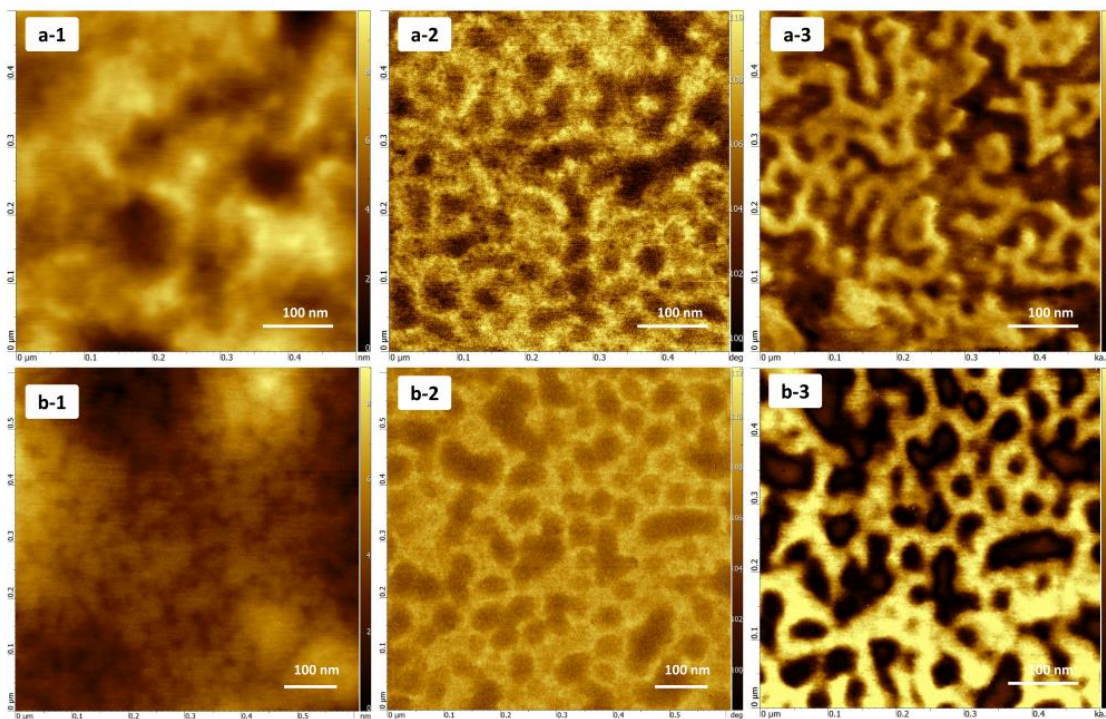


Figure 4.14 AFM of FIF-10: a-1) topology, a-2) phase contrast, a-3) force modulation and FIF-14: b-1) topology, b-2) phase contrast, b-3) force modulation.

had a significant effect on the T_g of PBF homopolymer. Among the additives, the initiation system of DME/*n*-BuLi T_g produced PBF with the highest T_g above 190°C.

References:

- [1]. (a) Szwarc, M. *Nature* **1956**, *178* (4543), 1168-1169; (b) Szwarc, M.; Levy, M.; Milkovich, R. *Journal of the American Chemical Society* **1956**, *78* (11), 2656-2657.
- [2]. Hadjichristidis, N.; Pitsikalis, M.; Pispas, S.; Iatrou, H. *Chemical Reviews* **2001**, *101* (12), 3747-3792.
- [3]. Hirao, A.; Goseki, R.; Ishizone, T. *Macromolecules* **2014**, *47* (6), 1883-1905.
- [4]. Hsieh, H.; Quirk, R. P., *Anionic polymerization: principles and practical applications*. CRC Press: 1996.
- [5]. Quirk, R. P., *Applications of anionic polymerization research*. American Chemical Society; Distributed by Oxford University Press: 1998.
- [6]. Holden, G. K.; Hans Rytger; Quirk, Roderic P. , *Thermoplastic Elastomers*. 3 ed.; Hanser-Gardner Publications: 2004.
- [7]. Holden, G.; Milkovich, R. Block polymers of monovinyl aromatic hydrocarbons and conjugated dienes. US 3265765 A, 1966.
- [8]. Handlin, D. L.; Trenor, S.; Wright, K., Applications of Thermoplastic Elastomers Based on Styrenic Block Copolymers. In *Macromolecular Engineering: Precise Synthesis, Materials Properties, Applications*, Matyjaszewski, K.; Gnanou, Y.; Leibler, L., Eds. Wiley-VCH: 2007; Vol. 4, pp 2001-2031.
- [9]. Fetters, L. J.; Morton, M. *Macromolecules* **1969**, *2* (5), 453-458.

- [10]. Bolton, J. M.; Hillmyer, M. A.; Hoyer, T. R. *ACS Macro Letters* **2014**, *3* (8), 717-720.
- [11]. Fetters, L. J.; Firer, E. M.; Dafauti, M. *Macromolecules* **1977**, *10* (6), 1200-1207.
- [12]. Kobayashi, S.; Kataoka, H.; Ishizone, T.; Kato, T.; Ono, T.; Kobukata, S.; Ogi, H. *Macromolecules* **2008**, *41* (14), 5502-5508.
- [13]. Alfonzo, C. G.; Fleury, G.; Chaffin, K. A.; Bates, F. S. *Macromolecules* **2010**, *43* (12), 5295-5305.
- [14]. Hucul, D. A.; Hahn, S. F. *Advanced Materials* **2000**, *12* (23), 1855-1858.
- [15]. Yu, Y.; Dubois, P.; Teyssié, P.; Jérôme, R. *Macromolecules* **1997**, *30* (15), 4254-4261.
- [16]. Yu, J. M.; Dubois, P.; Jérôme, R. *Macromolecules* **1997**, *30* (21), 6536-6543.
- [17]. Yu, J. M.; Dubois, P.; Jérôme, R. *Macromolecules* **1996**, *29* (26), 8362-8370.
- [18]. Yu, J. M.; Dubois, P.; Jérôme, R. *Macromolecules* **1996**, *29* (23), 7316-7322.
- [19]. Fodor, Z.; Kennedy, J. P. *Polymer Bulletin* **1992**, *29* (6), 697-704.
- [20]. Puskas, J. E.; Kaszas, G.; Kennedy, J. P.; Hager, W. G. *Journal of Polymer Science Part A: Polymer Chemistry* **1992**, *30* (1), 41-48.
- [21]. Li, D.; Faust, R. *Macromolecules* **1995**, *28* (14), 4893-4898.
- [22]. Kennedy, J. P.; Puskas, J. E.; Kaszas, G.; Hager, W. G. Thermoplastic elastomers of isobutylene and process of preparation US 4946899 A, 1990.
- [23]. Imaeda, T.; Hashimoto, T.; Irie, S.; Urushisaki, M.; Sakaguchi, T. *Journal of Polymer Science Part A: Polymer Chemistry* **2013**, *51* (8), 1796-1807.

- [24]. Mosnáček, J.; Yoon, J. A.; Juhari, A.; Koynov, K.; Matyjaszewski, K. *Polymer* **2009**, *50* (9), 2087-2094.
- [25]. Juhari, A.; Mosnáček, J.; Yoon, J. A.; Nese, A.; Koynov, K.; Kowalewski, T.; Matyjaszewski, K. *Polymer* **2010**, *51* (21), 4806-4813.
- [26]. Kosaka, Y.; Kitazawa, K.; Inomata, S.; Ishizone, T. *ACS Macro Letters* **2013**, *2* (2), 164-167.
- [27]. Kosaka, Y.; Goseki, R.; Kawauchi, S.; Ishizone, T. *Macromolecular Symposia* **2015**, *350* (1), 55-66.
- [28]. Kosaka, Y.; Kawauchi, S.; Goseki, R.; Ishizone, T. *Macromolecules* **2015**, *48* (13), 4421-4430.
- [29]. Data, M. P. Kraton® D1112P (SIS) Linear Block Copolymer. <http://www.matweb.com/search/datasheet.aspx?matguid=ec777ddb6a3540ae977fb8f9a53c4d64&ckck=1>.
- [30]. Uhrig, D.; Mays, J. W. *Journal of Polymer Science Part A: Polymer Chemistry* **2005**, *43* (24), 6179-6222.
- [31]. Klüppel, M.; Schramm, J. *Macromolecular Theory and Simulations* **2000**, *9* (9), 742-754.
- [32]. Skoulios, A. E., *In Developments on Block Copolymers-I* Applied Science Publishers: New York, 1982.

Chapter 5: Polybenzofulvene Based Thermoplastic Elastomers: Effects of Partial and Full Hydrogenation

Abstract: In this work we report the effects of partial and fully hydrogenation on the thermal stability, mechanical and morphological properties of high temperature thermoplastic elastomers comprised of polybenzofulvene-polyisoprene-polybenzofulvene triblock copolymer with 14 volume percentage of polybenzofulvene (FIF-14). “Partial hydrogenation” (PH-FIF-14) indicates saturated polyisoprene backbone and double bond in the five membered ring of polybenzofulvene (PBF) whereas “fully hydrogenation” (FH-FIF-14) indicates completely saturated FIF-14 into a polyolefin. Compared with FIF-14, FH-FIF increased degradation temperature from 245 °C to 350 °C. Ultimate stress was increased from 14.3 MPa to 17.8 MPa whereas strain at break decreased from 1394 % to 744 %. Dynamic mechanical analysis showed that the upper service temperature of fully hydrogenated FIF (FH-FIF-14) is 130 °C. Microphase separation of FH-FIF-14 triblock copolymers was observed by atomic force microscopy. Homopolymers of polybenzofulvene of two different microstructures were prepared and the effects of the hydrogenation on the glass transition temperature and thermal stability was evaluated. After complete hydrogenation, glass transition temperature (T_g) of PBF with 22% of 1,2-addition was reduced from 146 °C to 126 °C. The hydrogenation process largely decomposed PBF with 99% of 1,2-addition, as evidenced by SEC.

Keywords: Thermoplastic elastomers, anionic polymerization, high temperature, block copolymer, hydrogenation and polyolefin

5.1 Introduction:

Styrenic thermoplastic elastomers (S-TPEs) are ABA-type triblock copolymers with polyisoprene (PI) or polybutadiene (PB) as the elastic middle block anchored by glassy polystyrene (PS) end blocks.^{1,2} Generally, these materials are prepared by anionic polymerization in hydrocarbon solvent at mild temperatures and applied in various fields including footwear, coatings, sealants, paving, roofing materials and medical tubing.³ Market predictions show an increasing trend of global consumptions of styrenic block copolymers increasing from 5.5 billion US dollars in 2013 to 8.4 billion in 2020 with an annual growth rate of 4.5 %.⁴

In SIS and SBS triblock copolymer type TPEs, the thermodynamic immiscibility between PS and polydiene leads to a physically crosslinked bi-phasic system combining the processability of thermoplastics with the mechanical properties of crosslinked rubbery materials. S-TPEs displayed similar mechanical properties as conventional vulcanized rubber without filler reinforcement. The advantage of S-TPEs over vulcanized rubber is its ability to be processed by high throughput plastic processing techniques such as injection molding and melt extrusion without application of a curing process.⁵ However, compared with saturated rubber, the presence of unsaturation in polydienes reduces their resistance to UV light and oxidation as compared. The glass transition temperature of PS ($T_g \sim 95$ °C), on the other hand, limits the service temperature range of S-TPEs. Tensile stress drops

sharply at 95 °C as a result of softening of PS domains.³ Much research in the field of TPEs was driven by the goal of improving chemical resistance and upper service temperature.^{6,7,8,9,10,11,12}

Benzofulvene (BF) is a conjugated diene monomer that can undergoes living anionic polymerization in both hydrocarbon solvent such as benzene at mild temperatures and in polar solvents such as THF at -78 °C.^{13,14,15} As a hydrocarbon monomer derived from fulvene, BF shows high anionic polymerizability as reported by Ishizone. Similar to other diene monomers such as isoprene,^{16,17} butadiene^{18,19} and 1,3-cyclohexadiene,²⁰ the ratio of 1,2- and 1,4-addition present in polybenzofulvene (PBF) depends on the choice of solvent, initiator, additives, temperature and polymerization mechanism. For a molecular weight above 10 kg/mol, free radically polymerized PBF showed a T_g above 142 °C with 9% 1,2-addition.¹³ Anionic polymerization of BF in hydrocarbon solvent yields polymers with T_g above 145 °C with 22% of 1,2-addition whereas polymerization in THF at -78 °C produced PBF with T_g above 153 °C with 40 % of 1,2-addition. PBF polymerized with n-BuLi as the initiator and dimethoxyethane (DME) as the additive in benzene at 5 °C displayed T_g above 190 °C with virtually 99% of 1,2-addition.²¹ Inspired by such high glass transition temperatures of PBF and the anionic polymerizability in hydrocarbon solvent at room temperature, PBF-b-PI-b-PBF (FIF) triblock copolymers with different composition ,were prepared in benzene at room temperature as a potential high temperature TPE. FIF

with 14 vol% of PBF displayed 14.3 MPa ultimate stress, 1390 % strain at break, with service temperature up to 140 °C.²¹

As evidenced by ethylene-propylene rubber which is absent of unsaturated carbon bonds, saturation improves rubber thermal stability at high temperature and its UV resistance.²² Historically, catalytic hydrogenation has been employed to saturate polyisoprene into poly(ethylene-co-propylene) (PEP)^{23,24} and polybutadiene into poly(ethylene-co-butylene) (PEB)^{25,26} to prepare S-TPEs with better UV resistance.²⁷ With ultra-wide pore silica-supported Pt catalyst,²⁸ aromatic carbon-carbon double bonds in PS were hydrogenated into poly(vinyl-cyclohexane) (PVCH) at lower temperatures and with less hydrogen pressure, and with reduced reaction time and catalyst consumption. PVCH is a low density glassy polymer with a T_g of 147 °C.²⁹ Complete hydrogenation of SIS yields high temperature TPEs with better UV resistance and thermal stability.³⁰

In this work, we used ultra-wide pore silica-supported Pt catalyst to fully hydrogenate PBF synthesized using two different initiation systems. For PBF prepared with sec-BuLi as the initiator without any polar additive, complete hydrogenation reduced the glass transition temperature from 146 °C to 126 °C. Complete hydrogenation largely decomposed PBF prepared using n-BuLi as the initiator and DME as the additive. The T_g , on the other hand, decreased from 197 °C to 147 °C. Furthermore, partial and complete hydrogenation of FIF triblock copolymers were carried out to evaluate the effects of hydrogenation on its mechanical properties. In the case of partial hydrogenation, the double

bond in the five membered ring of PBF, along with unsaturation in PI, was hydrogenated whereas complete hydrogenation saturated FIF into a polyolefin. Dynamic mechanical analysis and tensile testing was used to evaluate the effects of partial and complete hydrogenation on the mechanical properties of FIF triblock copolymers. Atomic force microscopy (AFM) was used to characterize the morphology of completely hydrogenated FIF polymers. Thermal stability of both PBF and FIF was improved, as evidenced by thermogravimetric analysis (TGA).

5.2 Experimental Section:

5.2.1 Materials: Isoprene (Fisher, >99 %), *n*-BuLi (Fisher, 2.5 M in hexanes), 2-chlorobutane (Fisher, >99 %), hexane (Fisher, >99.5 %), methanol (Fisher, ≥99.9 %), benzene (Aldrich, ≥99.9 %), cyclohexane (Fisher, >99 %), 2-butanol (Aldrich, >99 %), 1,3-bis(1-phenylvinyl)benzene (PEB, donated by Dow Chemical, >95 %) were purified by high vacuum techniques.³¹ The hexane solution of *sec*-BuLi and *sec*-BuOLi and benzene solution of (1,3-phenylene)bis(3-methyl-1-phenylpentylidene) dilithium initiator (DLI) were prepared according to reported procedures and diluted to the desired concentration.³¹ 1,2-Dimethoxyethane (DME, Aldrich, >99.9 %) was distilled over CaH₂, potassium dispersion (two times), diluted with anhydrous benzene and ampulized under high vacuum. Lithium (Aldrich, >99 %, granular), sodium (Aldrich, >99.9 %, cubes), potassium (Aldrich, >98 %, chunks), indene (TCI, 95 %), paraformaldehyde (Aldrich, 95 %, powder),

potassium tert-butoxide (TCI, 1.0 M in tetrahydrofuran), ethylmagnesium bromide (Aldrich, 3.0 M in diethyl ether), butylhydroxytoluene (BHT, Aldrich, >99 %) were used as received. A heterogeneous Pt-Re/SiO₂ catalyst provided by Dow Chemical Company was used for the hydrogenation reaction. Benzofulvene monomer was synthesized based on the literature,¹³ diluted with anhydrous benzene (0.3 to 0.5M), and ampulized under high vacuum condition. All ampules of monomer, initiator, and additives were stored at -30 °C.

5.2.2 Anionic polymerization: All anionic polymerizations were carried out with pre-purged, customized glass apparatus under high vacuum conditions (10⁻⁶ torr). In the homopolymerization of BF, a solution of *sec*-BuLi (0.0211 mmol) in hexane was introduced into BF (0.200g, 1.56 mmol) solution in benzene at room temperature. An excess of degassed methanol was added to quench the reaction after 30 min. 0.5 wt% of BHT was added into the polymer solution before precipitating into methanol. Size exclusion chromatography (SEC), ¹H-NMR, differential scanning calorimetry (DSC) and thermogravimetric analysis (TGA) were used to characterize the resulting polymer. The yield of the polymer is quantitative. (11.6 kg/mol, 100%, M_w/M_n=1.04, T_g = 146 °C **Table 5.1**, run 1). In the triblock copolymerization of FIF, living difunctional polyisoprenyllithium was prepared by initiating isoprene (5.47g, 80.3 mmol) from DLI (0.0377 mmol) and *sec*-BuOLi (0.473 mmol) mixture in benzene. BF (1.024 g, 8.0 mmol)

Table 5.1: Anionic polymerization and complete hydrogenation of polybenzofulvene

Run	Name	M_n^a (kg/mol)	M_w^a (kg/mol)	PDI ^b	Microstructure		T_g^c (°C)	T_d^d (°C)
					1,2-	1,4-		
1	PBF-12	11.6	12.1	1.04	22%	78%	146	255
2	PBF-DME	158.1	190.0	1.20	>99%	<1%	197	256
3	H-PBF-12	12.2	13.2	1.08			126	360
4	H-PBF-DME	10.5	20.4	1.90			147	356

^a M_n and M_w was characterized by SEC equipped with refractive index detector calibrated with polystyrene standard. ^b M_w/M_n was calculated by SEC with polystyrene standard in THF. ^c T_g was measured by DSC on the second heating scans. ^d T_d was measured by TGA under nitrogen.

was introduced into the polymer solution after complete consumption of isoprene as monitored by SEC over 5 days. Degassed methanol was used to quench the reaction after 8 h. The resulting polymer was precipitated into a large excess of methanol containing 0.5 wt% of IRGANOX[®] B 225 as the long-term thermal stabilizer. Precipitates were filtered and dried in a vacuum oven for 48h. Triblock copolymer in 98 % yield was recovered and characterized by SEC against polystyrene standard calibration, ¹H-NMR, DSC and TGA. (**Table 5.2**, run 5, 79.4 kg/mol, PDI=1.24, T_{g,1}=-56 °C, T_{g,2}=145 °C, T_d=245 °C) The weight percentage of PBF in the triblock copolymer was calculated from ¹H-NMR to be 14.1%.

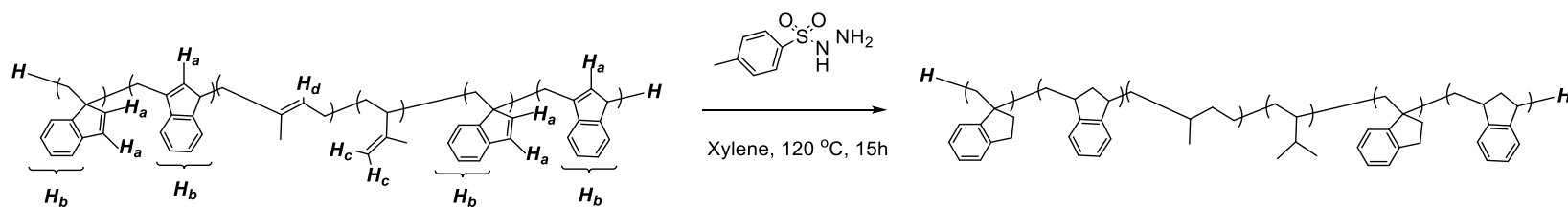
5.2.3 Hydrogenation: Partial hydrogenation of FIF was performed in a 500 ml three-neck round bottom flask. Typically, 2 g of polymer (FIF-14, M_n=79.4 kg/mol) was dissolved into 180 ml of xylene, mixed with 35 g of p-toluenesulfonhydrazide and 25 mg of 3,5-di-tert-butyl-4-hydroxytoluene as anti-oxidant. After refluxing at 120 °C for 15 h, the solution was precipitated into a large excess of methanol three times and dried. (**Scheme 5.1**, PH-FIF-14, Table 2, run 6, M_n=82.4 kg/mol, PDI=1.25) Complete hydrogenation reactions were performed in a 1 L pressurized vessel by Parr Instrument Company. In each reaction cycle, 1.0 g of FIF-14 and 1.0 g of Pt-Re/SiO₂ catalyst were mixed in 500 mL of solvent (cyclohexane or decalin, purchased from Sigma-Aldrich) and pressurized with H₂ to 500 psi. The reactions were conducted at 170 °C for 17 h, after

Table 5.2 Anionic polymerization, partial and complete hydrogenation of FIF-14

Run	Name	M_n^b (kg/mol)	M_w^b (kg/mol)	PDI ^c	$T_{g,1}^d$ (°C)	$T_{g,2}^e$ (°C)	T_d^f (°C)
5	FIF-14 ^a	79.4	98.5	1.24	-56	145	245
6	PH-FIF-14	82.4	105.9	1.25	-54	125	275
7	FH-FIF-14	82.6	113.1	1.37	-54	132	350

^a Weight percentage of polybenzofulvene was calculated by ¹H-NMR. ^b M_n and M_w was characterized by SEC equipped with refractive index detector calibrated with polystyrene standard. ^c M_w/M_n was calculated by SEC with polystyrene standard in THF. ^d $T_{g,1}$ was measured by DSC on the second heating scans. ^e $T_{g,2}$ of PH-FIF-14 was measured by DSC on the second heating scans. $T_{g,2}$ of FIF-14 and FH-FIF-14 was measured by DMA.

^f T_d was measured by TGA under nitrogen.

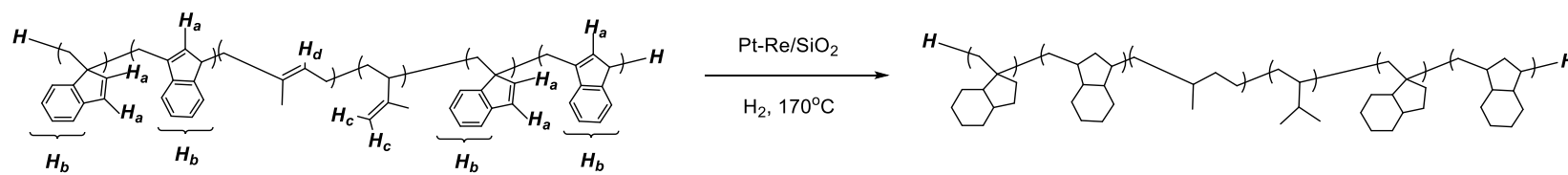


Scheme 5.1 Partial hydrogenation of FIF-14

which the solutions were filtered through a Millipore 0.2 μm filter. The filtered solutions were subsequently poured into 2 L of cool methanol or acetone for precipitation. The precipitates were recovered and dried for further characterization. (**Scheme 5.2**, FH-FIF-14, Table 2, run 7, $M_n=82.6$ kg/mol, PDI=1.37).

5.2.4 Preparation of samples: Type 5A, ISO 527/2 specimens was used by stamping polymer films casted from 1 g of polymers in 40 ml of toluene. The film was evaporated slowly over 7 days and annealed at 70 $^{\circ}\text{C}$ under vacuum (10^{-1} torr) upon removing residual solvent. Similar solvent casting procedures were used to prepare samples with thickness around 0.5-0.6 mm for dynamic mechanical analysis. Films with diameter of 4 mm were prepared by solvent casting and annealed at 155 $^{\circ}\text{C}$ for 12 h under dynamic high vacuum (10^{-6} Torr) for small angle X-ray scattering analysis. Spin casted films from 2 mg/ml polymer in toluene solutions were prepared and annealed at 155 $^{\circ}\text{C}$ for 12 h under dynamic high vacuum for atomic force microscopy measurements.

5.2.5 Measurements: ^1H - and ^{13}C -NMR spectra were obtained on a Varian Mercury 500 instrument using deuterated chloroform (CDCl_3) for homopolymers of PBF, partially hydrogenated FIF-14, and completely hydrogenated FIF, and using deuterated tetrahydrofuran ($\text{THF-}d_8$) for FIF-14. Molecular weight and molecular weight distribution was measured by size exclusion chromatography in THF at 40 $^{\circ}\text{C}$ with a flow rate of 0.35 ml/min using a Tosoh EcoSEC GPC system equipped with two TSKgel Super Multipore



Scheme 5.2 Complete hydrogenation of FIF-14

HZ-V columns calibrated using standard polystyrenes with molecular weight from 580 to 7.5×10^6 g/mol. Glass transition temperature was measured using a TA Instruments Q-2000 differential scanning calorimeter (DSC) from -80 °C to 200 °C at a heating rate of 10 °C/min with a 5 minute isothermal hold at the maximum and minimum temperatures. Reported glass transition temperatures were measured on the second (or third) heating scans. Thermal stability was examined using a TA instruments Q-50 TGA. A 5-10 mg sample was placed on a platinum pan and equilibrated at 30 °C. The temperature was ramped from 30-800 °C at a rate of 10 °C/min under nitrogen atmosphere. Atomic force microscopy (AFM) measurements were performed with Asylum Cypher in tapping mode in air. The probe used for AFM measurement is HiRes-C19/Cr-Au (MikroMasch) with 6 nm radius and 75 kHz resonance. Tensile tests were performed with a Zwick Z050 at the speed of 15 mm/ min, clamping distance of 50 mm and measuring distance of 15 mm. Each sample was measured three times. Dynamic mechanical analysis was carried out by a TA Q-800 instrument with force control, temperature sweep mode at 1Hz from -80°C to 160°C.

5.3 Results and Discussion:

5.3.1 Anionic polymerization and complete hydrogenation of homopolybenzofulvene: Polybenzofulvene (PBF) was prepared using two initiation systems in order to compare the effects of hydrogenation on the thermal properties of PBF with different microstructures. With *sec*-BuLi as the initiator and polymerization in

benzene at room temperature, PBF-12 (run 1, **Table 5.1**) displayed predicted molecular weight (11.6 kg/mol) and narrow molecular weight distribution (PDI=1.04) (**Figure 5.1, a**) with 22 % of 1,2- addition. However, a coupling peak was observed which might due to the presence of oxygen when quenching the reaction. The glass transition of PBF-12 was 145.7 °C as measured by DCS. When n-BuLi was used as the initiator with DME as the polar additive, polymerized in benzene at 6 °C, PBF-DME (run 2, **table 5.1**) showed molecular weight of 158.1 kg/mol with PDI of 1.20 (**Figure 5.1, b**). Almost 99% of 1,2- addition was observed in PBF-DME with T_g of 196.8 °C.

Complete hydrogenation of PBF-12 and PBF-DME were carried out in a Parr reactor with Pt catalyst. As showed in **Table 5.1**, run 3, after hydrogenation, the molecular weight of PBF-12 was increased slightly with PDI lower than 1.09 based on polystyrene calibration. No obvious decomposition was observed for H-PBF-12 as evidenced by SEC. In the $^1\text{H-NMR}$ analysis, signals from 5.50 ppm to 7.60 ppm (H_a and H_b in **Figure 5.2**), which corresponds to protons on the unsaturated carbon in PBF, completely disappeared after hydrogenation. While the degradation temperature in nitrogen of PBF-12 was increased from 255 °C to 360 °C (**Figure 5.3**), the glass transition temperature was decreased from 146 °C to 126 °C (**Figure 5.4, a**). The decreasing trend of glass transition temperature was also observed for the complete hydrogenation of PBF-DME from 197 °C to 147 °C (**Figure 4, 2**). However, PBF-DME was largely decomposed during the

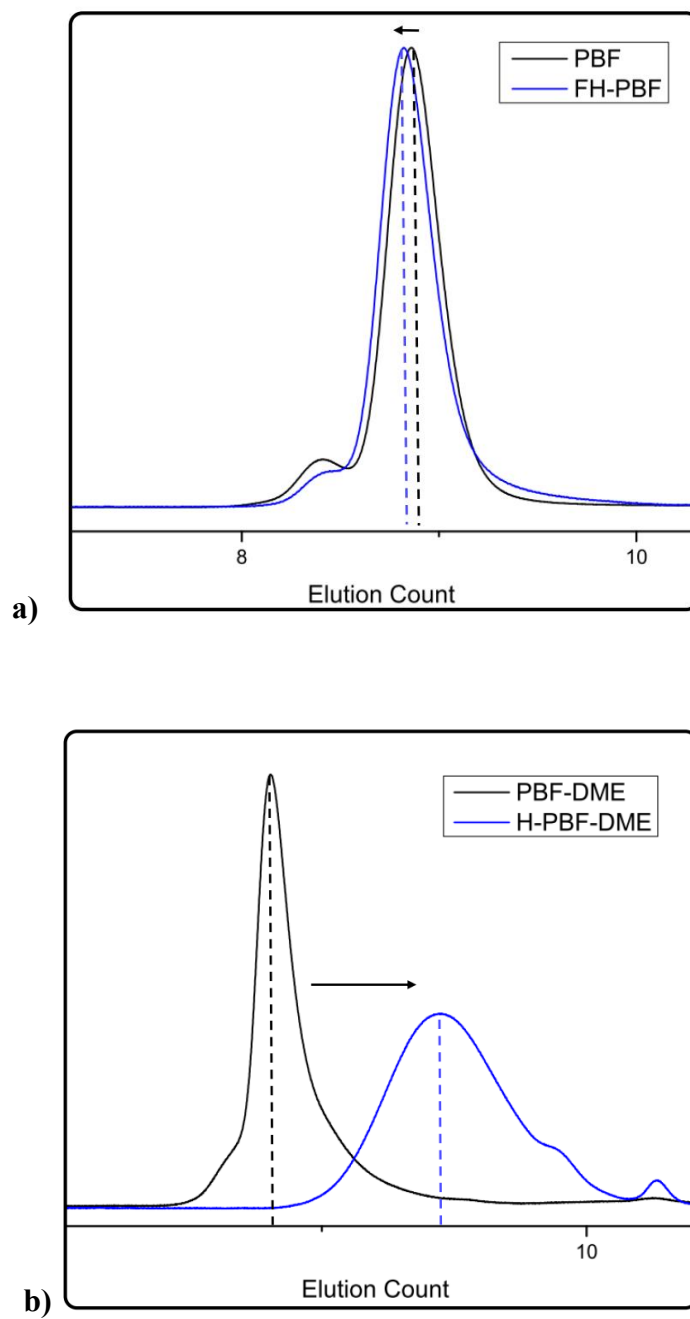


Figure 5.1: GPC of completely hydrogenated: a) PBF-12 and b) PBF-DME

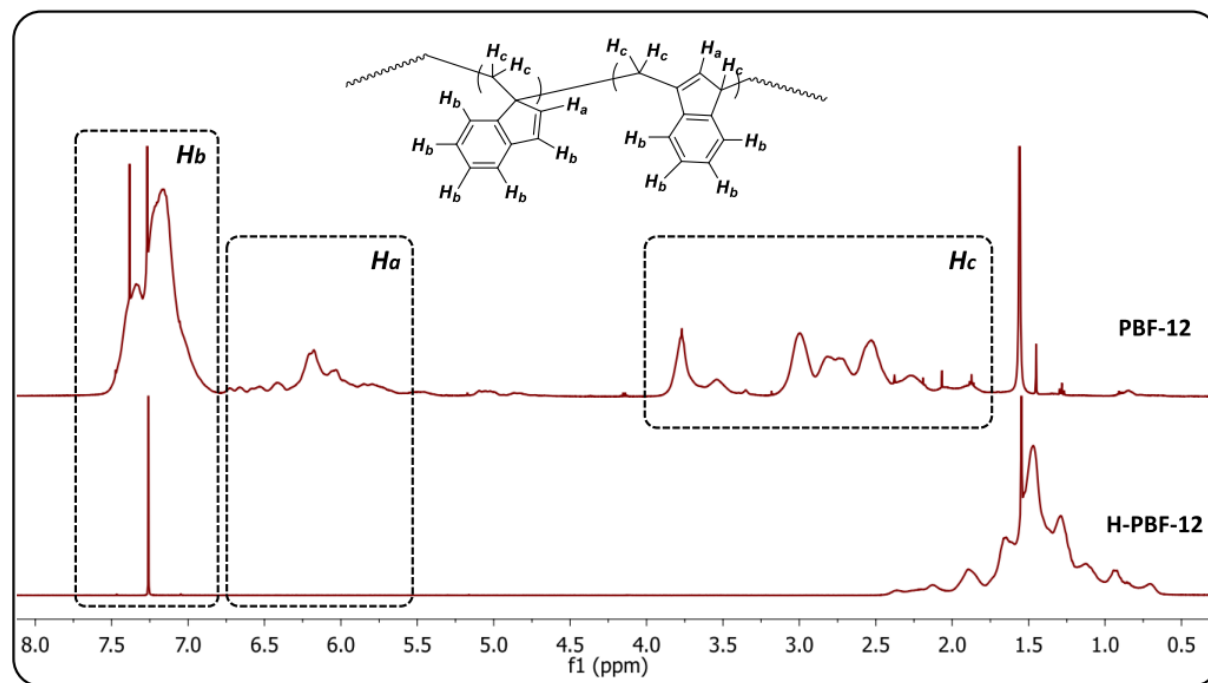


Figure 5.2 NMR of complete hydrogenation of PBF-12

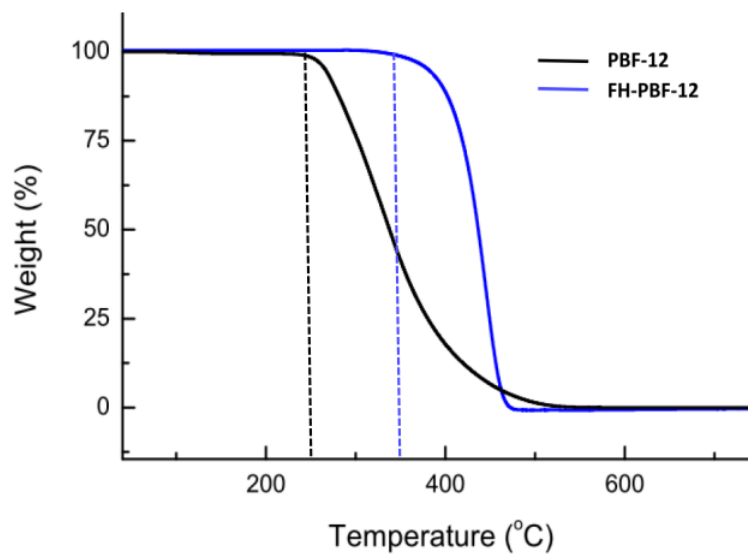
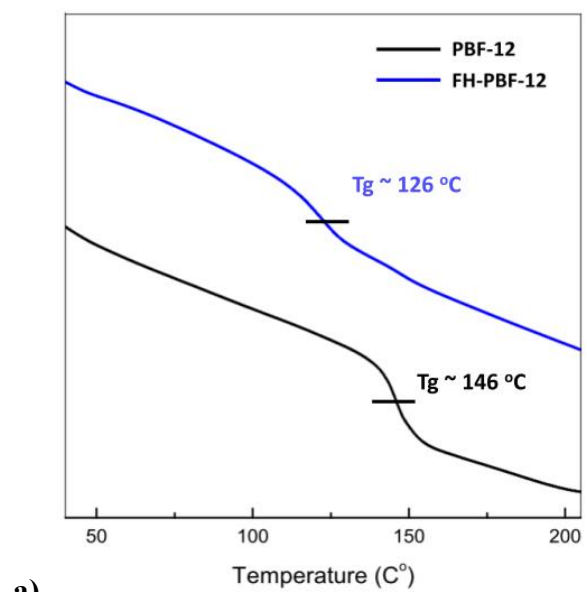
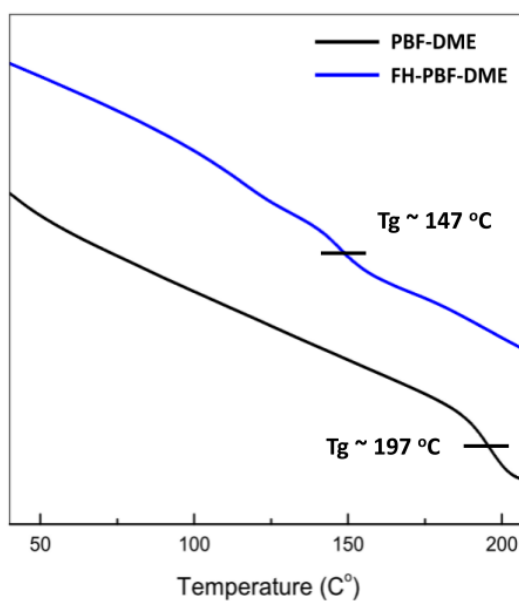


Figure 5.3: TGA of complete hydrogenation of PBF-12



a)



b)

Figure 5.4 DSC of complete hydrogenation of a) PBF-12 and b) PBF-DME

hydrogenation process. After hydrogenation, the molecular weight of PBF-DME was decreased from 158.1 kg/mol to 10.5 kg/mol, whereas the PDI was increased from 1.20 to 1.90.

5.3.2 Anionic polymerization and hydrogenation of polybenzofulvene-b-polyisoprene-b-polybenzofulvene (FIF): Triblock copolymer of polybenzofulvene-b-polyisoprene-b-polybenzofulvene was synthesized by living anionic polymerization using a difunctional lithium initiator in benzene following a previously reported method. Volume percentage of polybenzofulvene (14 vol%) was calculated by integrating of proton signals from 4.60 ppm to 4.75 ppm (3,4- addition of PI, H_c), 5.05 ppm to 5.25 ppm (1,4-addition of PI, H_d), 5.50 ppm to 6.75 ppm (allylic proton of PBF, H_a) and 6.75 ppm to 7.60 ppm (aromatic proton, H_b) from ¹H-NMR analysis (**Figure 5.5**). The density of PI used was 0.920 g/cm³ and 1.146 g/cm³ for PBF. The number average molecular weight was 79.4 kg/mol with PDI of 1.24 based polystyrene calibration (**Figure 5.6**, black line). After partial hydrogenation FIF-14 with p-toluenesulfonylhydrazide in xylene at 120 °C for 15 h (**Scheme 5.1**), allylic proton signals including protons from five carbon ring on polybenzofulvene (H_a) and 1,4-(H_d), 3,4-(H_c) addition in PI disappeared from the ¹H-NMR spectrum (**Figure 5.6**). The apparent molecular weight was increased to 82.4 kg/mol with PDI of 1.25. Complete hydrogenation of FIF-14 with Pt-Re catalyst (**Scheme 5.2**) produced polymers with M_n of 82.6 kg/mol with PDI of 1.37 (**Table 5.2**). The shoulder in the low

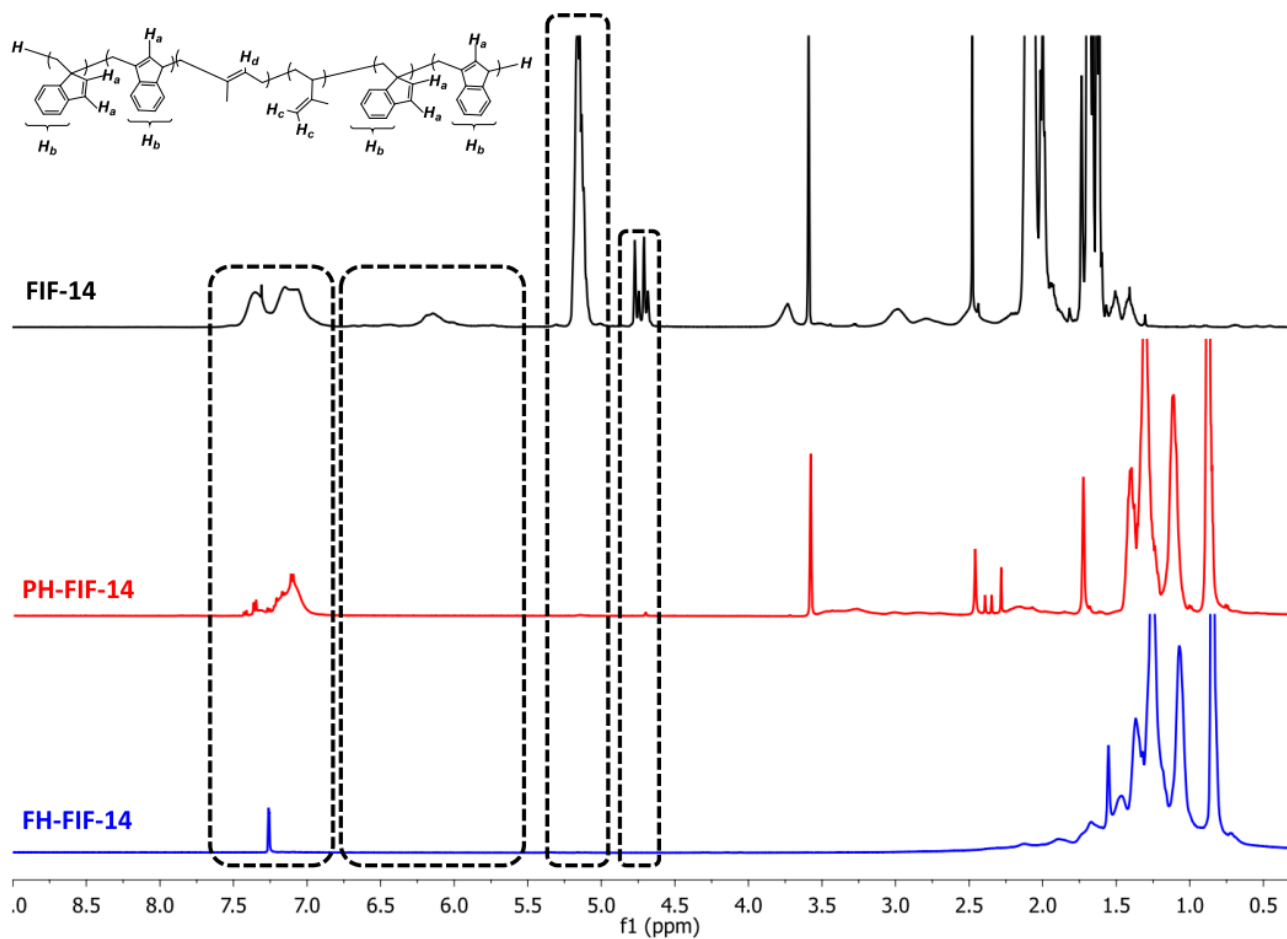


Figure 5.5 $^1\text{H-NMR}$ of partial and complete hydrogenation of FIF-14

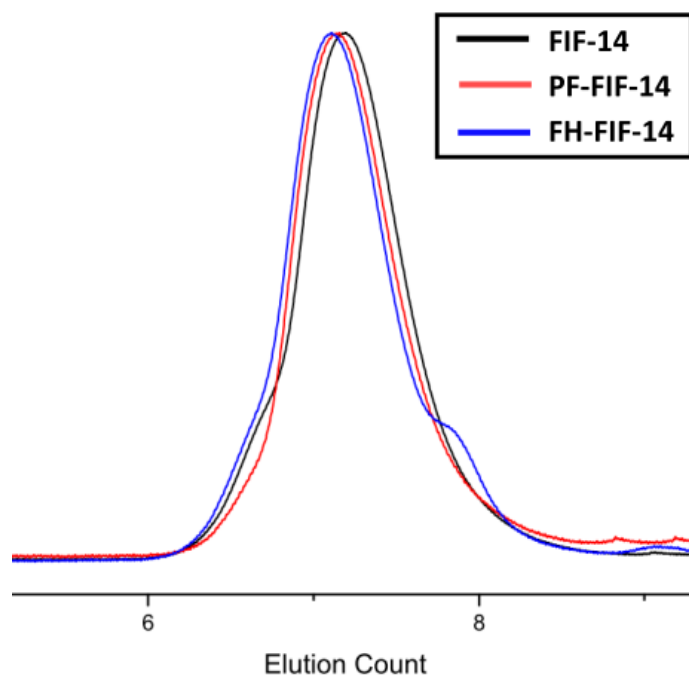


Figure 5.6: GPC of partial and completely hydrogenated FIF-14

molecular weight range of FH-FIF-14 indicated FIF-14 might slightly decompose during hydrogenation. This decomposition might be avoided by reducing the reaction time or pressure during the reaction. All NMR signals from protons associated to carbon-carbon double bonds in FIF-14 disappeared in the ^1H -NMR spectrum (**Figure 5.5**).

5.3.3 Thermal properties: Generally, hydrogenation has been applied to improve the UV resistance and thermal stability of polydiene-based thermoplastic elastomers. After partial hydrogenation of FIF-14, the degradation temperature was improved from 245 °C to 275 °C. Two step degradation was observed in PH-FIF-14 with 17.5% weight lost from 275 °C to 375 °C and 82.5% weight lost from 375 °C to 455 °C. Based on the chemical composition, the first 17.5% weight loss might be subjected to the hydrogenated 1,2-addition units in PBF. The complete hydrogenation further improved the degradation temperature up to 312 °C (**Figure 5.7**). The glass transition of PI was increased slightly from -56 °C to -54 °C as shown in DSC. The T_g of PBF was not observed in non-hydrogenated FIF-14, which indicates a certain level of phase blending between PI and PBF with such compositions. The strength of phase separation was increased after partial hydrogenation as evidenced by a clear T_g corresponding to partially hydrogenated PBF that was observed in DSC at 125 °C. The glass transition temperature of completely hydrogenated PBF was not observed in fully saturated FH-FIF-14 (**Figure 5.8**).

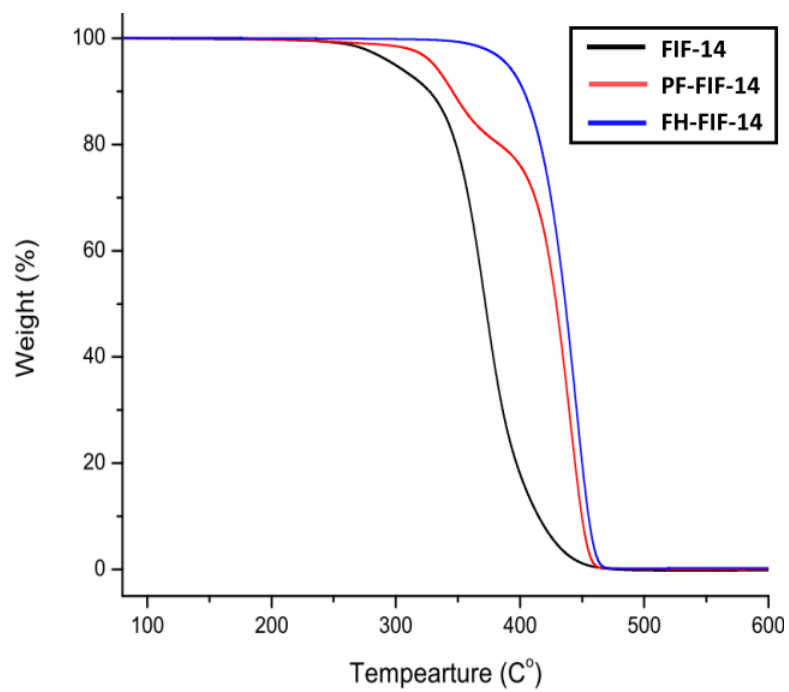


Figure 5.7 TGA of partial and complete hydrogenation of FIF-14

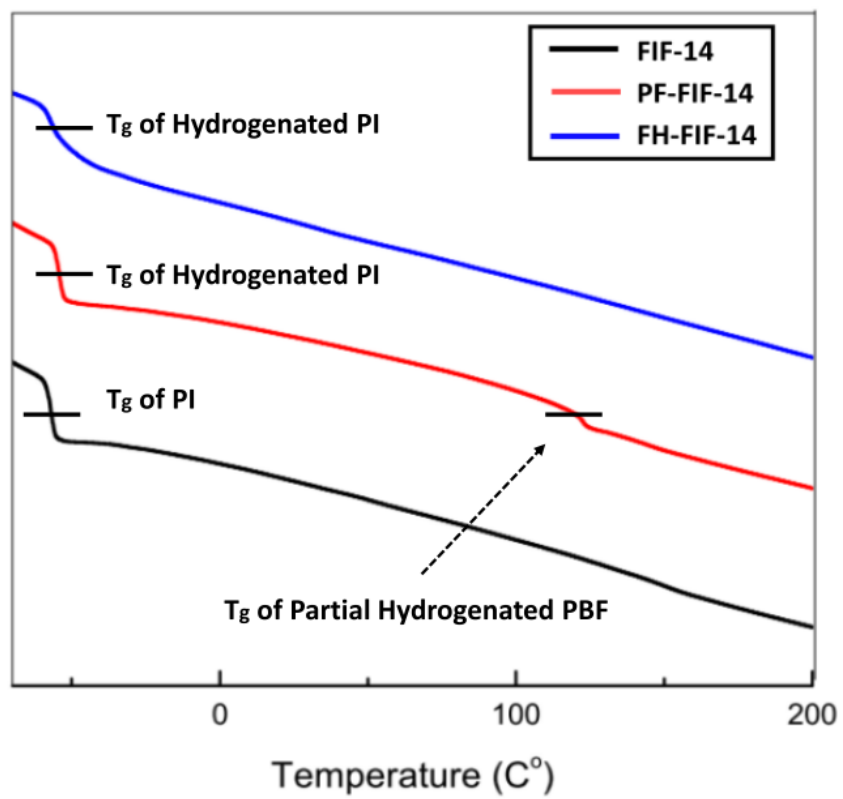


Figure 5.8 DSC of partial and complete hydrogenation of FIF-14

5.3.4 Dynamic mechanical analysis: Since the T_g of FIF-14 and FH-FIF-14 were not observed from DSC, we employed DMA, which is a more sensitive method, to measure T_g or upper service temperature of these two samples. Both measurements were carried out by ramping the temperature from $-80\text{ }^\circ\text{C}$ to $160\text{ }^\circ\text{C}$ with a frequency of 1 Hz. For FIF-14, the first transition was observed at $-54\text{ }^\circ\text{C}$ for PI, which was consistent with DSC measurements. When the temperature was lower than $-54\text{ }^\circ\text{C}$, the storage modulus (G') of FIF-14 was around 990 MPa. As the temperature increased, the rubbery plateau of FIF-14 was observed starting from $-25\text{ }^\circ\text{C}$ to $145\text{ }^\circ\text{C}$ with G' around 20 MPa. The second T_g was observed at $145\text{ }^\circ\text{C}$ for the PBF component in FIF-14 (**Figure 5.9, a**). In the DMA analysis of FH-FIF-14, G' was about 990 MPa in the glassy region. The first glass transition temperature was observed at $-37\text{ }^\circ\text{C}$ for hydrogenated polyisoprene. The rubbery plateau started from $-8\text{ }^\circ\text{C}$ to $130\text{ }^\circ\text{C}$ with G' around 25 MPa. Thus, the service temperature range of FIF-14 was from $-25\text{ }^\circ\text{C}$ to $145\text{ }^\circ\text{C}$ and for FH-FIF-14 was $-8\text{ }^\circ\text{C}$ to $130\text{ }^\circ\text{C}$ (**Figure 5.9, b**).

5.3.5 Tensile Testing: Previously, we reported mechanical properties of FIF triblock copolymers with different volume fractions of PBF. For triblock copolymer FIF-14 which contained 14% volume fraction of PBF, the highest ultimate tensile stress of 1394.4 % was observed with strain at break of 14.3 MPa (**Figure 5.10**, black line). Both partial and complete hydrogenation saturated polyisoprene into poly(ethylene-co-

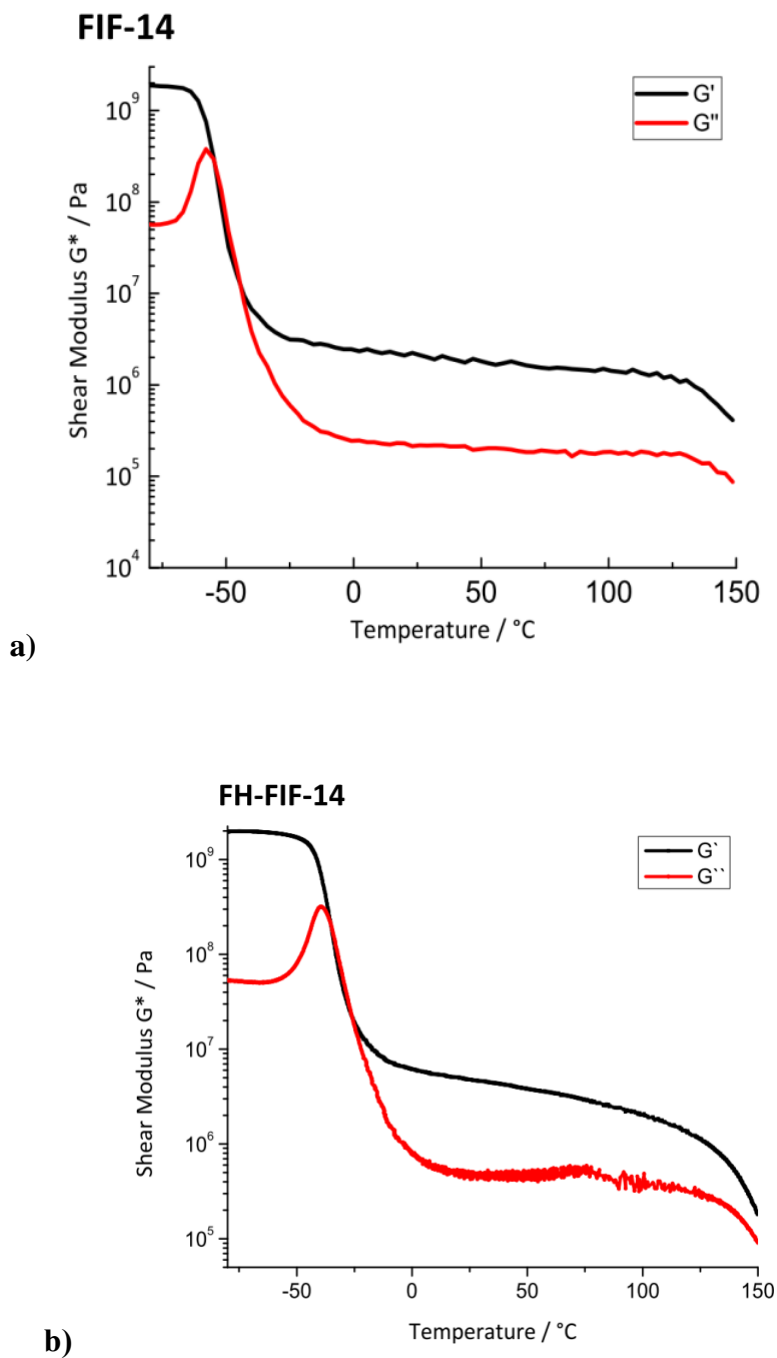


Figure 5.9 DMA of a) FIF-14 and b) FH-FIF-14

propylene) with higher entanglement molecular weight which lead to lower strain at break. PH-FIF-14 displayed 773.9 % strain at break with ultimate stress of 11.4 MPa (**Figure 5.10**, red line). The Young's modulus increased from 2.57 MPa to 3.57 MPa. Tensile tests of FH-FIF-14 was made with a dynamic mechanical analyzer with a controlled forced experiment. FH-FIF-14 did not break at 510 % strain with stress of 16.8 MPa (**Figure 5.11**). The Young's modulus of FH-FIF-14 was 36.9 MPa, higher than both FIF-14 and PH-FIF-14 (**Table 5.3**).

Table 5.3 Mechanical properties of triblock copolymers

Name	Ultimate stress (%)	Strain at break (MPa)	Young's Modulus (MPa)
FIF-14	1394.4 ± 65.7	17.85 ± 1.12	2.57 ± 0.24
PH-FIF-14	773.9 ± 51.4	11.4 ± 0.29	3.57 ± 0.06
FH-FIF-14	>510	>16.8	36.9

5.3.6 Atomic force microscopy (AFM): The phase separation in FIF-14 and FH-FIF-14 was characterized by AFM because no known staining reagent is available to selectively react with one block in both the above mentioned triblock copolymers. By spin coating polymer solutions in toluene onto mica surface, tapping mode AFM was carried out on the surface of two annealed samples. Both samples showed smooth surfaces as observed from height images (**Figure 5.12**, a and c). In the phase image, bright spots

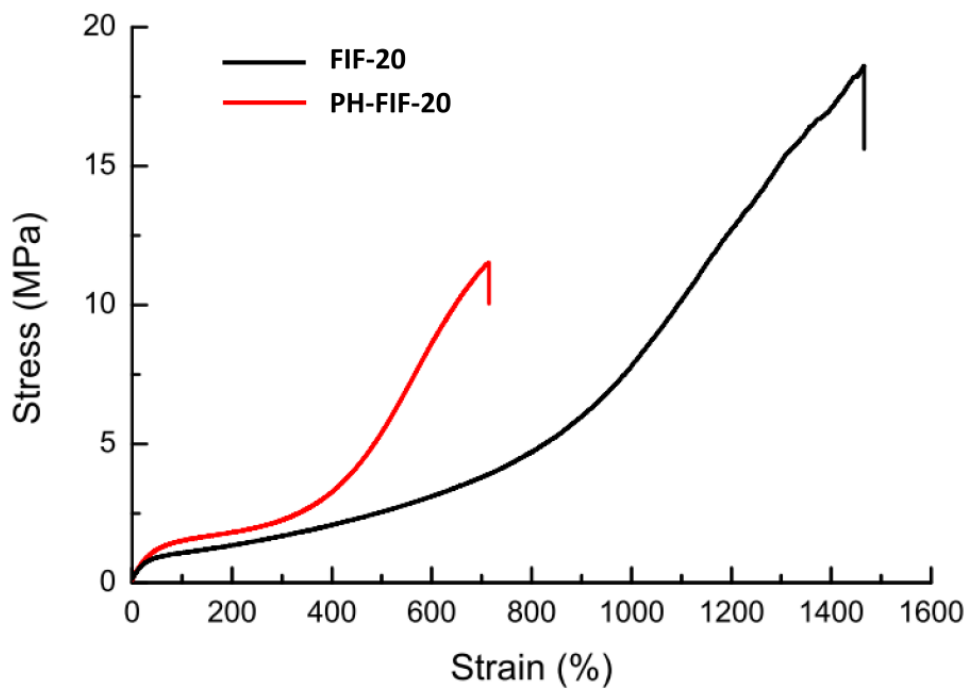


Figure 5.10: Tensile test of FIF-20 and PH-FIF-20

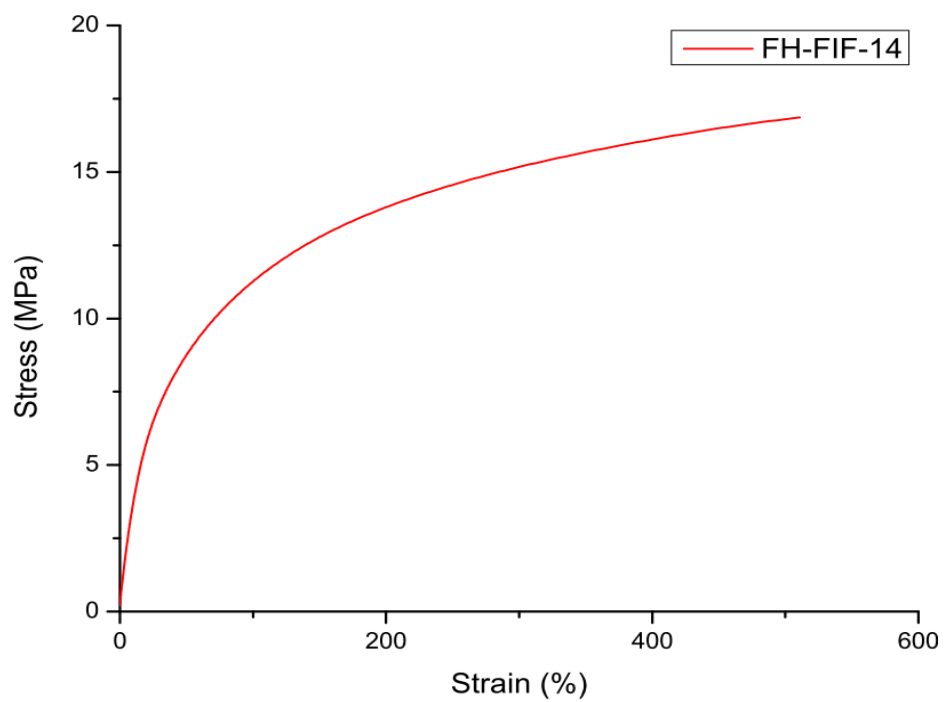


Figure 5.11: Tensile test of FH-FIF-20

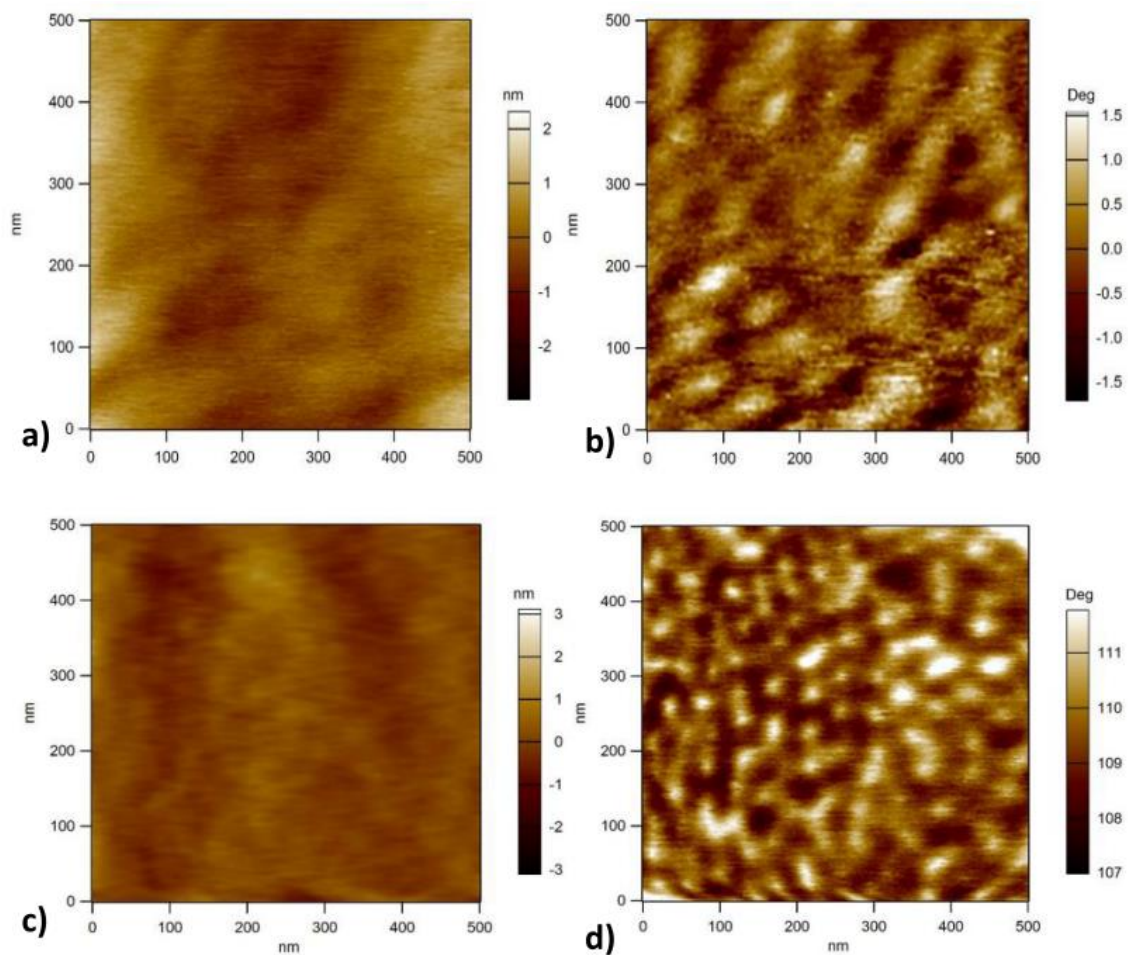


Figure 5.12: AFM of a) Height Image of FIF-14, b) Phase Image of FIF-14, c) Height Image of FH-FIF-14, d) Phase Image of FH-FIF-14.

indicate glassy domains and dark regions represent the elastic domains. In the phase image of FIF-14, phase separation was observed between PBF and PI with spherical PBF domains dispersed in a PI matrix (**Figure 5.12**, b). The domain sizes of PBF averaged from 35 to 55 nm. In the height image of FH-FIF-14, smaller spherical glassy domains were found dispersed in an elastic matrix (**Figure 5.12**, d). The average domain size of fully hydrogenated PBF was from 15 to 33 nm. With smaller domain size, more physical crosslinks were present in the same volume for FH-FIF-14 as compared with FIF-14. This might contribute to the higher tensile stress displayed in the completely hydrogenated triblock copolymers.

5.4 Conclusions:

Complete hydrogenation of PBF with two types of microstructure was carried out with ultra-wide pore silica supported Pt catalyst. After complete hydrogenation of polybenzofulvene, the glass transition of PBF was decreased from 146 °C to 126 °C for PBF with 22% of 1,2-addition. The hydrogenation of PBF with 99% of 1,2-addition decomposed the polymer. Partial and complete hydrogenation of FIF with 20 weight percentage PBF was successful with minor decomposition for complete hydrogenation. Both hydrogenations improved the phase separation, Young's modulus and thermal stability.

References:

- [1]. Holden, G. K., Hans Rytger; R.P. Quirk, *Thermoplastic Elastomers*. 3 ed.; Hanser-Gardner Publications: 2004.
- [2]. Hsieh, H.; Quirk, R. P., *Anionic polymerization: principles and practical applications*. CRC Press: 1996.
- [3]. Handlin, D. L.; Trenor, S.; Wright, K., Applications of Thermoplastic Elastomers Based on Styrenic Block Copolymers. In *Macromolecular Engineering: Precise Synthesis, Materials Properties, Applications*, Matyjaszewski, K.; Gnanou, Y.; Leibler, L., Eds. Wiley-VCH: 2007; Vol. 4, pp 2001-2031.
- [4]. Grand View Research Inc., Styrenic Block Copolymers (SBCs) Market Analysis And Segment Forecasts To 2020. <http://www.grandviewresearch.com/industry-analysis/styrenic-block-copolymers-sbcs-industry>, (accessed Oct. 09).
- [5]. Geoffrey, H.; Milkovich, R. Block polymers of monovinyl aromatic hydrocarbons and conjugated dienes. US 3265765 A, 1966.
- [6]. Fetters, L. J.; Morton, M. *Macromolecules* **1969**, 2 (5), 453-458.
- [7]. Fetters, L. J.; Firer, E. M.; Dafauti, M. *Macromolecules* **1977**, 10 (6), 1200-1207.
- [8]. Kobayashi, S.; Kataoka, H.; Ishizone, T.; Kato, T.; Ono, T.; Kobukata, S.; Ogi, H. *Macromolecules* **2008**, 41 (14), 5502-5508.
- [9]. Bolton, J. M.; Hillmyer, M. A.; Hoye, T. R. *ACS Macro Letters* **2014**, 3 (8), 717-720.

- [10]. Yu, J. M.; Dubois, P.; Jérôme, R. *Macromolecules* **1996**, *29* (26), 8362-8370.
- [11]. Yu, J. M.; Dubois, P.; Jérôme, R. *Macromolecules* **1996**, *29* (23), 7316-7322.
- [12]. Yu, J. M.; Dubois, P.; Jérôme, R. *Macromolecules* **1997**, *30* (21), 6536-6543.
- [13]. Kosaka, Y.; Kitazawa, K.; Inomata, S.; Ishizone, T. *ACS Macro Letters* **2013**, *2* (2), 164-167.
- [14]. Kosaka, Y.; Goseki, R.; Kawauchi, S.; Ishizone, T. *Macromolecular Symposia* **2015**, *350* (1), 55-66.
- [15]. Kosaka, Y.; Kawauchi, S.; Goseki, R.; Ishizone, T. *Macromolecules* **2015**, *48* (13), 4421-4430.
- [16]. Worsfold, D. J.; Bywater, S. *Canadian Journal of Chemistry* **1964**, *42* (12), 2884-2892.
- [17]. Bywater, S.; Worsfold, D. J. *Canadian Journal of Chemistry* **1967**, *45* (16), 1821-1824.
- [18]. Halasa, A. F.; Lohr, D.; Hall, J. *Journal of Polymer Science: Part A Polymer Chemistry Edition* **1981**, *19* (6), 1357-1360.
- [19]. Garton, A.; Bywater, S. *Macromolecules* **1975**, *8* (6), 694-697.
- [20]. Hong, K.; Mays, J. W. *Macromolecules* **2001**, *34* (4), 782-786.
- [21]. W, Wang, R. Schlegel, T.White, K.Willimson, D.Voyloy, A. Goodwin, E. B. Coughlin, S. Gido, M. Beiner, K. Hong, N.G. Kang, J.Mays, High temperature

thermoplastic elastomers synthesized by living anionic polymerization in hydrocarbon solvent at room temperature. (Unpublished)

[22]. Amberg, L. O.; Robinson, A. E. *Industrial & Engineering Chemistry* **1961**, *53* (5), 368-370.

[23]. Gotro, J. T.; Graessley, W. W. *Macromolecules* **1984**, *17* (12), 2767-2775.

[24]. Leclerc, M. K.; Waymouth, R. M.. *Angewandte Chemie International Edition* **1998**, *37* (7), 922-925.

[25]. Mohammadi, N. A.; Rempel, G. L. *Journal of Molecular Catalysis* **1989**, *50* (3), 259-275.

[26]. Krigas, T. M.; Carella, J. M.; Struglinski, M. J.; Crist, B.; Graessley, W. W.; Schilling, F. C. *Journal of Polymer Science: Polymer Physics Edition* **1985**, *23* (3), 509-520.

[27]. Bhattacharjee, S.; Rajagopalan, P.; Bhowmick, A. K.; Avasthi, B. N. *Journal of Applied Polymer Science* **1993**, *49* (11), 1971-1977.

[28]. Hucul, D. A.; Hahn, S. F. *Advanced Materials* **2000**, *12* (23), 1855-1858.

[29]. Bates, F. S.; Fredrickson, G. H.; Hucul, D.; Hahn, S. F. *AIChE Journal* **2001**, *47* (4), 762.

[30]. Mahanthappa, M. K.; Lim, L. S.; Hillmyer, M. A.; Bates, F. S. *Macromolecules* **2007**, *40* (5), 1585-1593.

[31]. Uhrig, D.; Mays, J. W. *Journal of Polymer Science. Part A: Polymer Chemistry* **2005**, *43* (24), 6179-6222.

Chapter 6: Synthesis and Characterization of Graft Copolymers Poly(isoprene-g-styrene) of High Molecular Weight by a Combination of Anionic Polymerization and Emulsion Polymerization

Abstract: In this work, high molecular weight “comb-shaped” graft copolymers, poly(isoprene-*g*-styrene), with polyisoprene as the backbone and polystyrene as side chains, were synthesized via free radical emulsion polymerization by copolymerization of isoprene with a polystyrene macromonomer synthesized using anionic polymerization. A small amount of toluene was used in order to successfully disperse the macromonomer. Both a redox and thermal initiation systems were used in the emulsion polymerization, and the latex particle size and distribution were investigated by dynamic light scattering. The structural characteristics of the macromonomer and comb graft copolymers were investigated through use of size exclusion chromatography, spectroscopy, microscopy, thermal analysis, and rheology. While the macromonomer was successfully copolymerized to obtain the desired multigraft copolymers, small amounts of unreacted macromonomer remained in the products, reflecting its reduced reactivity due to steric effects. Nevertheless, the multigraft copolymers obtained were very high in molecular weight ($5\text{--}12 \times 10^5$ g/mol) and up to 10 branches per chain, on average, could be incorporated. A material incorporating 29 wt% polystyrene exhibits a disordered microphase separated morphology and elastomeric properties. These materials show promise as new, highly tunable, and potentially low cost thermoplastic elastomers.

Keywords: graft copolymer; anionic polymerization; emulsion polymerization; macromonomer; rheology

6.1 Introduction:

Graft copolymers have attracted much attention in many fields over the past few decades.¹⁻² As compared to block copolymers, graft copolymers provide additional architectural flexibility, since graft (side chain) density, graft length, and backbone length can be systematically varied¹⁻³. By judicious choice of monomers used and by controlling the macromolecular composition and architecture, the resulting graft copolymers may find a range of applications, including water-dispersible nanostructures with potential for carrying drugs and other biological cargo, nanostructured materials, photonic materials, and tough renewable materials.^{1-2, 4-6} Multigraft copolymers with polyisoprene (PI) as backbones and polystyrene (PS) as side chains constitute a novel class of thermoplastic elastomers called “superelastomers”.⁷⁻⁸ Superelastomers have advantageous properties as compared to commercial linear thermoplastic elastomers, such as larger elongation at break, lower residual strain, and highly tunable modulus.⁹⁻¹⁰ These property advantages reflect enhanced interactions between the glassy nanodomains and the rubbery matrix and the ability to tune morphology independent of composition.

Graft copolymers are synthesized by three main strategies: “grafting onto”, “grafting from”, and “grafting through” (also known as the macromonomer technique).¹⁻² When living polymerization methods are employed, graft copolymers having narrow polydispersity backbones and/or side chains can be synthesized.^{3, 11} However, the precise

number of side chains per molecule, the placement of the branch points along the backbone, and the number of branches per branch point could not be readily controlled until recently, as discussed in detail in a recent review.¹¹ As part of a systematic study on structure-property relationships for graft copolymers, Mays et al. developed a novel strategy for synthesis of multigraft copolymer. In this work, near-monodisperse backbone segments (of PI) and side chains (of PS), made by living anionic polymerization, were linked together via chlorosilane linking chemistry in order to achieve regular branch point spacing and control of the number of side chains per branch point. The resulting regular “comb”, “centipede” and “barbwire” multigraft copolymers were endowed with one, two, and four branches per branch point, respectively.¹²⁻¹³ As noted above, certain of these poly(isoprene-*g*-styrene) multigraft copolymers behave as thermoplastic elastomers and exhibit exceptional properties.⁷⁻¹⁰ Unfortunately, their synthesis by anionic polymerization is very demanding and time consuming.¹²⁻¹³

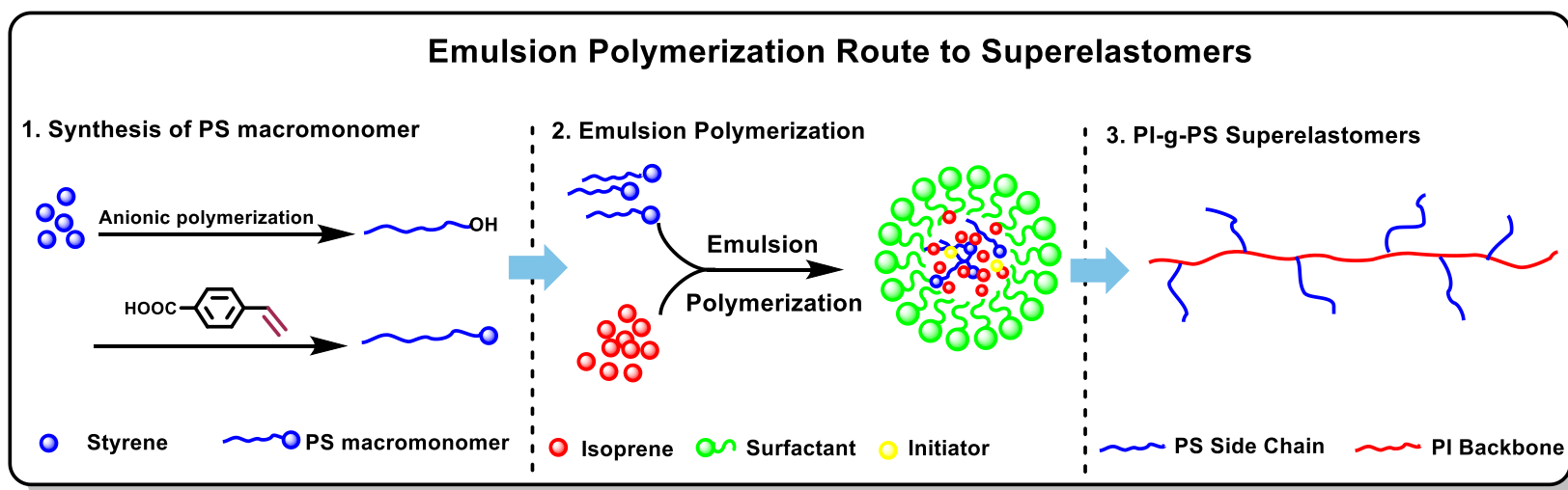
The grafting through or macromonomer method offers a simpler approach for the synthesis of multigraft copolymers which have controlled number of side chains per branch point. Thus, while the use of a conventional “single-tailed” macromonomer yields a single side chain (comb), a “double-tailed” macromonomer yields two side chains (centipede), and a “triple-tailed” macromonomer yields three side chains per branch point, as demonstrated by Hadjichristidis et al. using anionic copolymerization.¹⁴⁻¹⁵ For these

materials, branch point spacing is not regular but is determined by the reactivity ratios of the two species, macromonomer and co-monomer. Disparities in reactivity preferences are generally greater with ionic mechanisms than in free radical polymerization, and thus it can in some cases be difficult or impossible to achieve the desired spacing of the side chains. We recently synthesized poly(isoprene-*g*-styrene) multigraft copolymers by anionic copolymerization of double-tailed PS macromonomer with isoprene in benzene using potassium alkoxide as a polar modifier. This modifier facilitates random copolymerization of the two monomers and gives high (90%) 1, 4-PI microstructure necessary for a low glass transition temperature (T_g) and good elastomeric properties. These random multigraft copolymers have been found to exhibit the same exceptional tensile properties as regularly spaced “superelastomers”, while being much easier to synthesize.

For several reasons it is desirable to develop a free radical approach to the synthesis of superelastomer materials. Free radical polymerization is applicable to a much wider range of monomers as compared to anionic polymerization. Radical polymerization requires far less stringent reaction conditions, and allows the use of lower cost initiators and a wider choice of dispersing media, including water. Also, macromonomers are solid materials that are extremely difficult to purify to the standards required for anionic polymerization.^{16,17} In addition, emulsion polymerization is well-suited to synthesis of

polymers and copolymers of very high molecular weight, which is necessary for producing multigraft copolymer elastomers having high tensile strength and large elongations at break.¹⁸ Furthermore, emulsion polymerization is used to produce styrene-butadiene rubber (SBR) on a massive scale, so it is compatible with hydrocarbon monomers (styrene and isoprene) using in our previous studies.¹⁹ Indeed, poly(isoprene-*g*-styrene) has been recently synthesized by emulsion copolymerization by grafting PS onto preformed nanosized PI particles.²⁰

Here we report the synthesis of comb branched poly(isoprene-*g*-styrene) multigraft copolymers having PI as the backbone and PS as side chains via a macromonomer method combining anionic polymerization and conventional free radical emulsion polymerization. Hydroxyl-terminated PS was synthesized via high-vacuum anionic polymerization and end-capping with ethylene oxide. The polystyrene macromonomer was obtained through Steglich esterification between the hydroxyl-terminated PS and 4-vinylbenzoic acid. The PS macromonomer was then copolymerized with isoprene in emulsion polymerization, initiated by use of either azobisisobutyronitrile (AIBN) or redox initiation, to produce comb graft copolymers (**Scheme 6.1**). The structural characteristics of both the macromonomer and the comb graft copolymers were investigated. The rheological properties of the comb graft copolymers were studied, and the elastomeric properties of the comb graft copolymers were confirmed.



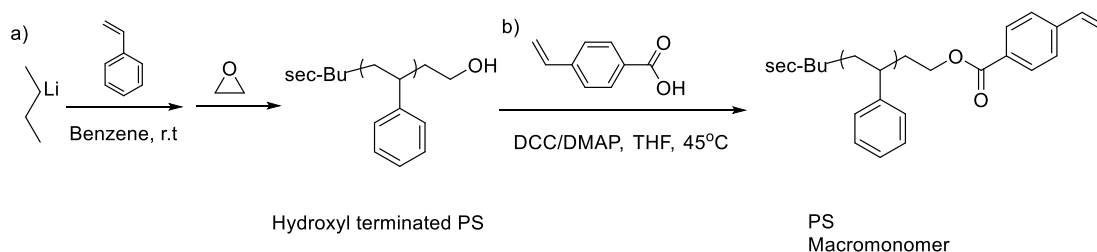
Scheme 6.1: Emulsion copolymerization strategy for obtaining graft copolymer by macromonomer method.

6.2 Experimental Section:

6.2.1 Materials: Sec-butyllithium (Aldrich, 1.4 M in cyclohexane) was used as received after double titration with allyl bromide to verify its concentration.²¹ Benzene (Sigma-Aldrich, $\geq 99.9\%$) and styrene (Sigma-Aldrich, $\geq 99\%$) were purified to the standards required for anionic polymerization as previously reported.¹⁶⁻¹⁷ Methanol (Sigma-Aldrich, $\geq 99.9\%$) was degassed on the vacuum line before distilling into ampules followed by flame sealing. Ethylene oxide (Aldrich, $\geq 99.5\%$) was purified by allowing it to stand over sodium–potassium alloy for 30 min after drying over calcium hydride. Other reagents in the syntheses were purified as per standard all glass high-vacuum anionic polymerization techniques.¹⁷⁻¹⁸ 4-(Dimethylamino)pyridine (DMAP, Aldrich, $\geq 99\%$) and N,N'-dicyclohexylcarbodiimide (DCC, Acros Organics, 99%) were both used as received. Sodium dodecylbenzenesulfonate (SDBS, Sigma-Aldrich, technical grade) was used as received. 2, 2-Azodiisobutyronitrile (AIBN, Aldrich, 90%) was recrystallized before use. 4-Vinylbenzoic acid (Aldrich, 97%) was used as received. The redox initiation system, cumene hydroperoxide ($C_9H_{12}O_2$, Aldrich, 80%), the reducing agent sodium formaldehyde sulfoxylate (SFS, $CH_3NaO_3S \cdot 2H_2O$, Aldrich, $\geq 98\%$), Iron (II) sulfate heptahydrate ($FeSO_4 \cdot 7H_2O$, Sigma-Aldrich, $\geq 99\%$) and ethylenediaminetetraacetic acid disodium salt dihydrate (EDTA- Na_2 , $C_{10}H_{14}N_2Na_2O_8 \cdot 2H_2O$, Sigma-Aldrich, 99%) were used as received. Deionized water (DI water) and other reagents were used as received. A stock solution of 100 mL was prepared from 0.0621 g $FeSO_4 \cdot 7H_2O$, 0.1365 g EDTA- Na_2 and

deionized water. The ratio of $\text{FeSO}_4 \cdot 7\text{H}_2\text{O}$ and EDTA-Na_2 was that suggested by Prince and Spitz²².

6.2.2 Synthesis of PS macromonomer: All anionic polymerizations were carried out in sealed, all-glass apparatuses using standard high-vacuum techniques.¹⁶⁻¹⁷ The synthesis procedure for hydroxyl-terminated PS was reported previously²³, and the reaction sequence is shown in **Scheme 2, a**. The number-average molecular weight (M_n) of the PS was designed to be 4800 g/mol. Macromonomers were synthesized by the well-known Steglich esterification reaction in the presence of DCC and DMAP²⁴, and the synthetic route is shown in **Scheme 2, b**.



Scheme 6.2: The synthetic route to PS macromonomer. (a) the synthesis procedure for hydroxyl-terminated PS; (b) Steglich esterification reaction for synthesis of PS macromonomer.

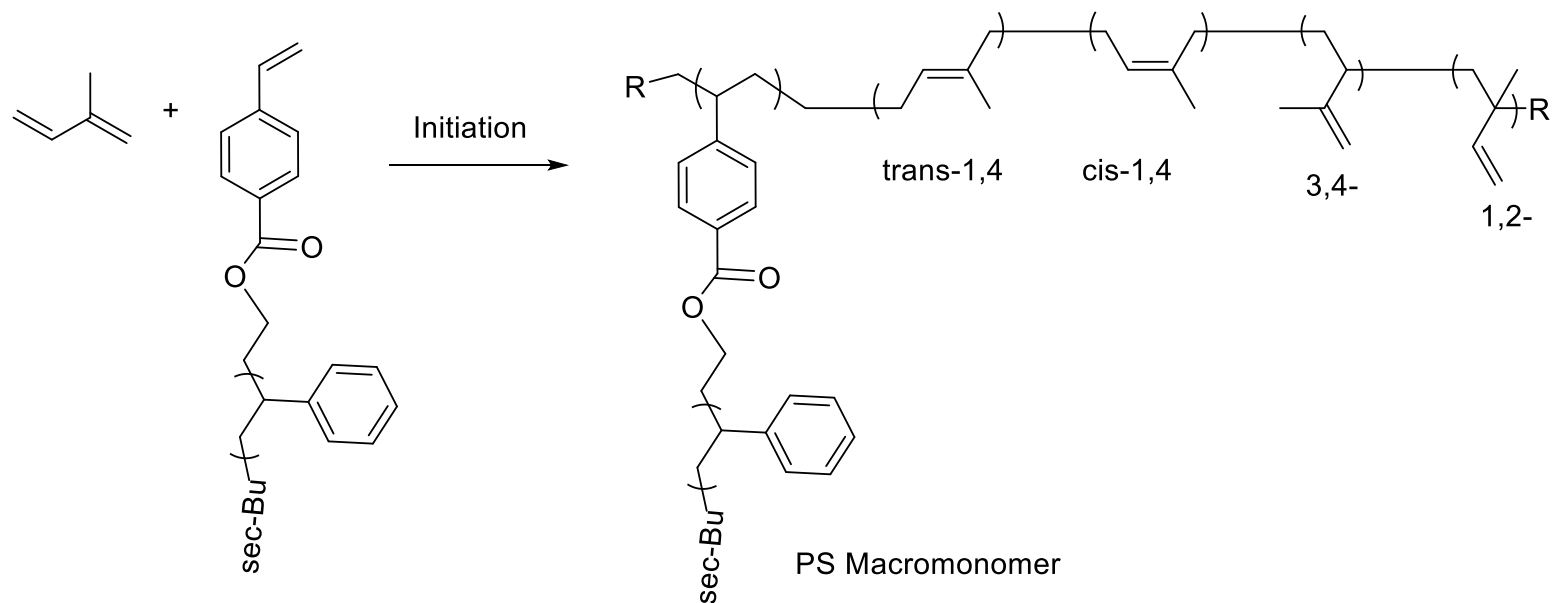
6.2.3 Synthesis of graft copolymers: PS macromonomer, isoprene, and toluene, in the amounts shown in **Table 6.1**, were mixed together to form a homogeneous solution under sonication while cooling with an ice bath, and then the initiator AIBN (or cumene

Table 6.1: Recipes for synthesis of PI-g-PS multigraft copolymers

Samples	MG-3-1	MG-3-2	MG-3-3	MG-3-4 ^d	MG-3-5
Ingredients					
SDBS (g)	0.0848	0.0807	0.081	0.0802	0.080
DI water (g)	6.0783	6.0804	6.08	6.1115	6.05
isoprene (g)	1.5	1.501	1.003	1.508	1.06
PS macromonomer (g)	0.31	0.2005	0.201	0.2003	0.206
toluene(g)	0.9023	0.6054	0.6046	0.6149	0.6018
AIBN	-	-	-	-	0.0252
EDTA-Na ₂ and FeSO ₄ ·7H ₂ O stock solution(mL)	1	1	1	1	-
Cumene hydroperoxide (g)	0.0133	0.0137	0.0139	0.0138	-
SFS (g)	0.0068	0.0069	0.0068	0.0066	-
Temperature (°C)	40	40	60	60	60
Reaction time (h)	24	24	8	24	8
C ^a (isoprene) (%)	21	24	56	73	29
C ^b (macromonomer)(%)	-	-	31	-	61
Latex particle diameter ^c (nm)	-	-	54	-	77
PDI ^e	-	-	0.41	-	0.25

^aConversion of isoprene measured by gravimetric method. ^bConversion of PS macromonomer calculated by the conversion of isoprene and ¹H-NMR of graft copolymer. ^cMeasured by dynamic light scattering. ^dGelation. ^eThe polydispersity values of latex particles were measured by DLS.

hydroperoxide for the redox initiation system) was added into the solution. The mixture was poured into a vial containing the SDBS aqueous solution, and the vial was placed into the sonicator while cooling with the ice bath for pre-emulsification. After 5 min, the emulsion was transferred to a glass flask equipped with a magnetic stirrer, reflux condenser, and nitrogen inlet. For the redox initiation system, the EDTA- Na_2 and $\text{FeSO}_4 \cdot 7\text{H}_2\text{O}$ stock solution with SFS were added into the pre-emulsion under nitrogen after the mixture was pre-emulsified. After 5 min of nitrogen purging, the flask was sealed and put into a thermostatted oil bath to initiate the polymerization. The polymerization was initiated under different temperatures. The polymerization was stopped by cooling after several hours, and the copolymer was obtained by breaking the emulsion using sodium chloride. The copolymer was purified three times by dissolving it in tetrahydrofuran (THF) and precipitating into methanol, and it was dried under vacuum at 30 °C for 24 h. The graft copolymers were further purified by fractionation to remove some unreacted macromonomer using toluene as solvent and methanol as non-solvent. **Scheme 6.3** shows the synthetic route to comb multigraft graft copolymers by emulsion copolymerization. A general nomenclature for these multigraft copolymers, MG-n-m, is employed. MG stands for “multigraft”, and n is the junction point functionality. The “m” represents different samples.



Scheme 6.3 The synthetic route to poly(isoprene-*g*-styrene) multigraft copolymer via free radical emulsion copolymerization.

6.2.4 Characterization: SEC (Size Exclusion Chromatography) was carried out at 40 °C using an EcoSEC GPC system (Tosoh Biosciences LLC) with a RI-8320 detector and two TSK gel super Multipore HZM columns. A six-point calibration was obtained using polystyrene standards (Tosoh, molecular weight range: 2.6×10^2 - 7.0×10^5 Da) and was used to obtain molecular weight characteristics and polydispersity indices (PDI). THF was used as the mobile phase at a flow rate of 0.35 mL/min. ^1H - and ^{13}C -NMR spectra were obtained on a Varian Mercury 500 instrument. Samples were dissolved in deuterated chloroform (CDCl_3). The MALDI-TOF mass spectra were recorded using a Bruker Autoflex II model smart-beam instrument equipped with a nitrogen laser (337 nm). Samples were dissolved in THF, dithranol was used as the matrix, and sodium trifluoroacetate was used as the cation source. The latex particle size was measured at 25°C using DLS (PD Expert System, Precision Detectors Inc., Bellingham, MA, USA). A laser of 683 nm wavelength was used as the light source, and light scattered by the sample was detected at 95°. Each sample was scanned 120 times, and the mean particle size was determined by averaging values from at least 10 different experiments. Thermal stability of the multigraft copolymers was examined using TGA (Discovery, TA Instruments, New Castle, DE). Briefly, 15-20 mg of sample was placed on platinum pans before equilibrating at 30°C. The temperature was then ramped to 650 °C at 10 °C/min. All TGA work was done under a nitrogen atmosphere. A TA Instruments Q2000 differential scanning calorimeter (DSC) was used to investigate thermal transitions of the

copolymers. Analysis was performed under a nitrogen purge at a heating rate of 10 °C/min from -80 °C to 150°C. The glass transition temperature (T_g) was determined from the second heating in order to erase the thermal history. T_g is reported as the temperature of the midpoint of the heat capacity change determined from the baseline tangents using Universal Analysis software (TA Instruments). A solution-cast film of graft copolymer was prepared from a nonselective solvent (toluene). The solvent was allowed to evaporate slowly over 7 days at room temperature. The film was then dried to a constant weight in a vacuum oven at 120°C for 3 days. Samples were embedded into low viscosity epoxy resin before cryo-microtoming into ~100nm thick slices. These sections were collected on TEM grids and stained in OsO₄ vapor for 30min. TEM experiments were performed in a Zeiss Libra 120 at 120kV with an emission current as low as 3μA and minimal exposure time to minimize electron-beam-induced morphological changes and damages. Thin film morphologies were examined using a PicoSPM II AFM (Molecular Imaging, Santa Clara, CA) instrument in tapping mode. Samples were prepared from a 1 wt% solution using toluene as solvent by spin coating onto small glass wafers. The observed surface structures were analyzed using WSxM 5.0 Develop 5.3 scanning probe microscopy software. The solid samples were analyzed on a parallel plate RDA II rheometer (Rheometrics). Polymer disks of 8 mm diameter and 0.5 to 2 mm thickness were chosen for this analysis. These samples were analyzed by strain-fixed dynamic rheology with a frequency sweep from 0.1 to 100 Hz at room temperature.

6.3 Results and Discussion

6.3.1 Synthesis of PS macromonomer: Polystyrene macromonomer was prepared by high-vacuum living anionic polymerization by combining the procedure described by Ji et al.²³ for synthesis of hydroxyl-terminated PS with Steglich esterification.²⁴ The resulting PS macromonomer has a sec-butyl group at the α -end and a polymerizable styryl group at the ω -end. Its structure and purity were thoroughly characterized by a combination of SEC, ¹H NMR and MALDI-TOF-MS. **Figure 6.1** shows the SEC curve for this material, exhibiting a symmetric and unimodal distribution, and the analysis of the chromatogram yielded M_n of 5100 g/mol with PDI=1.08. The ¹H NMR spectrum of the PS macromonomer is shown in **Figure 6.2**. The characteristic peaks for vinyl protons from the styryl group (Ha and Ha', 2H, δ 5.2 and 5.7 ppm) and methyl protons from the sec-butyl initiator fragment (Hc, 6H, δ 0.5-0.8 ppm)²⁵⁻²⁶ can be clearly seen in **Figure 6.2**. Moreover, the characteristic peaks of phenyl protons (Hb, 5H, δ 6.2-7.2 ppm) are also observed in **Figure 6.2**. **Figure 6.3** shows the MALDI-TOF spectrum of the PS macromonomer, and it confirms the uniformity and well-defined nature of the material. M_n and PDI values of 4900 g/mol and 1.02, respectively, were calculated from the MALDI-TOF spectrum. A representative monoisotopic mass peak at m/z 4727.3 corresponds to the 43-mer of (ω -vinylbenzyl)-polystyrene, $C_4H_9-(C_8H_8)_{43}-C_{11}H_{11}O_2 \cdot Na^+$, with calculated monoisotopic mass $[57(C_4H_9)+43 \times 104(C_8H_8)+175(C_{11}H_{11}O_2)+23(Na^+)]=4727$ g/mol. Overall, no dimer peak was found in the SEC chromatogram, and the MALDI-TOF result did not show

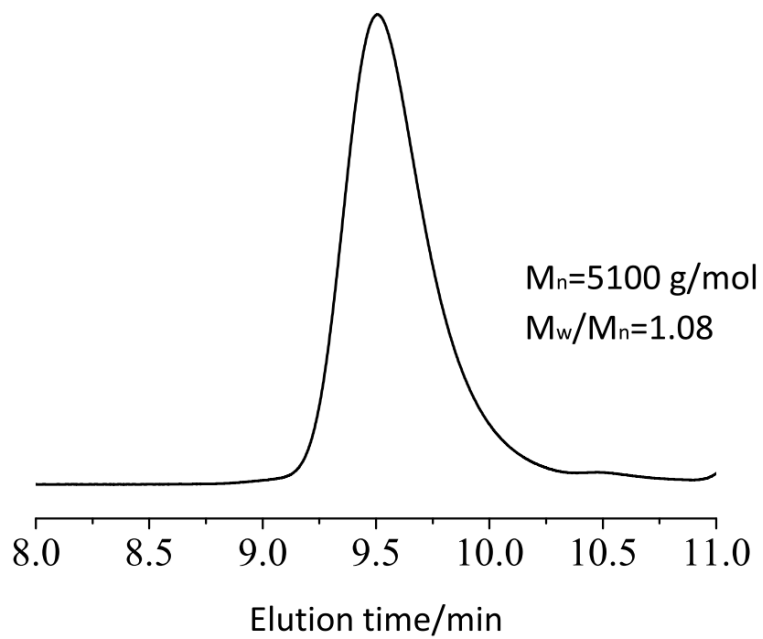


Figure 6.1 SEC chromatogram for polystyrene macromonomer.

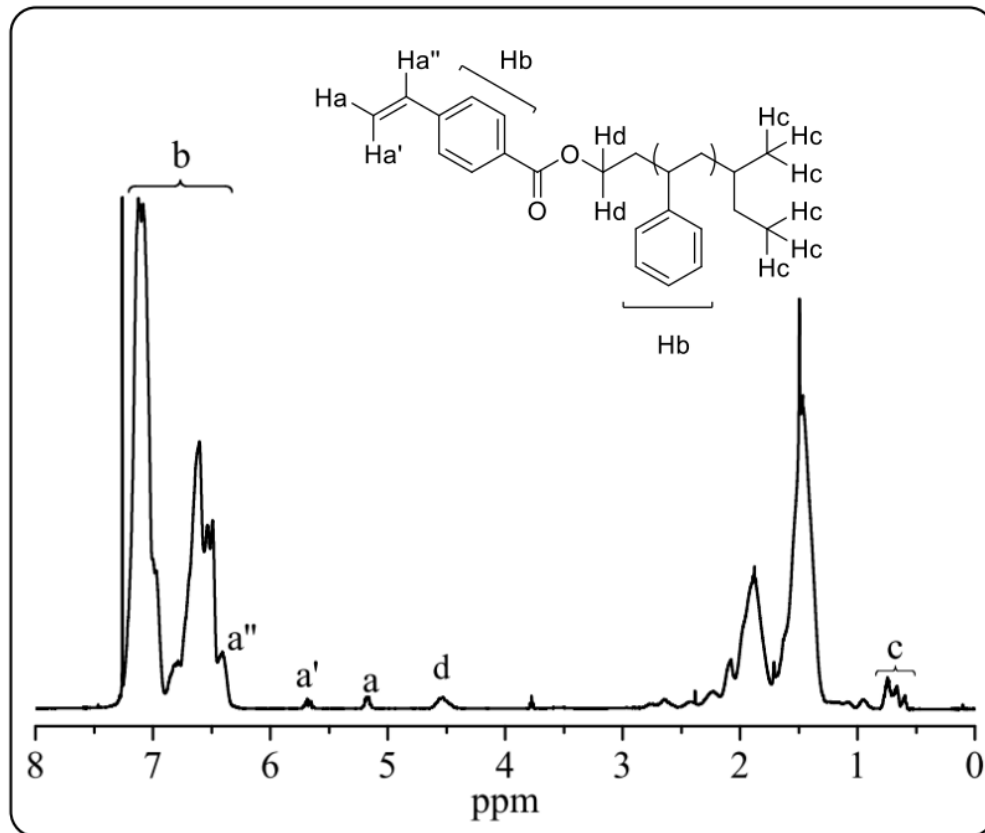


Figure 6.2 $^1\text{H-NMR}$ spectrum of polystyrene macromonomer.

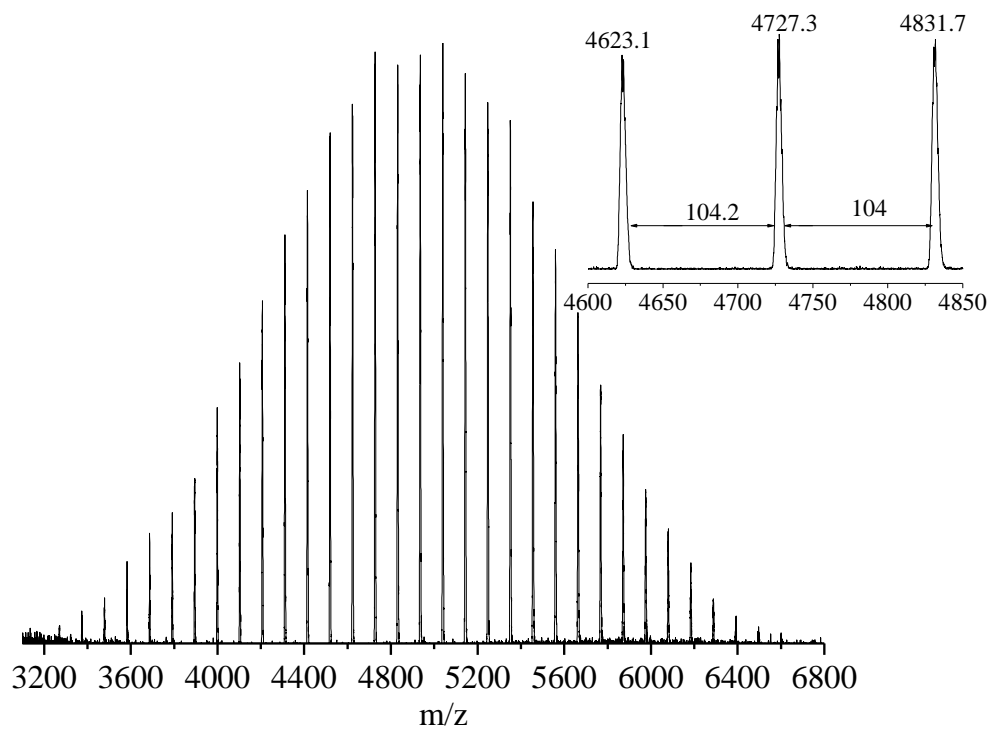


Figure 6.3 MALDI-TOF mass spectrum of PS macromonomer.

unfunctionalized species. These results, together with the NMR result, support the efficient synthesis of macromonomer with controlled molecular weight, narrow PDI and 100% styryl end functionality.

6.3.2 Characterization of latex particles composed of graft copolymers: From **Table 6.1**, it can be seen that the copolymerization of PS macromonomer and isoprene was carried out at different temperatures. When the temperature was 40 °C, the copolymerization rate was low and the conversion of isoprene was only 21% and 24% in MG-3-1 and MG-3-2 after 24 h, respectively. When the temperature was 60 °C, gelation occurred after 24 h in MG-3-4. This long reaction time and high temperature apparently leads to free radicals attacking residual double bonds of PI leading to crosslinking. Therefore, polymerizations to yield MG-3-3 and MG-3-5 were carried out at 60 °C using a different initiation system. The size and size distribution of graft copolymer latex particles in MG-3-3 and MG-3-5 initiated by AIBN and redox initiation were characterized by DLS, and the results are shown in **Figure 6.4** and **Table 6.1**. From **Figure 6.4**, we can see that the latex particles have average diameters of 50 to 80 nm, with narrow size distributions. The PDI of two samples were 0.41 and 0.25, respectively. Therefore, the emulsion latex incorporating the macromonomer was stable enough for the emulsion polymerization to proceed successfully.

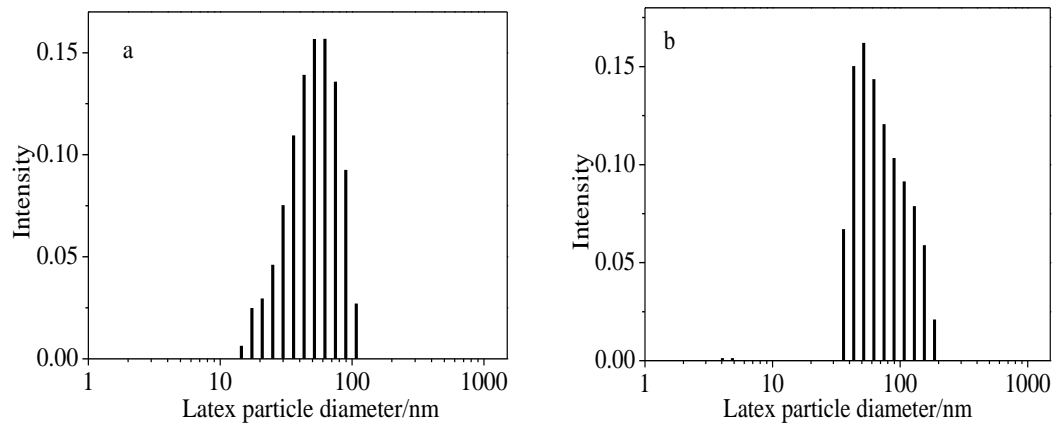


Figure 6.4 DLS size results for latex particles formed by graft copolymerization of macromonomer and isoprene, (a) for sample MG-3-3; (b) for sample MG-3-5.

6.3.3 Characterization of “comb” graft copolymers: The molecular weights and molecular weight distributions of the graft copolymers before and after fractionation were investigated by SEC, and the chromatograms are shown in **Figure 6.5**. The SEC curve of the PS macromonomer is also shown in Figure 6.5 for comparison. From Figure 6.5, we can see that there was a small amount of residual PS macromonomer in the graft copolymers before fractionation. This is attributed to the PS macromonomer being less reactive in copolymerization because of steric effects (vinyl group sterically hindered within a polymer coil). However, the low molecular weight peak in SEC curves disappeared after fractionation and the peaks of grafted copolymers are shifted to much higher molecular weight as compared to that of the macromonomer. Thus, non-polymerized macromonomer was removed completely from the product by fractionation. The apparent number-average and weight-average molecular weights and PDIs based on the polystyrene calibration curve are presented in **Table 6.2**. Comparing the molecular weights and PDIs of MG-3-3 and MG-3-5, we can see that the molecular weight of MG-3-5 synthesized by AIBN initiation is much higher than that of MG-3-3 initiated by redox reaction. In addition, the PDI of MG-3-5 is lower than that of MG-3-3, although it is not clear that PDI is an important parameter in determining the elastomeric properties of these materials.

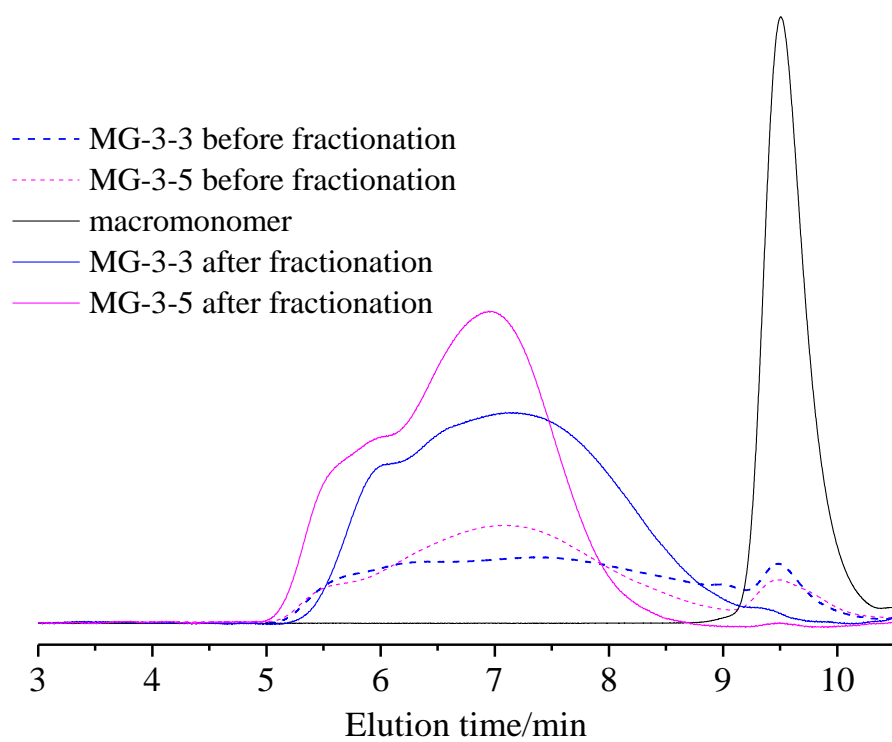


Figure 6.5. SEC chromatograms for PS macromonomer and multigraft copolymers before and after fractionation.

Table 6.2 Average molecular weights and compositions of macromonomer and multigraft copolymers as measured by SEC and $^1\text{H-NMR}$.

Sample	Mn (g/mol)	Mw (g/mol)	PDI	no. of junction points/molecule ^b	PS (wt%) ^c	PS (wt%)
PS Macromonomer	5100	5510	1.08	-	-	100
MG-3-3	66100	520000	7.9	1.3	16.7	9.8 ^a
MG-3-5	182000	1160000	6.3	10.3	16.3	28.9 ^a

^aThe mass ratio of PS in the graft copolymer was calculated from the integral area of protons of PI and PS in $^1\text{H-NMR}$. ^bNumber of junction points per molecules were calculated according to the total Mn of multigraft copolymer and the mass ratio of PI and PS. ^cThe theoretical weight ratio of PS according to the feeding weight

The compositions of graft copolymers were measured by ^1H -NMR (**Figure 6.6, a**) and ^{13}C -NMR (**Figure 6. 6, b**) to certify the copolymerization of isoprene and macromonomer. From **Figure 6.6.a**, the sharp chemical shifts of methyl protons from *trans*-1,4 (*dH*), *cis*-1, 4 (*jH*), 3,4-addition (*nH*) and 1,2-addition (*rH*) polyisoprene can be observed at 1.58 ppm and 1.68 ppm.²⁷⁻²⁸ The peaks at 5.71-5.8 ppm (*sH*) from 1,2-addition are seen in **Figure 6.6.a**. The methylene protons of *trans*-1, 4 (*aH*, *eH*), *cis*-1, 4 (*fH*, *iH*) and methine protons of 3, 4-addition (*lH*) are shown at 1.91-2.19 ppm²⁹. The other chemical shifts of protons in polyisoprene are also marked in **Figure 6.6.a**. The peaks of phenyl protons (*uH*) at 6.2-7.2 ppm²⁹ can be seen in **Figure 6.6.a** indicates that copolymerization of macromonomer with isoprene occurred and the desired graft copolymer was obtained. The compositions of graft copolymers were calculated from ^1H -NMR according to the integral area of protons in polystyrene and polyisoprene, and the results are shown in **Table 6.2**. From ^{13}C -NMR spectrum in Figure 6.6.b, it can be demonstrated that PI with the desired high 1, 4- microstructure was obtained because of the strong and sharp peaks at 27.0 ppm, 124.4 ppm, 16.1 ppm and 39.7 ppm.²⁷

6.3.4 Microphase separation of graft copolymer: The microphase separation of graft copolymer MG-3-5 was observed by AFM and TEM, and the images are shown in **Figure 6.7** and **Figure 6.8**. From the AFM phase image, regions of different colors, corresponding to materials having different hardnesses, can be seen. These data indicate

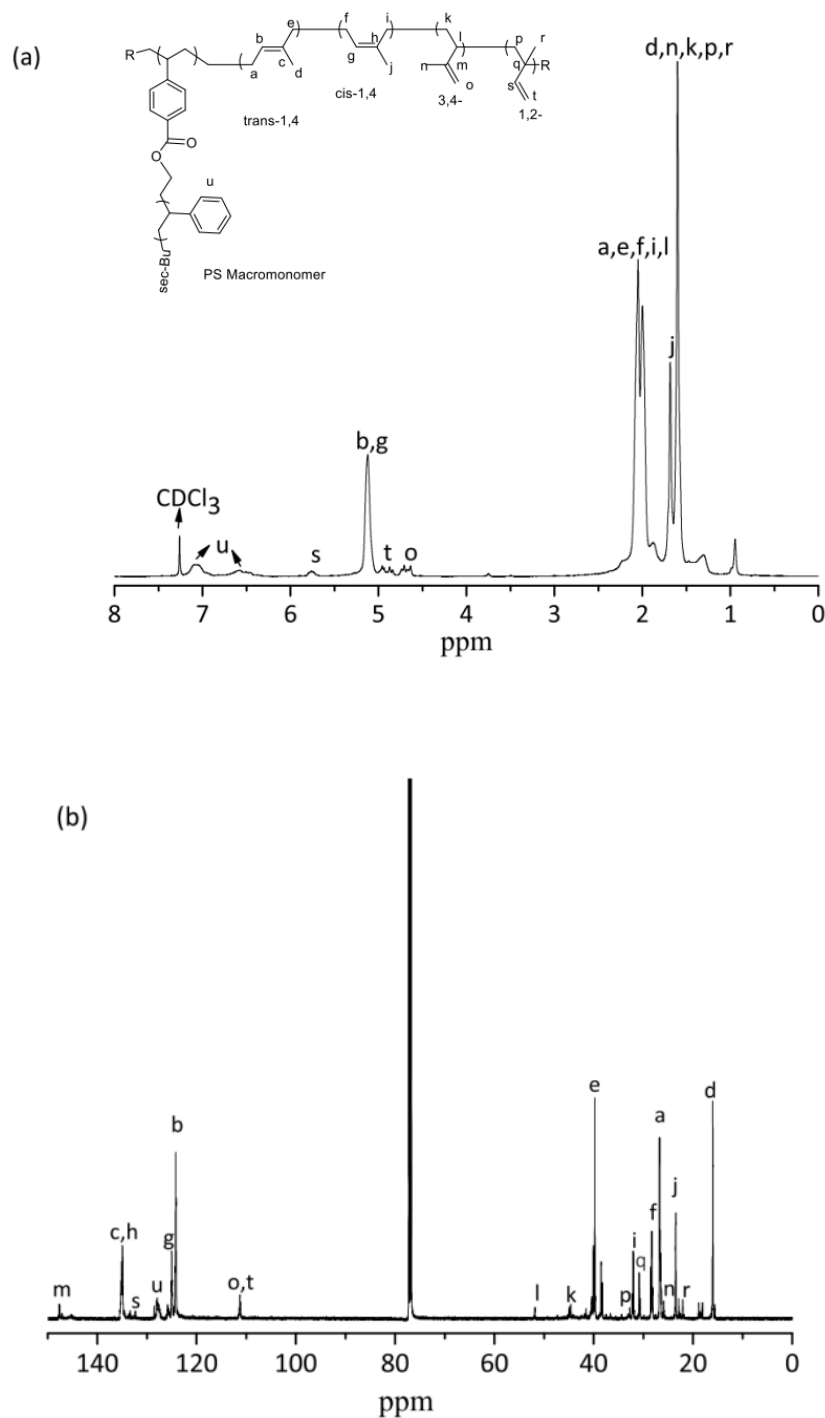


Figure 6.6 a) The chain structure and ^1H -NMR spectrum of MG-3-3 dissolved in CDCl_3 ;
 b) ^{13}C -NMR spectrum of MG-3-3 dissolved in CDCl_3 .

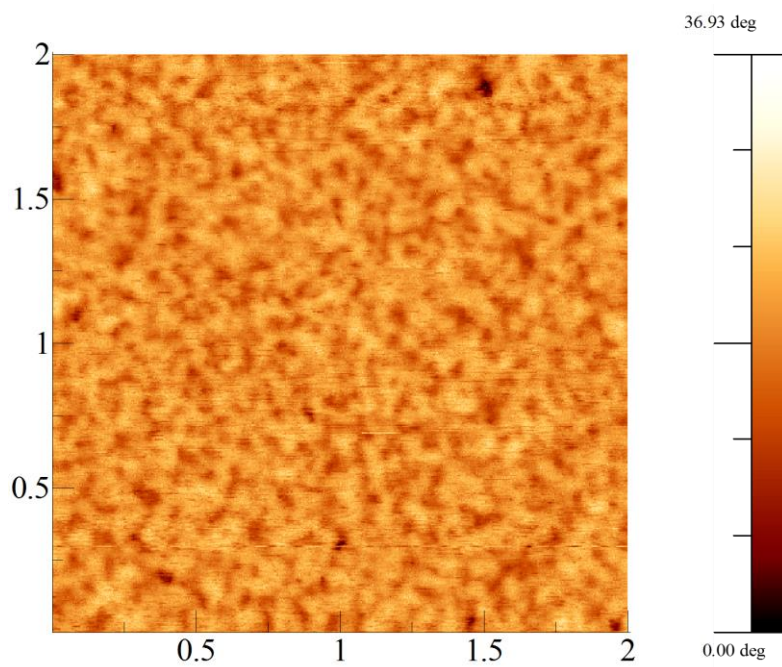


Figure 6.7: AFM phase image of MG-3-5 over an area of 2 μm x 2 μm .

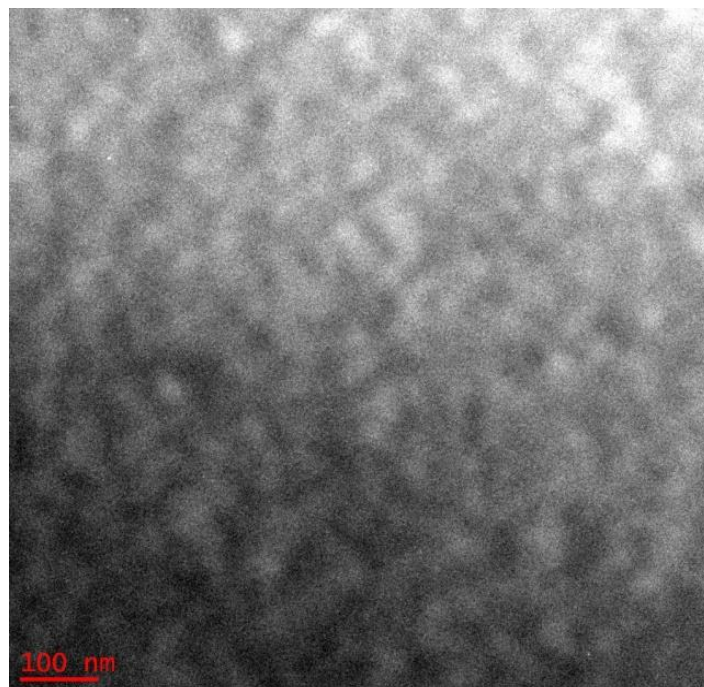


Figure 6.8: TEM image of MG-3-5

that microphase separation of the graft copolymer occurred, yet the morphology is not well-ordered, which might be related to the broad molecular weight distribution³⁰ as well as the branched architecture.^{7-10,18} Indeed, the system is strongly segregated since the product of Flory-Huggins interaction parameter χ times overall degree of polymerization N equals to about 200, over an order of magnitude higher than the critical value for microphase separation.³¹⁻³³ However, even though the system is strongly segregated it does not form the well-ordered morphologies observed for monodisperse diblock and triblock copolymers. The morphology of microphase separated polymers is affected by the polydispersity and structure (molecular architecture) of the copolymers. Graft copolymer is nonlinear block copolymer, and the ability to form well-ordered morphology is hindered as the number of junction points per molecule increases, most likely due to the kinetic limitations imposed by large number of junction points and high molecular weight. In our extensive prior work with well-defined multigraft copolymers having very narrow PDIs, we consistently observed poor or no long range order, even for samples subjected to extensive thermal annealing, particularly as the number of branch points was increased.^{7-10, 18} This result also probably reflects the strong barriers to motions necessary for reorientation of the chains because of the high molecular weight, branched nature of these materials. Thus, while these materials undergo phase separation, they do not exhibit morphologies having long range order.

6.3.5 Thermal properties of the graft copolymers: The thermal properties of the graft copolymers were evaluated using TGA and DSC. **Figure 6.9** shows the TGA thermograms, and the decomposition temperature of 5% weight loss (T_{5d}) was 348 °C and 350 °C for samples MG-3-3 and MG-3-5, respectively. These results are similar to the decomposition temperature of 5% weight loss (T_{5d}) of Kraton SIS triblock copolymer.³⁴ DSC was utilized to measure the T_g s of the graft copolymers (shown in **Figure 6.10**). For comparison, we also measured the T_g s of PI homopolymer synthesized by emulsion polymerization and PS macromonomer. The T_g s of PI and PS are -58 °C and 87 °C, respectively. The low T_g value for PI reflects its high 1,4- microstructure and is identical to the value of -58 °C measured using DSC for anionically synthesized polyisoprene.³⁵ The T_g value of the PS macromonomer is lower than the value for high molecular weight PS of about 100 °C, reflecting its low molecular weight. It may be initially surprising that the DSC curves for MG-3-3 and MG-3-5 exhibit only a single T_g which is very close to the T_g of PI homopolymer, and no clear T_g for PS is observed. However, this result is in complete agreement with the findings of Mijovic and co-workers³⁶ who carried out an extensive study of poly(isoprene-*g*-styrene) multigraft copolymers of comb, centipede, and barbwire architectures having from 19 to 67 % PS content and PS side chain molecular weights of 13,000 to 77,000 g/mol. These workers observed by DSC a midpoint T_g of -56 °C for PI but found that T_g of the PS side chain blocks could not be readily determined by DSC because the transition is not sharp, occurring over a wide temperature range.³⁶ This likely

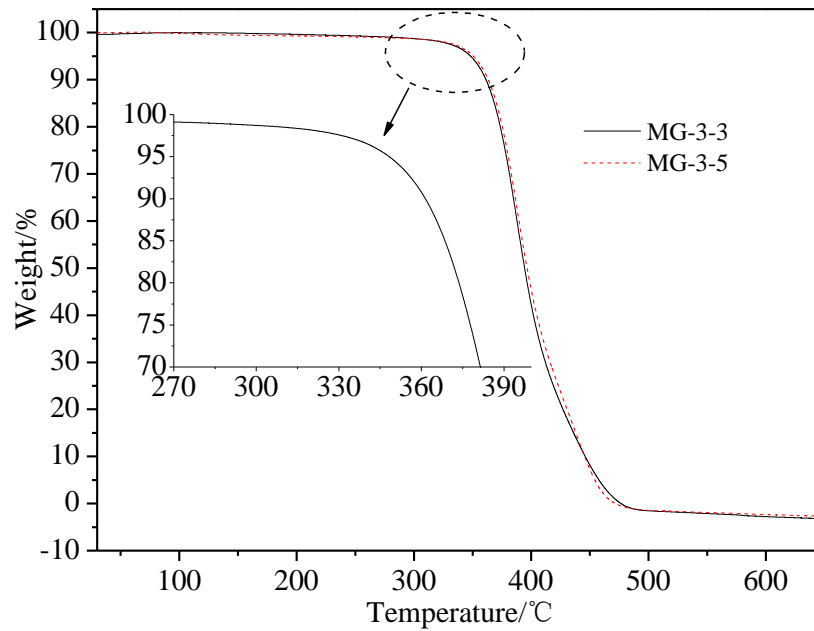


Figure 6.9: TGA thermograms for poly(isoprene-g-styrene) multigraft copolymers.

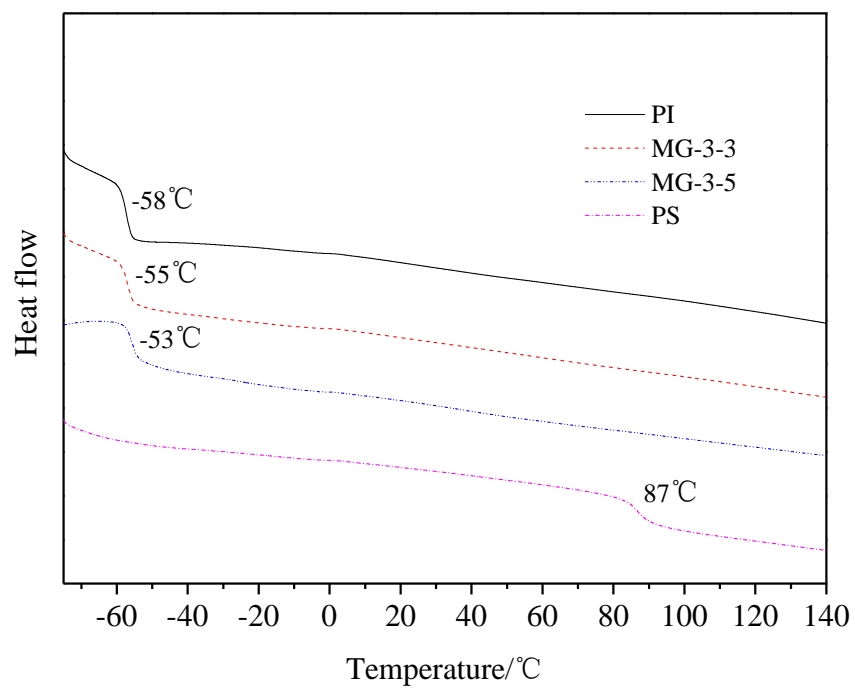


Figure 6.10: DSC thermograms for PI homopolymer, MG-3-3, MG-3-5, and PS macromonomer.

reflects the different environments in which the PS side chains reside due to the very poorly ordered microphase separated morphology. Another possible explanation is the large polydispersity of MG-3-3 and MG-3-5, which can lead to substantial dissolution of short and hard PS branches inside neighboring PI soft microdomains, which is similar to the case of block copolymer.³⁷

6.3.6 Rheological properties of graft copolymers: Comb-branched multigraft copolymers of appropriate composition and molecular weight behave as novel thermoplastic elastomers.^{8-10, 38} Since the main focus of this work was to attempt the first emulsion polymerization synthesis of multigraft copolymer superelastomers, the synthesis was carried out on a very small scale, and the amount of copolymer available is inadequate for detailed study of tensile properties. Nevertheless, we did observe through physical handling that both samples were highly elastic and decided to perform some preliminary rheological measurements on these materials. **Figure 6.11** shows the frequency dependence of rheological properties (storage modulus G' and loss modulus G'') of MG-3-3 and MG-3-5. From **Figure 6.11**, it is seen that G' is an order of magnitude larger than G'' over the frequency range probed for each sample. Therefore the graft copolymers exhibit elastic properties at room temperature.³⁹ Furthermore, we can see that G' increases with increasing frequency. This is attributed to time being adequate for entangled chains to relax, which reduces the modulus at low frequency. However, the entangled polymer

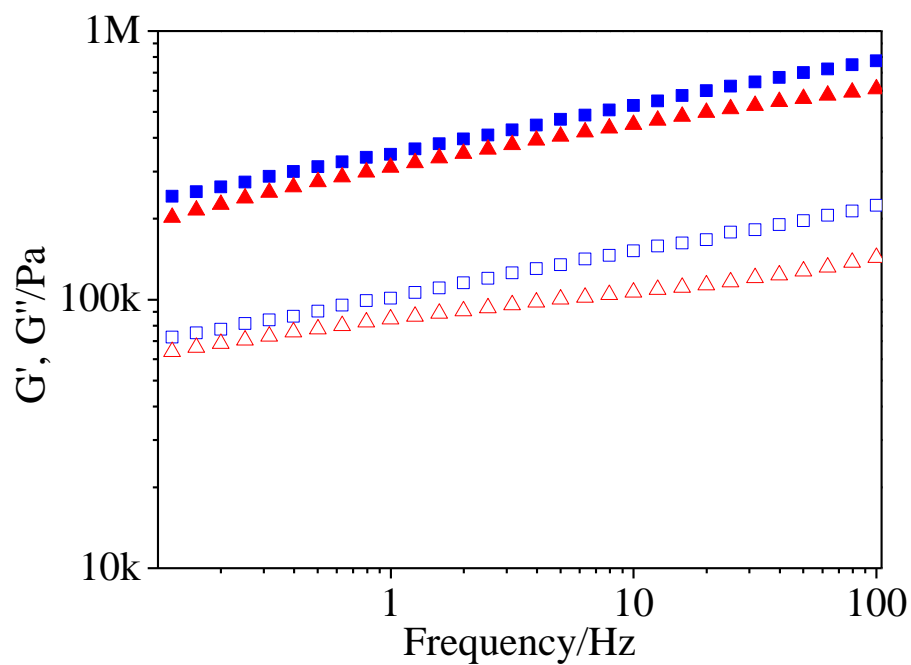


Figure 6.11: Storage modulus G' (solid symbols) and loss modulus G'' (hollow symbols) for MG-3-3 (■, □) and MG-3-5 (▲, △) as a function of frequency.

chains have less time for reorientation at higher frequency, resulting in higher G' values. Moreover, the storage modulus (G') of MG-3-5 is lower than that of MG-3-3, which means that the former graft copolymer exhibits better elastic properties and larger elongation at break if loaded with the same stress. The molecular weight of MG-3-5 is much higher than that of MG-3-3, and the weight fraction of polystyrene in MG-3-5 is also higher than that of MG-3-3. Higher molecular weight results in more chain entanglements, which is beneficial to the mechanical properties of elastomeric materials, and the content of PS controls the morphology and thus the nature of the physical cross-linking domains in microphase separated multigraft copolymers.³⁸ In addition, **Figure 6.12** illustrates the results of $\tan \delta$ versus frequency, and MG-3-5 exhibits lower $\tan \delta$ values at most frequencies, verifying its superior elasticity,⁴⁰ which is in agreement with the above discussion. Moreover, we can see from Table 2 that the number of junction points per molecule in MG-3-5 is greater than that of MG-3-3, which is also one reason for better elasticity of MG-3-5.⁹

6.4 Conclusions:

Poly(isoprene-*g*-styrene) multigraft copolymers having high molecular weights and containing up to 29 wt% PS, were synthesized successfully by copolymerizing a well-defined PS macromonomer with isoprene in emulsion copolymerization initiated by either

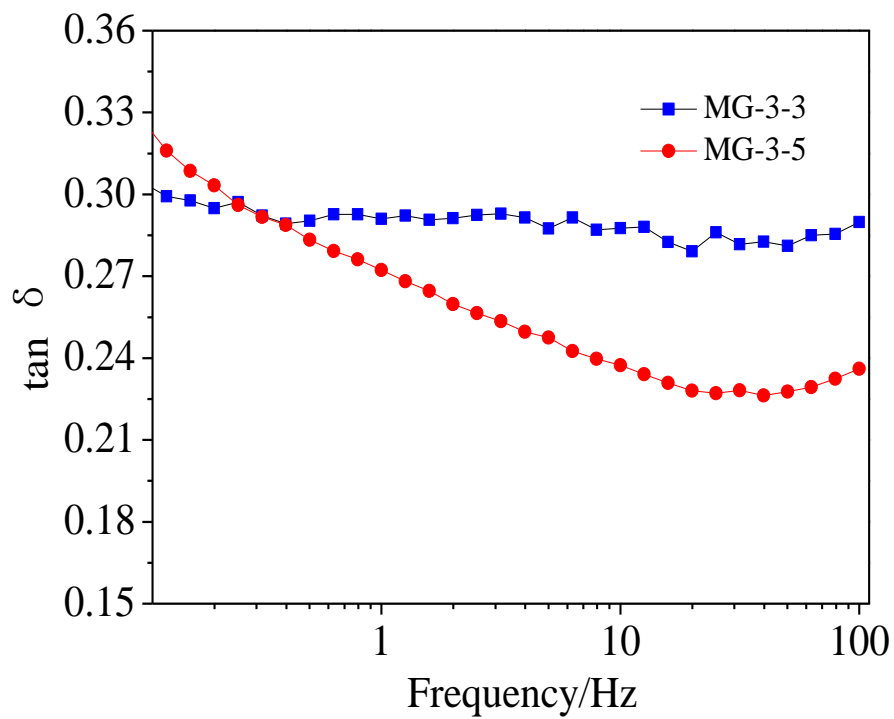


Figure 6.12: Tan δ versus frequency for MG-3-3 and MG-3-5.

AIBN or a redox initiator. DLS indicates that stable latexes were obtained either by AIBN initiation or by redox initiation by emulsifying the PS macromonomer using toluene. The graft copolymer having $M_w=1,200,000$, an average of 10 branches per chain, and containing 29 wt% PS exhibits microphase separation without long range order, as observed by AFM and TEM, while DSC only detected the T_g of the PI backbone, in agreement with prior extensive results on poly(isoprene-*g*-styrene) multigraft copolymers. From its rheological properties and handling characteristics, it is concluded that this polymer is promising as a thermoplastic elastomer. It thus appears that emulsion copolymerization of glassy macromonomers with co-monomers that yield rubbery backbones is a promising low cost and greener alternative to solution-based anionic polymerization for the synthesis of novel thermoplastic elastomer materials. In addition, this emulsion polymerization approach is well-suited to the synthesis of high molecular weight multigraft copolymers having large numbers of branch points. We have previously shown that increasing the number of branch points leads to an increase in both tensile strength and elongation at break of such materials.^{7-10, 18}

In future work, we will synthesize PS macromonomers having higher molecular weights and different structures, e.g. double-tailed, and utilize the emulsion copolymerization method reported herein to synthesize “comb” and “centipede” graft copolymers of PI-*g*-PS in quantities adequate for the detailed investigation of mechanical properties, in particular tensile properties.

References:

- [1]. Hadjichristidis, N.; Pispas, S.; Pitsikalis, M.; Iatrou, H.; Lohse, D., Graft copolymers, *Encyclopedia of Polymer Science and Technology. John Wiley & Sons, Inc., Hoboken, New York* **2004**.
- [2]. Cowie, J., Block and graft copolymers. *Pergamon Press plc, Comprehensive Polymer Science: the Synthesis, Characterization, Reactions & Applications of Polymers.* **1989**, 3, 33-42.
- [3]. Hadjichristidis, N.; Iatrou, H.; Pitsikalis, M.; Mays, J. *Prog. Polym. Sci.* **2006**, 31 (12), 1068-1132.
- [4]. Gramlich, W. M.; Theryo, G.; Hillmyer, M. A.. *Polym. Chem.* **2012**, 3 (6), 1510-1516.
- [5]. Feng, C.; Li, Y.; Yang, D.; Hu, J.; Zhang, X.; Huang, X. *Chem. Soc. Rev.* **2011**, 40 (3), 1282-1295.
- [6]. Theryo, G.; Jing, F.; Pitet, L. M.; Hillmyer, M. A. *Macromolecules* **2010**, 43 (18), 7394-7397.
- [7]. Mays, J. W.; Uhrig, D.; Gido, S.; Zhu, Y.; Weidisch, R.; Iatrou, H.; Hadjichristidis, N.; Hong, K.; Beyer, F.; Lach, R.; Buschnakowski, M. *Macromol. Symp.* **2004**, 215 (1), 111-126.

- [8]. Uhrig, D.; Schlegel, R.; Weidisch, R.; Mays, J. *Eur. Polym. J.* **2011**, *47* (4), 560-568.
- [9]. Zhu, Y.; Burgaz, E.; Gido, S. P.; Staudinger, U.; Weidisch, R.; Uhrig, D.; Mays, J. W. *Macromolecules* **2006**, *39* (13), 4428-4436.
- [10]. Staudinger, U.; Weidisch, R.; Zhu, Y.; Gido, S.; Uhrig, D.; Mays, J.; Iatrou, H.; Hadjichristidis, N. *Macromol. Symp.*, **2006**, pp 42-50.
- [11]. Uhrig, D.; Mays, J. *Polym. Chem.* **2011**, *2* (1), 69.
- [12]. Iatrou, H.; Mays, J. W.; Hadjichristidis, N. *Macromolecules* **1998**, *31* (19), 6697-6701.
- [13]. Uhrig, D.; Mays, J. W. *Macromolecules* **2002**, *35* (19), 7182-7190.
- [14]. Driva, P.; Iatrou, H.; Lohse, D. J.; Hadjichristidis, N. *J. Polym. Sci. Part A: Polym. Chem.* **2005**, *43* (18), 4070-4078.
- [15]. Nikopoulou, A.; Iatrou, H.; Lohse, D. J.; Hadjichristidis, N. *J. Polym. Sci. Part A: Polym. Chem.* **2007**, *45* (16), 3513-3523.
- [16]. Hadjichristidis, N.; Iatrou, H.; Pispas, S.; Pitsikalis, M. *J. Polym. Sci. Part A: Polym. Chem.* **2000**, *38* (18), 3211-3234.
- [17]. Uhrig, D.; Mays, J. W. *J. Polym. Sci. Part A: Polym. Chem.* **2005**, *43* (24), 6179-6222.
- [18]. Weidisch, R.; Gido, S. P.; Uhrig, D.; Iatrou, H.; Mays, J.; Hadjichristidis, N. *Macromolecules* **2001**, *34* (18), 6333-6337.

- [19]. Minari, R. J.; Rodriguez, V. I.; Estenoz, D. A.; Vega, J. R.; Meira, G. R.; Gugliotta, L. M. *J. Appl. Polym. Sci.* **2010**, *116* (1), 590-601.
- [20]. Suppaibulsuk, B.; Rempel, G. L.; Prasassarakich, P. *Polym. Adv. Technol.* **2012**, *23* (11), 1473-1483.
- [21]. Gilman, H.; Cartledge, F. K. *J. Organomet. Chem.* **1964**, *2* (6), 447-454.
- [22]. Prince, A.; Spitz, R. *Ind. Eng. Chem. Res.* **1960**, *52* (3), 235-238.
- [23]. Ji, H.; Sato, N.; Nonidez, W. K.; Mays, J. W. *Polymer* **2002**, *43* (25), 7119-7123.
- [24]. Neises, B.; Steglich, W. *Angew. Chem. Int. Ed.* **1978**, *17* (7), 522-524.
- [25]. Quirk, R. P.; Pickel, J. M.; Arnould, M. A.; Wollyung, K. M.; Wesdemiotis, C. *Macromolecules* **2006**, *39* (5), 1681-1692.
- [26]. Liu, B.; Quirk, R. P.; Wesdemiotis, C.; Yol, A. M.; Foster, M. D. *Macromolecules* **2012**, *45* (23), 9233-9242.
- [27]. Cheong, I. W.; Fellows, C. M.; Gilbert, R. G. *Polymer* **2004**, *45* (3), 769-781.
- [28]. Kongsinlark, A.; Rempel, G. L.; Prasassarakich, P. *J. Appl. Polym. Sci.* **2013**, *127* (5), 3622-3632.
- [29]. Wang, W.; Zhang, H.; Geng, W.; Gu, J.; Zhou, Y.; Zhang, J.; Zhang, Q. *J. Colloid Interface Sci.* **2013**, *406*, 154-164.
- [30]. Wei, R.; Luo, Y.; Zeng, W.; Wang, F.; Xu, S. *Ind. Eng. Chem. Res.* **2012**, *51* (47), 15530-15535.

- [31]. Zhang, J.; Yu, X.; Yang, P.; Peng, J.; Luo, C.; Huang, W.; Han, Y. *Macromol. Rapid Commun.* **2010**, 31, 591-608.
- [32]. Khandpur, A. K.; Foerster, S.; Bates F. S.; Hamley I. W.; Ryan A. J.; Bras W.; Almdal K.; Mortensen K. *Macromolecules* **1995**, 28, 8796-8806.
- [33]. Olvera de La Cruz, M.; Sanchez I. C. *Macromolecules* **1986**, 19, 2501-2508.
- [34]. Peng Wu; Shuhua Qi; Nailiang Liu; Kangqing Deng; Haiying Nie. *J. Elastom. Plast.* **2011**, 43 (4), 369-386.
- [35]. Frick, B.; Fetters, L. J. *Macromolecules* **1994**, 27 (4), 974-980.
- [36]. Mijović, J.; Sun, M.; Pejanović, S.; Mays, J. W. *Macromolecules* **2003**, 36 (20), 7640-7651.
- [37]. Nicolas, J.; Ruzette, A.V.; Farcet, C.; Gérard, P.; Magnet, S.; Charleux, B., *Polymer* **2007**, 48, 7029-7040.
- [38]. Duan, Y.; Rettler, E.; Schneider, K.; Schlegel, R.; Thunga, M.; Weidisch, R.; Siesler, H. W.; Stamm, M.; Mays, J. W.; Hadjichristidis, N. *Macromolecules* **2008**, 41 (13), 4565-4568.
- [39]. Singh, M.; Odusanya, O.; Wilmes, G. M.; Eitouni, H. B.; Gomez, E. D.; Patel, A. J.; Chen, V. L.; Park, M. J.; Fragouli, P.; Iatrou, H. *Macromolecules* **2007**, 40 (13), 4578-4585.
- [40]. Poongavalappil, S.; Svoboda, P.; Theravalappil, R.; Svobodova, D.; Danek, M.; Zatloukal, M. *J. Appl. Polym. Sci.* **2013**, 128 (5), 3026-3033.

Chapter 7: Conclusions and Future Perspectives

7.1 Conclusions:

Overall, this dissertation was aimed at developing thermoplastic elastomers with higher upper service temperature and lower cost:

We prepared polybenzofulvene-polyisoprene-polybenzofulvene triblock copolymers and evaluated their mechanical properties as a new class of high temperature thermoplastic elastomers. For a FIF triblock copolymer with 14 vol% of PBF, tensile test indicated ultimate stress of 14.3 ± 1.3 MPa with strain at break of 1394 ± 66 % which was competitive with commercial Kraton SIS triblock copolymer type TPEs. The upper service temperature of TPEs based on PBF as the glassy block were 145°C as confirmed by dynamic mechanical analysis. Microphase separation of FIF triblock copolymers was observed by small angle X-ray scattering and AFM. The ability to synthesize FIF triblock copolymers in hydrocarbon solvent at room temperature distinguishes these materials from other types of high temperature TPEs synthesized by cationic polymerization, controlled radical polymerization or anionic polymerization in THF at -78°C , and enable PBF based TPEs with great commercial potential.

Furthermore, the effects of partial and complete hydrogenation on the thermal stability, mechanical and morphological properties of FIF triblock copolymers were investigated and compared with hydrogenation of SIS triblock copolymers. Tensile tests showed higher Young's modulus for partially and completely hydrogenated FIF. Dynamic

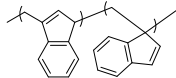
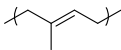
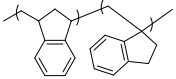
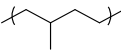
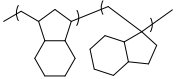
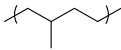
mechanical analysis showed that the upper service temperature of completely hydrogenated FIF (FH-FIF-14) is 130 °C. After complete hydrogenation, the degradation temperature of FIF was improved from 245 °C to 350 °C. The mechanical properties are summarized in **Table 7.1**

Besides developing TPEs with higher upper service temperature, we also explored the possibility of preparing TPEs with cost efficient emulsion polymerization techniques. High molecular weight “comb-shaped” graft copolymers, poly(isoprene-g-styrene), with polyisoprene as the backbone and polystyrene as side chains, were synthesized via free radical emulsion polymerization by copolymerization of isoprene with a polystyrene macromonomer synthesized using anionic polymerization. The multigraft copolymers obtained were very high in molecular weight ($5-12 \times 10^5$ g/mol) and up to 10 branches per chain, on average, could be incorporated. A material incorporating 29 wt% polystyrene exhibits a disordered microphase separated morphology and elastomeric properties. These materials show promise as new, highly tunable, and potentially low cost thermoplastic elastomers.

7.2. Future Perspectives:

Most aspects of the task of developing high temperature TPEs and lower cost TPEs in this dissertation were accomplished. However, many intriguing topics are still worth further

Table 7.1 Mechanical properties of PBF based TPEs

Hard Segment (T_g , °C)	Soft Segment (T_g , °C)	Mechanical Properties			Synthetic Methods
		Stress / MPa	Strain / %	wt %	
 (145 °C)	 (-56 °C)	14.3 MPa	1390%	20%	
 (125 °C)	 (-48 °C)	11.2 MPa	750%	20%	Anionic PLZ (benzene, r.t.) Catalytic Hydrogenation
 (135 °C)	 (-48 °C)	17.0MPa>	500%>	20%	

exploration for the interest of both fundamental research in academia and performance materials in industry:

7.2.1. Composition Dependence of the Morphology in PBF/PI block copolymers: In order to optimize the mechanical performance of FIF triblock copolymers, a comprehensive understanding of the chemical composition dependence of the morphology in PBF/PI block copolymers is critical. However, elucidating the morphology of FIF by transmission electron microscopy (TEM) is challenging due to the unsaturated carbon-carbon double bonds in both the PBF and PI blocks. Traditional block copolymer staining reagents such as OsO₄ or RuO₄ have little or no selectivity between these double bonds in both the rigid and soft blocks in FIF polymers. For similar reasons small angle x-ray scattering provides very little contrast. Due to the limitations of using TEM or SAXS to determine the phase behavior of PBF-PI block copolymers, we propose to synthesize PBF-PI block copolymers with deuterated isoprene blocks (**Figure 7.1**) and use small angle neutron scattering (SANS) to determine the composition dependence of their morphology.

For these experiments, we will synthesize two groups of PBF-*b*-PI diblock copolymers by anionic polymerization with deuterated isoprene. In order to span the phase diagram, the first group of diblock copolymers will target an overall molecular weight of 100k. The weight percentage of PBF in these copolymers will be varied from 5%, 15%, 25%, 35%, 50%, 65% and 85%. To further understand the order-disorder transition

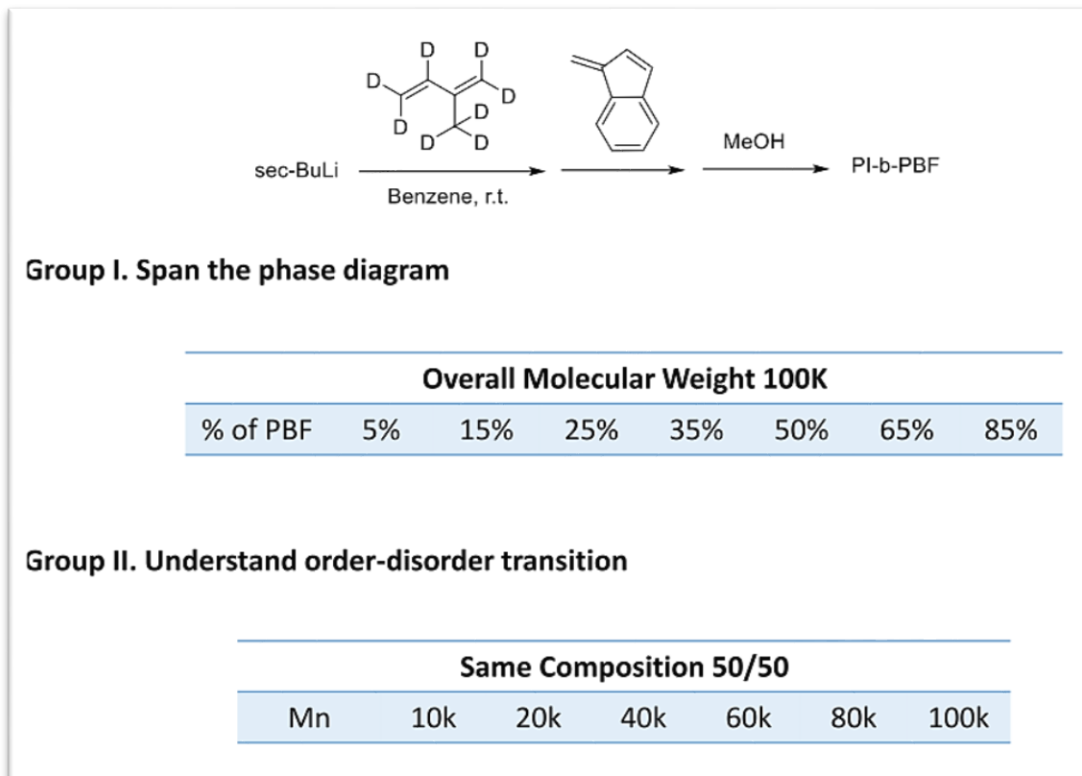


Figure 7.1: Proposed research on composition dependence of the morphology in PBF/PI block copolymers

behavior, a second group of PBF-PI copolymer will be synthesized with a composition of 50/50 but changing the overall molecular weight from 100k to 80k, 60k, 40k, 20k and 10k.

(Figure 7.1)

7.2.2 Effects of additives on the characteristic ratio of PBF: Similar to other conjugated dienes, the microstructure of PBF also shows dependence on initiators, additives, polymerization solvents and temperature. Different microstructures of polydiene generally lead to different characteristic ratio and glass transition temperature and would affect bulk morphology in diblock copolymers due to conformational asymmetry. Thus, from the prospect of fundamental research, study of the effects of additives on the microstructure, glass transition temperature and characteristic ratio of PBF is proposed to further explore the basic physical properties of benzofulvene based polymers. The scheme is proposed in **Figure 7.2** with polar additives such as: 1,2-dipiperidinoethane (DiPIP), 1,2-dimethoxyethane (DME), 1,4-diazabicyclo[2.2.2]-octane (DABCO), tetramethylethylenediamine (TMEDA) and sec-Butoxide (sec-BuOLi).

7.2.3: Benzofulvene-Butadiene Rubber: Styrene-Butadiene Rubber (SBR) was first developed in 1929 by randomly copolymerizing styrene and butadiene in a ratio of 1:3 in either emulsion or solution, and is currently of huge importance in the synthetic rubber industry, especially in compounding tires. Additionally, SBR is widely applied in the field of footwear, polymer modifications and adhesive with a predicted global market worth of

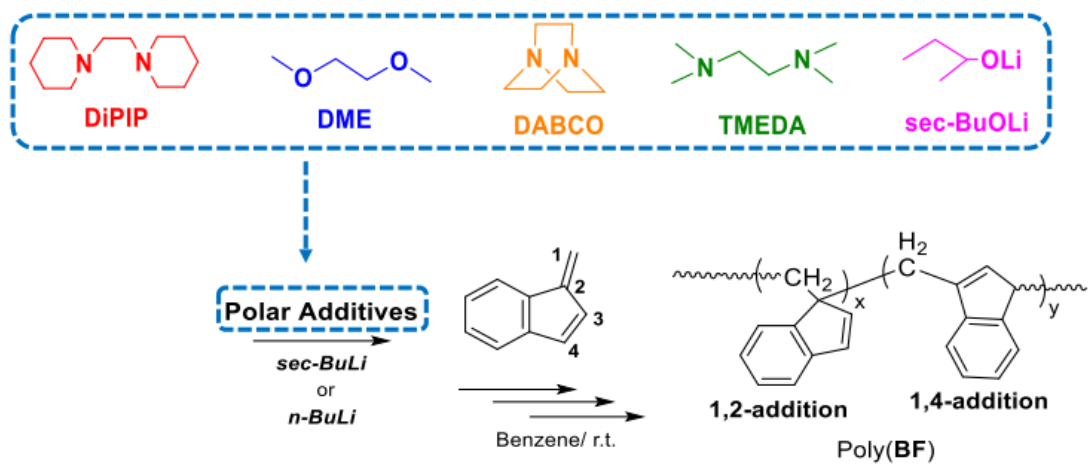


Figure 7.2: Proposed Study of Effects of Additives on PBF

\$23 billion in 2020. Most SBR end-applications require vulcanization to chemically crosslink the carbon-carbon double bond in the butadiene units (curing process) to improve mechanical properties and oxidation resistance. However, this curing process only attacks unsaturated polybutadiene units. Here, we propose to incorporate benzofulvene as additional cross-linkable repeat units, replacing styrene as co-monomer, together randomly copolymerizing with butadiene or isoprene to prepare a new class of synthetic rubber: Benzofulvene-Butadiene Rubber (BBR) (**Figure 7.3**) and Benzofulvene-Isoprene Rubber (BIR).

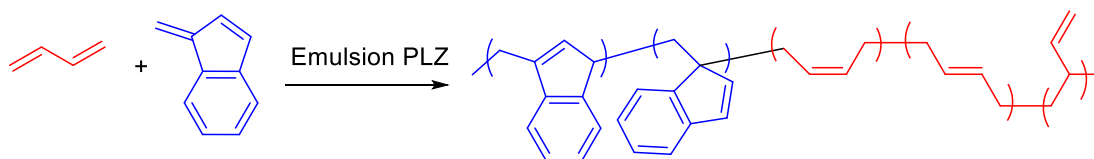


Figure 7.3: Benzofulvene-Butadiene Rubber

Unlike SBR rubber which curing process only crosslinks butadiene units. BBR contains additional unsaturated double bond in benzofulvene units. We are eager to compare how this additional double bond in BF will affect classical curing process and eventually, mechanical properties of benzofulvene-butadiene rubber (BBR). Considering the difficulty in lab to handle gas type monomer butadiene, we will choose isoprene to evaluate the reactive ratio between benzofulvene and isoprene by radical and emulsion polymerization.

Vita

Weiyu Wang was born in Gansu, China. He obtained the Bachelor of Science Degree in Chemistry in July 2011 from Hunan University, joined Dr. Jimmy Mays' research group in November 2011, and graduated in December 2015 with a PhD. Degree in Polymer Chemistry focused on developing thermoplastic elastomers with higher service temperature and lower cost.

During his four years and half stay in the University of Tennessee, he co-published six papers and contributed to one book chapter about anionic polymerization. He presented his research on various occasions including ACS National Meeting, International Conference of Polymer Analysis and Characterization (ISPAC), Gordon Research Conference, research seminar at Eastman Chemical Co. and a special seminar in the Department of Polymer Science and Engineering in the University of Massachusetts, Amherst. He has been honored with the Gleb Mamantov Graduate Chemistry Scholar (2015), Graduate Student Senate Travel Award (2015) from the University of Tennessee and won the Summer Fellowship from Eastman Chemical Co.